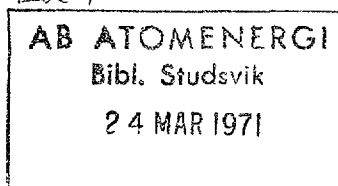


AE-409

# X-Ray Powder Diffraction with Guinier - Hägg Focusing Cameras

A. Brown

*Ex 1*



AKTIEBOLAGET ATOMENERGI  
STUDSVIK, NYKÖPING, SWEDEN 1970



X-RAY POWDER DIFFRACTION  
WITH GUINIER - HÄGG FOCUSING CAMERAS

Allan Brown

ABSTRACT

The Guinier - Hägg focusing camera is discussed with reference to its use as an instrument for rapid phase analysis. An actual camera and the alignment procedure employed in its setting up are described. The results obtained with the instrument are compared with those obtained with Debye - Scherrer cameras and powder diffractometers. Exposure times of 15 - 30 minutes with compounds of simple structure are roughly one-sixth of those required for Debye - Scherrer patterns. Coupled with the lower background resulting from the use of a monochromatic X-ray beam, the shorter exposure time gives a ten-fold increase in sensitivity for the detection of minor phases as compared with the Debye - Scherrer camera.

Attention is paid to the precautions taken to obtain reliable Bragg angles from Guinier - Hägg film measurements, with particular reference to calibration procedures. The evaluation of unit cell parameters from Guinier - Hägg data is discussed together with the application of tests for the presence of angle-dependent systematic errors. It is concluded that with proper calibration procedures and least squares treatment of the data, accuracies of the order of 0.005 % are attainable.

A compilation of diffraction data for a number of compounds examined in the Active Central Laboratory at Studsvik is presented to exemplify the scope of this type of powder camera.

## LIST OF CONTENTS

1.	INTRODUCTION	4
2.	GENERAL CONSIDERATIONS	7
2.1.	Diffraction in Crystals	7
2.2.	The Debye - Scherrer Effect	9
2.3.	Influence of Specimen Condition on Pattern Definition	10
2.4.	Requirements and Problems of Powder Photography	11
2.5.	Problems Associated with the X-ray Spectrum	14
2.6.	Crystal Monochromatization	15
2.6.1.	Parallel X-ray Beams	15
2.6.2.	Geometrical Conditions for the Focusing of Divergent Beams	16
3.	PRACTICAL CONSIDERATIONS: THE GUINIER-HÄGG CAMERA	17
3.1.	Guinier Focusing Geometry	17
3.2.	The Monochromator Crystal	18
3.3.	Mounting the Crystal	20
3.4.	The X-ray Source	21
4.	SETTING UP THE CAMERA	22
4.1.	Component Parts	22
4.2.	Preliminary Steps	23
4.3.	Adjustment of Monochromator (Sample Assembly Absent)	23
4.4.	Adjustment of the Sample-Film Cassette Assembly	26
4.5.	Final Adjustment	27
5.	EXAMINATION OF POWDER SAMPLES IN THE GUINIER - HÄGG CAMERA	29
5.1.	Specimen Treatment	29
5.2.	Encapsulated Materials	30
5.3.	Fluorescent Specimens	31
6.	EVALUATION OF THE GUINIER - HÄGG CAMERA AS AN ANALYTICAL INSTRUMENT	32
6.1.	Exposure Times and General Sensitivity	32
6.2.	Treatment of Diffracted Intensities	34
6.3.	Pattern Definition, Calibration and the Measurement of $\theta$	36

6. 3. 1.	Precision of Film Measurement	36
6. 3. 2.	The Camera Constant and the Origin of Systematic Errors in the Measurement of $\theta$	37
6. 3. 3.	Calibration of Guinier - Hägg Patterns	38
6. 3. 4.	Film Measurement and Derivation of K	39
6. 3. 5.	The Magnitude of Residual Systematic Errors in $\theta$	40
6. 4.	Unit Cell Dimensions from Guinier - Hägg Film Measurements	41
6. 4. 1.	Evaluation of Cell Dimensions and their Probable Errors	41
6. 4. 2.	Significance Tests for Residual Systematic Errors	43
7.	APPLICATIONS	46
	ACKNOWLEDGEMENT	48
	REFERENCES	49

#### TABLES

1. Linear Equations for the Relationship between Bragg Angle, Miller Indices and Unit Cell Parameters for Monoclinic to Cubic Symmetries.
2. Calibration Data for Silicon Powder.
3. Camera Constants and their Deviations Obtained with Silicon Calibrant for 80 mm Diameter Cassette.
4. Comparison of Cell Dimension Calculations from Guinier - Hägg Data Using Least-Squares and Likelihood-Ratio Methods.
5. Comparison of Cell Dimensions from Guinier - Hägg Data with Literature Values.

#### PLATES I & II

Comparison Photographs of Powder Patterns.

#### APPENDIX I

Listing of Computer Programme Mott.

#### APPENDIX II

Results Obtained from Measurements of Some Guinier - Hägg Patterns Obtained in Routine Studies

## 1. INTRODUCTION

X-ray powder diffraction is a well established technique for the phase analysis of solids. Studies of minerals, reaction products of laboratory and technical-scale processes, surface coatings and corrosion products have all benefited from the introduction of powder-pattern characterization. A related application, the measurement of the dimensions and angles of the crystallographic unit cell, has afforded a powerful means for studying and understanding the phenomenon of solid solubility. At a fundamental level these cell parameter measurements serve to convert the atomic parameters, obtained in crystal structure studies, into the spatial realities of bond distances and angles for subsequent correlation with physical and chemical properties.

For most of these applications a photographic method is preferred for recording the powder pattern, largely because of its cheapness, but also because it is simple to apply. Only where accurate X-ray intensity measurements are required, as in quantitative analysis, or line profile studies, is the camera superseded by the electronically recording diffractometer.

Devices used for powder photography are usually based on the cylindrical camera, first used by Debye and Scherrer. The most popular version of this instrument in current use is the camera developed by Staumanis for precision lattice parameter measurements. Although simple to operate and maintain in routine application, this type of camera, with its  $1^\circ$  per 2 mm film ratio, suffers from limitations of resolution and line definition. Accordingly the interpretation of complex patterns is at best qualitative. Increased resolution is obtained up to a point by increasing the camera diameter (from 11.46 cm in the Straumanis to 19 cm in the Bradley - Jay camera) but the exposure times are then considerably increased. X-ray beams from conventional Coolidge tubes are divergent and an increased path length necessitates the use of more stringent collimation in order to maintain acceptable line definition.

Because of the need for collimation the Debye - Scherrer camera utilises only a fraction of the divergent X-ray beam. Improvements in camera performance have therefore been sought through beam focusing.

This is achieved in the Seeman - Bohlin and Westgren - Phragmén cameras by reflecting the primary beam from a specimen curved to fit a circle defined by the X-ray source and the recording film. In a further development, due to Guinier, a focused beam is obtained by setting up a curved quartz crystal in the path of the divergent primary X-rays. The beam diffracted from the quartz crystal is then transmitted through the specimen which, in the form of a powder, is spread over a paper tissue. This method has the added attraction that only a narrow band of wavelengths is employed to obtain the power pattern, the curved crystal functioning as a monochrometer.

A considerable disadvantage of the focusing camera is the limitation imposed on the angular range of the pattern available for recording on a single film ( $\theta_{\max} \leq 50^\circ$  in the low angle range). For the Guinier camera there are added difficulties in aligning and maintaining in effective operation, the optically sensitive system of bent crystal, specimen holder, film cassette and associated slit systems. As a result opinion regarding the value of this type of camera is generally guarded. Thus, while text books devoted to X-ray technique invariably give full accounts of the Debye - Scherrer camera and powder diffractometer, the Guinier camera is either given a passing mention or ignored altogether.

A typical evaluation is that the Guinier camera is capable of giving diffraction patterns with a resolution approaching that of the powder diffractometer for an exposure time comparable to that of the Debye - Scherrer camera. It is often pointed out, moreover, that direct measurement of Bragg angles is not possible in the Guinier camera, since the relationship between film circle and specimen plane is not ideal. The use of an internal calibrant becomes necessary in order to determine the ratio between film distance and Bragg angle at different points along the film.

In view of the past performance of some early commercial Guinier cameras, such remarks are justified. It should be pointed out, however, that the introduction of the fine-focus X-ray tube during the early 1960's afforded a possibility for a major improvement in Guinier camera performance. This is due to the increase in the definition of the X-ray

source which governs the line definition of the pattern and the ease with which the characteristic radiation is freed from the  $\alpha_2$  component. An added bonus is the possibility of much reduced exposure times arising from the greater intensity of the fine-focus-beam.

Full advantage of the improvements in X-ray tube performance is taken in the version of the Guinier camera developed in Uppsala by Prof. G. Hägg during the early 1950's. In 1958, two examples of this Guinier - Hägg camera were constructed for operation with  $\text{CuK}\alpha$  radiation at the Stockholm laboratories of AB Atomenergi under professor Hägg's guidance. In 1966 the present writer replaced the normal focus X-ray tube used with these cameras by a Philips fine-focus tube. Subsequent attempts to realign the optical system of the instruments indicated that the monochromator support was insufficiently stable under the critical conditions imposed by the fine-focus source.

Consultation with Dr. Per Spiegelberg of the Institute for Metals Research, Stockholm, led to the abandonment of the original arrangement for pivoting the crystal and setting it at the required distance from the fine-focus anode. A new device, constructed by Mr. K. Kranz of the Institute for Metals Research and described in this report has proved to be both highly flexible for adjustment purposes and mechanically stable under long term usage. Operated with strictly monochromatic  $\text{CuK}\alpha_1$  radiation, exposures are suitably short (15 - 30 minutes) for purposes of rapid phase analysis. The line definition is such that Bragg angle measurements from silicon calibrated patterns, are sufficiently precise to permit detection of cell parameter changes at the 0.01 % level, independent of cell symmetry. This degree of precision has been found to have particular value in connection with the indexing of powder patterns of new structures.

Since the main problem with the Guinier-type camera is to ensure that performance is consistently of the above quality, a description of these cameras and the method adopted for their adjustment seems called for. A brief summary of the principles and problems of powder diffraction is included as a means of highlighting the special advantages of the focusing camera. The report is supplemented with some results of an investigation into the reliability of cell dimension measurements based on calibrated Guinier - Hägg patterns.



The abbreviations D - S and G - H used throughout refer to Debye - Scherrer and Guinier - Hägg respectively, in the context of the cameras associated with these workers.

## 2. GENERAL CONSIDERATIONS

### 2.1. Diffraction in Crystals

The diffraction of X-rays in crystals can be understood with reference to Fig. 1a. The crystal is imagined as comprising sets of parallel planes which have the property of being able to scatter X-rays. Each set of planes is characterized by a particular separation, the interplanar distance  $d$ , measured along the normal.

A parallel beam of X-rays is defined by placing a collimator close to the irradiated crystal. X-rays travelling along the beam are then associated with a wave front perpendicular to the beam axis; wave fronts travel down the beam from the source with a separation of  $\lambda$ , the wavelength of the radiation.

As each component of a wave front strikes a crystal plane, scattering of a fraction of the radiation occurs at the point of impact, the scattered radiation being spherically distributed. The occurrence of scattering in successive crystal planes gives rise to interference phenomena as shown in Fig. 1a. Here, the components A, B and C are seen to strike the first three planes of a set at points O, P and Q along the normal. Inclination of the wave front at  $\theta$  to the normal leads to a path difference for the front, as it strikes successive planes at these points, which reaches a maximum at  $\theta = 90^\circ$ . When  $\theta$  attains an angle such that the path difference corresponds to an integral number of wavelengths,  $n\lambda$ , radiation scattered elastically at O, P and Q will reinforce to produce a wavefront at the same angle to, but on the opposite side of, the normal. This "reflected" wavefront is contained entirely in the plane defined by the path of the incident beam and the normal to the set of diffracting planes.

From a simple consideration of the quantities involved in Fig. 1c the condition for the generation of a diffracted beam is then given by the Bragg equation,

$$n\lambda = 2d \sin \theta$$

The normal to each set of crystal planes is inclined at a specific angle to the crystal axes, the angle being defined by the Miller indices  $hkl$  of the planes and by the dimensions of the unit cell  $a_0, b_0, c_0$  measured along the cell ledges and the interaxial angles,  $\alpha, \beta, \gamma$ . A purely trigonometrical relationship can be derived to relate these quantities and the  $d$  spacing along the normal to a set of planes  $hkl$ . Substituting for  $d$  in the Bragg equation, the general, triclinic case can be described by the linear expression

$$Q_{hkl} = Ah^2 + Bk^2 + Cl^2 + Dh\ell + Ekl + Fhk = n^2/d_{hkl}^2$$

where

$$Q_{hkl} = 4 \sin^2 \theta_{hkl} / \lambda^2$$

$$A = b^2 c^2 \sin^2 \alpha / V^2$$

$$B = c^2 a^2 \sin^2 \beta / V^2$$

$$C = a^2 b^2 \sin^2 \gamma / V^2$$

$$D = 2 ab^2 c \sin \alpha \sin \gamma (\cos \alpha \cos \gamma - \cos \beta / \sin \alpha \sin \gamma) / V^2$$

$$E = 2 a^2 bc \sin \beta \sin \gamma (\cos \beta \cos \gamma - \cos \alpha / \sin \beta \sin \gamma) / V^2$$

$$F = 2 abc^2 \sin \alpha \sin \beta (\cos \alpha \cos \beta - \cos \gamma / \sin \alpha \sin \beta) / V^2$$

and  $V$ , the volume of the unit cell is given by

$$abc(1 + 2 \cos \alpha \cos \beta \cos \gamma - \cos^2 \alpha - \cos^2 \beta - \cos^2 \gamma)^{1/2}$$

Simplifications of this expression obtained with increase of symmetry are given in Table 1.

Accordingly if the  $hkl$  indices corresponding to a number of independent reflections are known, measurement of the angles,  $2\theta_{hkl}$ , between the diffracted and transmitted beams can be used to determine the unit cell dimensions.

In a single crystal, each set of crystal planes and the associated normal, have a specific orientation with respect to the crystal axes. Diffraction from such a crystal therefore yields a pattern of reflected

beams which have a three dimensional distribution. This pattern is related to the symmetry and size of the unit cell and its orientation in the primary beam.

The measurement of  $2\theta$  in this three dimensional distribution presents serious problems of instrumentation since, in order to bring the different sets of  $hkl$  planes into the reflecting position, the crystal must be rotated through two mutually perpendicular arcs with respect to the X-ray beam [1]. These rotations must be known with a precision of at least  $0.01^\circ$  in order to obtain reliable values of  $2\theta$  for the measurement of accurate cell dimensions [2].

## 2.2. The Debye - Scherrer Effect

If the single crystal is reduced to a powder comprising a large number of randomly oriented crystallites, a given set of crystal planes of spacing  $d_{hkl}$  will be associated with a corresponding number of normals having spherical distribution. On irradiation with a parallel beam of X-rays, only those planes whose normals make an angle  $\phi$  ( $= 90 - \theta_{hkl}$ ) with the incident beam fulfill the Bragg condition. These normals lie on the surface of a cone of semi-angle  $\phi$  with the incident X-ray beam as cone axis. Each normal gives rise to a diffracted beam and these accordingly lie on the surface of a second cone of semi-angle  $2\theta$  to the transmitted beam. The process of cone formation, described by Debye and Scherrer [3], is depicted in Fig. 1b.

The three dimensional resolution afforded by single crystal diffraction is clearly lost when the specimen is a polycrystalline mass. Whereas in a single crystal, each set of  $hkl$  planes gives rise to a narrow, discrete beam of reflected X-rays, the set is represented in a polycrystalline specimen by a cone of reflection. The diffraction pattern accordingly comprises a family of such cones with the primary X-ray beam as common axis as depicted in Fig. 2a.

In compensation for the loss of three dimensional resolution, the powder pattern offers a considerable simplification of the requirements for measuring  $\theta_{hkl}$ . For a specimen with a truly random distribution of crystallites, all the reflections can be found on a single circle centred on the specimen with the X-ray beam as diameter. In the simplest

powder diffraction instrument, the Debye - Scherrer (D - S) camera, the reflections are recorded by placing a strip of photographic film on this circle as shown in Fig. 2a. The angle  $\theta_{hkl}$  is then proportional to the interval S measured between the exit point of the primary beam and the point on the equator (defined by the tangent between film cylinder and recording circle) where the cone of reflection emerges.

As cell dimensions grow larger and cell symmetries become lower the crowding of powder cones increases, particularly at values of  $\theta$  between 40 and 60°. Vand has considered the general distribution of reflections in a powder pattern in terms of the interaction of the Ewald sphere with the reciprocal lattice [4]. For reflection down to  $\theta_{hkl}$  corresponding to interplanar spacing  $d_{hkl}$  the radius of the reflecting sphere in reciprocal space is  $1/d$  and its volume is accordingly  $4 \pi/3d^3$ . For a unit cell of volume V, the reflecting sphere will contain  $4 \pi V/3d^3$  reciprocal lattice points each of which gives rise to a cone of reflection in the powder sample. Symmetry, however, limits the number of independent reciprocal lattice points, an effect represented by the multiplicity factor p for general hkl reflections. Thus p is 2 for triclinic, 4 for monoclinic, 6 for orthorhombic, 8 for tetragonal and 48 for cubic crystals. Neglecting the special cases where, for example, one or two indices are identical or zero the average number of powder lines is given approximately by

$$\begin{aligned} \bar{n} &= 4 \pi V/3pd^3 \\ &= (32 \pi V/3p\lambda^3) \cdot \sin^3 \theta \end{aligned}$$

The average number of reflections per unit of Bragg angle is then

$$d\bar{n}/d\theta = (32 \pi V/p\lambda^3) \sin^2 \theta \cos \theta$$

Fig. 2b shows the curve of this expression as a function of  $\theta$  together with a representation of the change in reflection density along the length of the powder pattern.

### 2. 3. Influence of Specimen Condition on Pattern Definition

The angular range,  $\Delta\theta$ , over which X-rays are diffracted by a set of crystal planes, spacing d, is governed by the number of planes N

which are stacked uniformly along the normal, and which contribute to reinforcement at Bragg angle  $\theta$  and cancellation at  $\theta \pm \Delta\theta/2$ . For values of  $N = 300$  and  $d = 1 \text{ \AA}$ , the resulting spread may be as large as  $2^\circ (2\theta)$ . As  $N$  exceeds 3000, however, 90 % of the diffracted radiation can be expected to lie within an angular range of  $0.2^\circ (2\theta)$ . The definition of the diffraction pattern is therefore determined to some extent by the crystallite size and the degree to which the presence of inelastic strains and chemical inhomogeneities in the crystallites disturb the regular stacking of reflecting planes.

Similarly, a powder specimen containing crystals above  $1 \mu$  in size tend to produce discontinuous powder rings. This effect is discounted for crystal sizes up to  $5 \mu$  by rotating the powder specimen in the X-ray beam to smooth out the individual reflections. It is enhanced, however, but the use of fine collimators such that the width of the X-ray beam approaches the mean size of the individual crystals. For crystal sizes beyond  $10 \mu$  a radial spread of the X-ray spots, leading to non-uniform broadening of the reflections, becomes evident. This is largely due to the effects of collimator geometry. In the case of non-monochromatic X-rays, it may also arise from the scattering of wavelengths within the spectral range but differing from those of the characteristic radiation (see section 2.5).

Optimum overall sharpness of the D - S pattern is afforded by crystallites with sizes between  $0.25$  and  $5 \mu$  in a strain-free condition. Departure from this condition has a particular bearing upon cell dimension measurements since line broadening clearly reduces the precision with which the diffraction angles can be determined. Specimen dependent line broadening is a function of diffraction angle, increasing as  $\theta$  increases. As a result, marked loss of pattern definition above  $40^\circ(\theta)$  is experienced for specimens which are either cold worked or comprise crystallites less than  $0.1 \mu$  in size. As will be described in the next section, the angular range above  $40^\circ(\theta)$  in D - S patterns is vital to the evaluation of reliable cell dimensions.

#### 2.4. Requirements and Problems of Powder Photography

Powder photography has two main applications in phase analysis, namely the identification of crystalline phases and the measurement of

the unit cell dimensions by which a phase is characterized. The main requirements for such work are good resolution and maximum sharpness of the pattern and a low background from unwanted components of the X-ray spectrum.

For the measurement of unit cell dimensions and angles, a guide to the precision of the measurement at different points on the pattern is given by differentiating the Bragg equation, whence

$$|\Delta d| = d \cot\theta \Delta\theta$$

Here  $\Delta d$  represents the random error in the measurement of  $d_{hkl}$  produced by a corresponding error  $\Delta\theta_{in}$  in the measurement of the Bragg angle.

Parish and Wilson [5] give curves (Fig 3) based on this expression for the percentage precision of  $d$  as a function of  $\theta$  for various values of the error  $\Delta\theta$ . The improvement in precision to be expected from measurements at high  $\theta$  is exemplified in the accompanying table constructed for a D - S camera of 11.46 cm diameter ( $l^o(\theta) = 2 \text{ mm(S)}$ , giving  $\Delta\theta = 0.005^o$  for a measurement error  $\sigma_s$  of 0.01 mm).

$\theta$	$ \Delta d/d  \cdot 10^3$
20	13.738
40	4.347
60	2.887
70	1.819
80	0.882
85	0.438

The random error is thus reduced to very small proportions at high Bragg angles and, using sophisticated methods for scanning the diffraction profile, accuracies of 1 part in  $10^6$  have been claimed. The measurements are open to systematic error, however, and for a number of reasons described briefly below and more exhaustively in ref. [6] it is rarely possible to achieve accuracies of better than 1 part in  $10^3$  from D - S films.

The main systematic errors in D - S measurements arise from diffraction in a cylindrical specimen which is ideally located at the exact centre of the recording circle. Divergence of the diffracted beam, ab-

sorption in the specimen and its eccentricity with respect to the recording circle all contribute to displace the diffraction peak to higher values of  $\theta$ . The effect diminishes with increasing  $\theta$  and mathematical expressions have been derived to permit correction of the D - S measurements for these  $\theta$  dependent errors (Taylor and Sinclair [7] and Nelson and Riley [8]). According to Cohen [9] the corrections are conveniently applied using the method of least squares, coefficients for the  $\theta$  dependent terms being derived from the analysis of a statistically suitable number of measurements. Accordingly, for hexagonal and tetragonal unit cells which are defined by two cell dimensions, the number of parameters to be determined is effectively doubled, necessitating a corresponding increase in the number of observations in order to maintain statistical accuracy.

As explained in 2.2, the D - S pattern attains maximum line density in the region  $40 - 60^\circ(\theta)$ . For non-cubic symmetries and CuK radiation, unit cells greater than 6 Å tend to produce line overlap in this region. At angles above  $60^\circ(\theta)$  small differences in cell dimensions produce appreciable changes in diffraction angle. Accordingly, for non-cubic cells, reflections may occur in a very different order to that expected on the basis of approximate cell dimensions. Clearly, in this region of the film the assignment of erroneous indices becomes increasingly possible.

Difficulties of a physical nature serve to reduce the definition of the pattern at successively higher angles. The effect of beam divergence,  $K\alpha$  doublet separation and the small but finite spread of  $\lambda$  about the value for the characteristic radiation all contribute to broaden the reflections. This broadening increases with  $\theta$ , the  $\alpha_1 - \alpha_2$  broadening affecting line definition at  $20 < \theta < 35$  while angular divergence and spectral spread exert their effects in the region  $\theta > 60^\circ$ . Specimen-dependent line broadening produced by micro-strains and sub-micron inhomogeneities is similarly marked in this angular range, as described in section 2.3, and careful treatment of the X-ray sample is necessary to optimize the sharpness of the pattern for precision measurements. Finally, thermal vibrations of the diffracting atoms lead to an attenuation of intensity, the effect becoming more pronounced with increasing  $\theta$ . For many organic materials, complexes and molecular

compounds, the effect of this temperature factor virtually eliminates all detail above  $50^\circ(\theta)$  in diffraction patterns obtained with  $\text{CuK}\alpha$  radiation.

Treated as a whole, the angular range above  $40^\circ(\theta)$  is seen to present considerable difficulties as regards the accurate location of the peak maximum for a given  $hkl$  reflection within the expected precision for the measurement. For the general, non-cubic case, there is, in fact, only a limited chance of obtaining reliable data from this region of the D - S pattern under routine conditions. There is, consequently, a very great risk that results obtained from reflections in the measurable part of the pattern will be severely affected by both random and systematic errors. To some extent the random error can be reduced by using a camera with a larger film radius but the effectiveness of this measure is limited by the increase in line width produced by beam divergence. Stricter collimation may be used to combat the effects of divergence but only at the expense of X-ray intensity and a useful exposure time. In any case, the sources of systematic error remain.

From the foregoing it is evident that a general purpose camera for powder diffraction work should overcome the principal limitations of the D - S camera. Thus, it should yield sharply defined reflections in the angular range up to at least  $45^\circ(\theta)$ . It should be capable of yielding good resolution, i. e. the effective camera diameter should yield at least  $2^\circ$  per mm film circumference. Finally the specimen should be ideally thin to minimize the systematic error produced by absorption.

In the following sections it will be shown that a carefully adjusted focusing camera of the Guinier type is capable of fulfilling these requirements.

### 2.5. Problems Associated with the X-ray Spectrum

A major contribution to the complexity of the powder pattern is the polychromatic character of the incident X-ray beam. The typical X-ray spectrum comprises a continuum of low intensity and characteristic peaks,  $\text{K}\beta_1$ ,  $\text{K}\alpha_1$ ,  $\text{K}\alpha_2$  etc. (Fig. 4) with wavelengths dependent on the nature of the element used as anode in the X-ray tube. For a copper anode  $\lambda\beta = 1.39217$ ,  $\lambda\alpha_1 = 1.54051$  and  $\lambda\alpha_2 = 1.54434$  Å.



In the instance of copper radiation, the above distribution permits the removal of the  $K\beta$  peak by absorption in a nickel foil. The intensity of the  $\alpha_1$  peak, however, is attenuated by roughly 45% in raising the ratio  $K\alpha_1/K\beta_1$  to 100/1 using such a filter. A narrow range of wavelengths about the combined  $K\alpha$  peak may be selected by transmitting the beam through balanced filters of Ni/Co foils. While useful in reducing the extent of background scattering due to the continuum, the discrimination achieved,  $\Delta\lambda = 0.12 \text{ \AA}$ , is insufficient to distinguish between the components of the  $\alpha_1\alpha_2$  doublet ( $\Delta\lambda\alpha_1\alpha_2 = 0.0038 \text{ \AA}$ ).

In the low-angle region of the D - S pattern, the  $\alpha_1\alpha_2$  doublet is unresolved. As  $\theta$  increases beyond  $20^\circ$ , however, reflections broaden as the  $\alpha_1$  and  $\alpha_2$  components separate in accordance with the requirements of the Bragg equation. In this angular region an estimate of diffraction angle corresponding to a particular value of  $\lambda$  may therefore be accompanied by a substantial error. Beyond  $\theta = 35^\circ$ , the spectral components of the reflections are resolved, thereby doubling the risk of overlapping and near coincidence in patterns of non-cubic materials.

## 2.6. Crystal Monochromatization

### 2.6.1. Parallel X-ray Beams

An effective method for isolating a narrow band of wavelengths from the X-ray spectrum utilises diffraction-reflection from a suitable face of a single crystal. The crystal is inclined at an angle to the primary beam so that for the wavelength selected, a set of strongly diffracting planes occupies the reflecting position in accordance with the Bragg condition. The principal weakness of the method is that only a fraction of the available X-rays is reflected, most being transmitted through, or absorbed in, the monochromator crystal. The practical application of crystal monochromatization therefore depends upon techniques for optimizing the diffraction conditions.

Diffraction from a plane crystal monochromator is depicted in Fig. 5a, the crystal surface being cut parallel to the reflecting planes. In Fig. 5b, the reflecting surface is cut at an angle,  $\alpha$ , to the diffracting planes. By this means an increase in beam density is achieved by shortening the view of the X-ray source. This tilted surface technique

is theoretically capable of yielding a nearly two-fold increase in intensity for a parallel beam. The gain is in fact limited to between 10 and 20 % by comparison with the plane-parallel method owing to intensity losses through extinction in the crystal.

Although the tilted surface effectively concentrates the primary beam, collimation, with attendant loss of intensity, is still necessary to obtain sharp definition, owing to the natural divergence of the primary X-ray beam. Curving the crystal serves, however, to focus the divergent beam and stringent collimation becomes unnecessary.

### 2.6.2. Geometrical Conditions for the Focusing of Divergent Beams

The principle of the focusing monochromator follows from the theorem that the chord of a circle subtends equal angles at all points on its arc. In Fig. 5c the divergent beam from source S is represented by two components which strike a reflecting curved surface at points A and B. This surface and the source lie on the same circle of radius R. If the components at A and B are reflected to yield the same angle,  $2\phi$  they will focus at point F, SF being the chord and SABF the arc referred to above.

In the simplest approach, due to Johann, the reflecting surface is a crystal cut in a direction parallel to a set of diffracting planes and curved to a radius of R (Fig. 6a). The diffracting condition is only fulfilled, however, when S, O and F lie on the surface of a circle of radius R/2; the crystal is accordingly only tangential to the focusing circle at O. The source is thus not clearly defined with respect to the diffracting surface and the focus has a width dependent upon the length of crystal irradiated, i. e. upon the positions of S and O relative to the focusing circle and the caustic circle, to which all diffracted rays are tangential.

The aberrations inherent in the Johann crystal are eliminated in the geometry due to Johansson. Here the diffracting surface of the crystal is first ground to a radius of 2R and then curved, by the application of pressure, to the radius R of the focusing circle (Fig. 6b). As in the case of the Johann crystal S and F are symmetrical about the point O about which the crystal is ground and bent. The angle  $\phi = \pi/2 - \theta$  and the source-crystal and crystal-focus distances are thus

$$SO = OF = 2R \sin \theta$$

Substituting  $\lambda/2d = \sin \theta$  from the Bragg equation these distances are seen to correspond to  $R\lambda/d$ .

Guinier [10] advises the use of an asymmetric version of the Johansson crystal to allow a greater crystal-focus separation, thus increasing the available working space while maintaining a short source-crystal separation (Fig. 7a). For this purpose the crystal is ground at an angle  $\alpha$  to the diffracting planes and the critical distances become

$$SO = 2R \sin (\theta - \alpha)$$

$$OF = 2R \sin (\theta + \alpha)$$

### 3. PRACTICAL CONSIDERATIONS

#### 3.1. Guinier Focusing Geometry

A powder specimen placed in the X-ray beam reflected from a curved crystal monochromator should give a pattern which is sharply defined along the circumference of a circle containing the powder specimen and the focus of the incident beam. The main requirement here is that the specimen should be infinitesimally thin. If film is used to record the pattern, it too should comply with this requirement, double coated film being stripped of emulsion on the side furthest from the specimen to avoid diffuse and staggered patterns.

In the symmetrical arrangement (Fig. 7b) the incident beam, normal to the plane of the specimen, forms a diameter of the recording circle. The expression for  $S$ , the diffraction interval along the circle, is then  $\pi R \theta / 45$ , an improvement by a factor of two over the resolution in a D - S camera of the same radius.

The main limitation of the symmetrical Guinier arrangement is the small angular range, roughly  $30^\circ(\theta)$ , which can usefully be recorded. For radiation containing both  $\alpha_1$  and  $\alpha_2$  components, there is, moreover, an asymmetry in the pattern due to differences in the way these peaks become separated on either side of the primary beam. Thus in the primary beam itself, the  $\alpha_2$  component is reflected from the crystal with a slightly greater Bragg angle (smaller  $\theta$ ) than the  $\alpha_1$  component. In

subsequent diffraction at the specimen surface, those rays taking a direction which is generally parallel to that of the beam striking the monochromator, experience a focusing effect as, with increasing  $\theta$ , the  $\alpha_2$  peaks first converge on, and then cross over the  $\alpha_1$  peaks (Fig. 8a). The effect is to produce reflections which are broad by comparison with the primary focus, resolution of  $\alpha_1$  and  $\alpha_2$  occurring at about  $25$  to  $30^\circ(\theta)$ . For X-rays reflected in the antiparallel direction on the other hand, the  $\alpha_1 - \alpha_2$  separation observed at the focus is further increased along the circumference of the recording circle as  $\theta$  increases (Fig. 8b). By comparison with the parallel direction, reflections on this side of the focus are sharper unless the pattern is of such complexity that  $\alpha_2$  peaks begin to merge with the  $\alpha_1$  peaks of neighbouring reflections.

An asymmetrical setting of the film cassette (Fig. 8) permits the recording of diffraction patterns up to  $45$  or  $50^\circ(\theta)$  depending upon the departure from  $90^\circ$  in the angle  $\zeta$ , between the monochromatic beam axis and the tangent to the recording circle. Whether the cassette is located in the parallel or antiparallel position is a matter of choice dictated by a consideration of the influence of the  $\alpha_1 \alpha_2$  separation on the sharpness, as opposed to the overall resolution, of the pattern.

### 3.2. The Monochromator Crystal

Elimination of the  $K\beta$  component from the X-ray beam is fairly easily achieved. The difference between the wavelengths of the  $K\alpha$  and  $K\beta$  components is such that a simple setting of the monochromator crystal to the angle prescribed by the Bragg condition is generally effective. In the instance of focusing monochromators discrimination is assisted by the requirement for wavelength-dependent distances between source, crystal and focus. These distances are so very different for the  $K\alpha$  and  $K\beta$  components, however, that a precise setting is not essential.

Discrimination between the components of the  $K\alpha$  doublet is clearly more difficult in view of their closely similar wavelengths. The main requirement is for an accurately defined focusing geometry. Otherwise the attenuation of the  $\alpha_1$  component will be too great when the angle of the crystal is adjusted to eliminate  $\alpha_2$ . Factors affecting the definition of the focusing geometry are the width of the X-ray source and the mosaic spread in the monochromator crystal. These, if too large, limit

discrimination. Alternatively a crystal which is too perfect, although offering good discrimination, yields a much weakened monochromatic beam owing to extinction effects.

A variety of materials have been tried in curved crystal monochromators for X-ray work. A compilation has been prepared based on the properties of the monochromatised beam, which should be strong with only a small width, and those of the crystal which should be physically and chemically stable, contain a low concentration of imperfections and be capable of being formed to the required curvature [11].

Quartz, cleaved parallel to  $(10\bar{1}1)$ , has traditionally been employed in Guinier cameras, owing to its good elastic properties and high discriminatory power. The main drawback is the relative weakness of the diffracted beam.

Ideally imperfect crystals should contain small mosaic blocks of  $10^{-3}$  mm size misoriented by not more than a few minutes of arc in order to minimize extinction. An approach to this condition in quartz crystals is made by subjecting them to an elastic stress; the reflected intensity can thus be increased by a factor of up to 20 [12]. The reflectance may also be increased by gently abrading the crystal face with a soft lead pencil to introduce a surface mosaic.

Oriented pyrolytic graphite appears to be superior to other materials as regards reflecting power; it gives a roughly fifteen-fold increase in the intensity of  $\text{CuK}\alpha$  radiation by comparison with quartz according to calculations by Renninger [13]. For a beam divergence which is less than the mosaic spread of the graphite the diffracted intensity is as much as 50% of the incident intensity for  $\text{CuK}\alpha$  radiation [14]. The main drawback to the use of pyrolytic graphite is the relatively high mosaic spread in the material, generally of the order of  $0.4^\circ$ , which severely limits peak resolution. Reduction of this spread by a factor of five or six is necessary before graphite can be considered suitable for Guinier camera application.

The quartz crystals employed in the cameras constructed at Atomenergi were manufactured by Messrs. A. Jobin and G. Yvon, 26 rue Berthollet, Arcueil (Seine), France. The specifications are for a quartz lamina with dimensions Length = 35 mm, Height = 15 mm, Thickness = 0.3 mm with H parallel to  $[010]$ . The face LH is cut at  $\alpha = 3^\circ$  to the

(10 $\bar{1}$ 1) set of crystal planes and ground to a radius of 500 mm (2R), the cylinder axis being parallel to H.

The lamina is mounted in a curved press which on tightening bends the crystal to the required radius of 250 mm. The press is mounted at the specified distance SO from the anode of the X-ray tube, O being the point about which the press is rotated to select the required wavelength. For use with a Cu anode the critical distances and angles for the three main spectral components are as follows, calculated on the basis of  $d_{10\bar{1}1} = 3.344 \text{ \AA}$ ,  $\alpha = 3^\circ$  and  $R = 250 \text{ mm}$ .

	$K\beta_1$	$K\alpha_1$	$K\alpha_2$
$\lambda(\text{\AA})$	1.39217	1.54051	1.54434
$\theta^\circ$	12.019	13.321	13.355
SO ( $D_1$ ) mm	78.4	89.6	89.9
OF ( $D_2$ ) mm	129.6	140.5	140.8

Experience shows that in fact quartz crystals generally exhibit departures in  $D_1$  and  $D_2$  from these figures, probably owing to variability in the angle  $\alpha$ . Thus for the instruments described here the  $D_1$  distances are 91 and 88 mm. Such departures are of little significance, however, as long as  $D_1$  does not exceed 100 mm and  $D_2$  is not less than 130 mm. A method for locating the crystal at the distance from the anode appropriate to the real values of  $R$  and  $\alpha$  is given in section 4.3b, based on the account given in ref. [10].

### 3.3. Mounting the Crystal

The crystal is supported in the press, A (Fig. 9) comprising two brass blocks with a cylindrical interface of radius 250 mm (R). The two halves of the press are drawn together by four spring-loaded bolts, B, until the lamina assumes the curvature of the interface. The crystal planes are now cylindrically curved with radius R. Care should be taken in drawing up the screws to avoid uneven pressures which might crack the fragile lamina. To this end, crystal and press surfaces are first washed free of dust particles with alcohol. In addition, a seating for the lamina can be improvised from a length of sellotape pressed against the

surface of the concave block, C, parallel to the lower edge. Resting the lamina on this thin edge ensures a common orientation for the cylinder axes of press and crystal during the tightening of the bolts.

The press is then mounted on plate D, which extends into an arm normal to the cylinder axis. This plate is, in turn, located on slide E which permits lateral translation of the crystal axis with respect to the primary beam. The stability of the alignment and, therefore, the performance of the camera as a whole, depends ultimately on the means used to unite slide and press, remembering that free rotation of the press is necessary to bring the crystal into the reflecting position. The device used here is that of a hollow, conical pivot, F, mounted on the underside of plate D and threaded to receive set screw G. Pivot F slots into the conical hole in slide E, the set screw being drawn up against the tension of spring H until the two surfaces of slide and plate are in firm contact. Experience shows that with lubricated surfaces, rotation of the press is smooth without being disturbed by rocking about the pivot axis.

The slide is now inserted into V-block I, and fastened in position, temporarily, with one of the fibre screws, J. The V-block, I, is located on the base plate of the camera with the help of pivot K and two bolts passed through the slotted holes L. These slots afford a limited rotation of  $3^\circ$  for the V-block, permitting a preliminary setting of the monochromator in accordance with the take-off angle selected for the primary beam axis.

#### 3.4. The X-ray Source

The use of a quartz crystal for discriminating between the  $\alpha_1$  and  $\alpha_2$  components of the X-ray spectrum is enhanced by the use of a fine focus X-ray source. In this respect the introduction of fine focus tubes in the early 1960's is to be regarded as a vital step in the application of Guinier cameras for routine X-ray analysis. These tubes are preferably used in the line focus orientation, the cylindrical axis of the crystal being parallel with the image of the filament on the anode of the tube. In this position, the Philips FF tube (Copper anode PW 25633/62) used with the Atomenergi cameras affords a line image which is 8 mm long

and 0.02 mm broad viewed at an angle of  $3^{\circ}$  to the plane of the anode. In addition to providing a more sharply defined camera geometry, such tubes afford X-ray beams which are less subject to air scattering than normal focus tubes. Experience shows, however, that setting up the monochromator and cassette with a fine-focus tube is a more critical operation owing, presumably, to the reduced tolerance in the SO and OF distances imposed by the sharp definition of the source.

In this connection, the mechanical stability of the X-ray tube shield with respect to the focusing camera is an important factor as regards long term performance. Brackets for mounting the tube shield in a horizontal direction are particularly susceptible to mechanical vibration. In the present case it became necessary to insert extra supports between the tube shield and the bench bearing the cameras. In this way mm-size variations in the height of the X-ray tube window, which had previously been encountered, were eliminated.

#### 4. SETTING UP THE CAMERA

##### 4.1. Component Parts

The interior of the Guinier - Hägg camera is depicted in Fig. 10. The component parts are mounted on a base plate, I, located inside a heavy-duty steel casing, II, with the help of three levelling screws, A, B and C, seated on a slot, a V and a plane respectively. The casing is mounted within a framework of flat rails III which permit translocation of the camera parallel to the X-ray tube axis. The casing may be locked in position by tightening a pair of setting screws K1, K2 against the front and rear walls; K1 may be fitted with a dial for precise setting.

Resting on the base plate are the monochromator assembly, IV, comprising crystal press and slit system, and the sample-holder/cassette assembly, V, mounted on a common plate U. This assembly, V, consists of a circular specimen holder, E, and its associated slit system, the film cassette, F, and the specimen rotating mechanism, G. The cassette is positioned with three legs on its own moveable plate, H, permitting adjustment with respect to the specimen surface so that the requirement of tangentiality with the focusing circle can be met.



#### 4.2. Preliminary Steps

- a) With the base plate resting on the bench, check that there is a common height above the plate for the mid-points of monochromator, sample holder, cassette window and the associated slit systems.
- b) Locate the cassette in its approximate position with the help of plate H; a line at  $30 - 40^\circ$  to the plane of the specimen should coincide with the line scored in the top of the cassette, passing from window to primary beam stop. The required distance from the specimen surface can be gauged with the help of a thin rod, cut to match the true cassette diameter. This is held inside the cassette with plasticine so that it coincides with the diameter normal to the window through which it projects. On completion of this adjustment the triangular plate, H, is secured in position (see, however, 4.5.f).
- c) The approximate height of the base plate above the floor of the casing is obtained as follows. With the base plate removed the X-ray beam is admitted through the entry port of the casing and its vertical extension is registered on a piece of fluorescent (ZnS) screen mounted in plasticine. The mid-point of this extension is noted with respect to a set of horizontal lines scored in the surface of the screen and its height from the floor of the cassette is then measured.

The levelling screws A, B and C are now adjusted until the midpoint of the monochromator press is at the same height from the bench top as the midpoint of the X-ray beam from the floor of the casing.

#### 4.3. Adjustment of Monochromator (Sample Assembly Absent)

- a) The primary (monochromator) slits are removed from the base plate which is then seated inside the casing. A piece of fluorescent screen is set up to register X-rays transmitted through the crystal and, with the X-ray tube operating at half power, the casing is translated past the open window until a broad, luminous area is seen on the screen.

With the crystal bathed in the primary beam, a shadow, due to absorption, is visible on the screen. Throughout the subsequent stages

of adjustment, this shadow should be maintained at the center of the illuminated field. This ensures that the rotation axis of the crystal lies on the primary beam axis (see Fig. 7a).

- b) While there are clearly two alternative ways of orienting the crystal in the press, only one is valid owing to the asymmetrical alignment of the  $(10\bar{1}1)$  planes relative to the cylinder axis. The prevailing orientation is determined by slowly rotating the press through its angular range and examining the effect on a fluorescent screen, the tube being operated at full power. The incorrect orientation is characterised by the appearance on the screen of a series of thin, bright lines. Removal of the press from its mounting plate, D, and inversion will now yield the correct orientation as demonstrated by the appearance of one or two bright bands on the screen during rotation of the press.
- c) Starting with the arm of the monochromator assembly pointing inwards towards the X-ray anode, rotation away from the tube (increasing  $\phi$ ) should yield in turn a bright and a dull, luminous band. These are the  $\alpha$  and  $\beta$  components of the X-ray spectrum which are separated by a roughly  $1^\circ$  rotation of the press for CuK radiation.
- d) If the X-ray source is correctly located on the circle defined by the curved crystal, the  $\alpha$  and  $\beta$  areas will be formed in turn by the coalescence of two separate bands. These move symmetrically towards each other as the wings of the crystal approach the circumference of the circle. This can be understood from Fig. 11. On passing through the reflecting angle, the fluorescent bands meet and then vanish promptly in a vertical direction as the near edge of the crystal passes into, and the far edge leaves the focusing circle. This is the condition to be aimed at for correct location of the crystal.

The presence of only one fluorescent band or the asymmetrical movement of two bands indicates that the distance between the X-ray source and the axis of crystal rotation departs from that specified for focusing (see section 3.2.). Thus, if the beam source lies outside the focusing circle the greatest movement of the fluorescent bands is towards the anode of the tube for a corresponding crystal rotation.

The press assembly is translated sideways by steps of 0.5 mm in the appropriate direction and the movement of the fluorescent bands re-examined at each interval until the axis of rotation is correctly located on the focusing circle.

- e) More serious departures from ideal focusing are indicated by striations and irregularities of the luminous area. These may arise from non-uniform stresses in a crystal clamped unevenly in the press, or from a crystal seated so that the cylinder axis does not coincide with the axis of the press. The press should be loosened slightly and the luminous field re-examined. If there is no improvement, slight rotations of the crystal in the plane of the press can be tried.
- f) Assuming that a broad (5 - 8 mm) band can be obtained on the screen placed one cm from the crystal, focusing of the reflected beam can be examined by moving the screen along the beam axis. With the screen normal to the axis, a fine intense line should be obtained at roughly 140 cm (for  $\text{CuK}\alpha$ ) from the monochromator axis. Inclination of the screen to the beam axis should resolve the  $\alpha_1\alpha_2$  doublet, the weaker  $\alpha_2$  component being nearer the front of the casing (smaller  $\phi$ ).

The crystal may now be locked in position, the fine-threaded screw N (Fig. 8) being used to set the angle of the press against the tension of the retaining spring, M. If the application of tension leads to any asymmetry of the luminous field it can be concluded that the press is too loosely seated and that screw G, on the underside of the slide, needs tightening. Before removing the slide, note its position in the V-block.

WARNING - Owing to the narrowness of the spot in fine-focus X-ray tubes, adjustment of the monochromator is exceedingly sensitive and with a good crystal, rotation of the press by a few seconds of arc separates the ideal setting from a non-reflecting position. Play in the moving parts of the monochromator is not permissible, nor is careless handling of the equipment during adjustment. The fine-focus beam is a particular hazard and hands should be kept clear when the beam is admitted into the casing.

A further danger is associated with the scattering of secondary radiation from the component parts of the camera, in particular the monochromator. Exposure to this radiation during the adjustment phase can be minimised by laying a plate of lead glass over the open camera when inspecting fluorescent pictures of the X-ray beam. On completion of the adjustment, the monochromator should be covered over with a housing of lead foil carrying a single exit slit, 10 mm square, for the monochromatised beam.

#### 4.4. Adjustment of the Sample-Film Cassette Assembly

- a) The primary slits, P, (Fig. 8) are screwed to the base plate, the vertical elements, Q, being opened to the fullest extent. With fluorescent screens in place, one to receive the primary beam and a second to receive the monochromatized beam, the horizontal elements are moved together with forceps until, on the first screen, only the shadow cast by the crystal remains.

If the luminous field on the second screen exhibits irregular edges, these can be eliminated by further closing the horizontal slits.

The monochromatized beam is now defined sufficiently to permit of setting up the sample holder.

- b) The sample-holder cassette assembly (slits removed) is set roughly in position so that the beam makes an angle  $\zeta$  of  $60 - 40^\circ$  with the plane of the sample holder. With a specimen of ZnS in the sample holder, the assembly is manoeuvred in the focusing beam until a vertical fluorescent band appears centrally on the specimen. Maintaining this condition, the cassette is positioned with the primary beam catcher, J, (Fig. 8) open and the metal shutter, L, removed. With a fluorescent screen in place of the film, the passage of the monochromatized beam through the cassette is checked, making small angular displacements of the assembly about the specimen axis. When the beam has been located centrally in the aperture of the catcher, the distance D2 may be set up, moving the assembly along the beam axis.
- c) The assembly is secured in its approximate position by bolts passing through guide slots cut in the supporting plate. A millimetre

scale is fastened against the edge of the assembly plate, parallel to the beam axis.

A standard specimen of lead nitrate (cubic,  $a_0 = 7.856 \text{ \AA}$ ) is next mounted in the camera and with film in the cassette an exposure of fifteen minutes is given. The primary beam is recorded in under two seconds with the tube operating at 12 kV and 6 mA. After developing the film, the sharpness of the reflections is examined at X 20 magnification.

- d) The assembly is moved along the beam axis in steps of 1 mm and patterns recorded at each step. With the assembly at the position yielding the sharpest pattern, the secondary (sample holder) slits, T, are inserted and the fluorescent specimen replaced. The vertical slits are closed until the luminous area is roughly 2 mm in height and distributed symmetrically in the vertical sense about the specimen centre.

The horizontal slits are now closed until they just graze the monochromatized beam (ZnS dusted along the edges of the slits serves to indicate their proximity to the beam). The slits may be closed in steps of 0.1 mm, with 15 minute exposures between each step: diffuse bands recorded on the film as a result of diffraction from the metal edges indicate too close a setting.

The luminous area at the centre of the fluorescent specimen should have a horizontal extension of  $\sim 1$  mm on either side of the centre point.

#### 4.5. Final Adjustment

- a) The above steps should yield a sharply defined pattern of lead nitrate over the whole  $\theta$  range. If the pattern is unsatisfactory, however, the position of the assembly along the beam axis should be re-examined with a series of 0.1 mm adjustments and 15 minute exposures. Failing this, the horizontal components of the primary slits may be closed to obtain a narrower beam, thus irradiating a smaller area of crystal.

- b) Curved tails at the top and bottom of low angle reflections are due to vertical divergence in the primary beam arising from the line focus of the X-ray tube. These are minimized by further closing the vertical elements of the secondary slits or, failing this, the primary slits.
- c) Non-parallel reflections in the pattern of the standard substance arise through a non-parallel condition of the base plate with respect to the primary beam. This effect may be examined by inserting shims under the edges of plate U in turn and recording pairs of patterns which are then placed bottom edge to top edge for comparison. When the correct inclination of the base plate has been found, the appropriate levelling screws are adjusted and the shims removed from beneath the assembly plate.
- d) Extinction of the  $K\alpha_2$  component is achieved by increasing the angle between the tube axis and the monochromator arm. The correction required is only about 2 minutes of arc for CuK radiation and should be followed with the aid of 15 minute exposures of the lead nitrate specimen. An approach to the correct condition is marked on the fluorescent screen placed about 2 cm from the crystal by a slight, barely visible, separation between the two luminous bands described in 4.3 c. Over-correction quickly leads to loss of X-ray intensity.
- e) The diffraction patterns of  $Pb(NO_3)_2$  obtained with  $CuK\alpha_1$  radiation should exhibit little or no background darkening after a thirty minute exposure. It is most probable, however, that the low angle region of the photograph will be heavily blackened owing to the presence of parasitic radiation scattered at the monochromator. Removal of this radiation is achieved by inserting shutter S (Fig. 9, 10) into the monochromator press until it just grazes the beam diffracted from the wing nearest to the X-ray tube. This position is found by examining the effect on a fluorescent screen as the shutter is pushed in.
- f) If it is observed that on moving the cassette-specimen holder assembly towards the monochromator, a region of maximum sharpness passes along the pattern, the position of plate H with respect to the specimen holder should be re-examined.

Non-linearity of the relationship between film measurement and diffraction angle arises through missetting of the specimen holder with respect to the recording circle as defined by the diameter of the cassette. Some observations made in connection with this effect are given in 6.3.2.

Measurement of a number of sharply defined patterns of a standard substance can be used to derive an average value for the camera constant defined by

$$\bar{K} = \frac{1}{n} \sum_{i=1}^n \theta_i / S_i$$

Slight adjustments to the separation of the cassette from the specimen holder and to the angle  $\zeta$  (4.4 e) can be used to follow the variation of  $K$  with  $\theta$  until a relationship has been obtained which is as nearly linear as possible (see section 6.3.1.).

NOTE - As originally designed, the Guinier - Hägg camera was operated in vacuo to eliminate background darkening due to the scattering of X-rays by air. Experience so far indicates that this precaution is unnecessary, at least for exposures with a fine-focus tube and  $\text{CuK}\alpha_1$  radiation. The heavy steel lid to the camera, essential for vacuum operation, has therefore been replaced by a light-weight cover of opaque plastic. There is, accordingly, less risk of disturbance to the critical adjustment of the monochromator from vibrations, which are unavoidably generated on closing the camera with a heavy metal cover. The beryllium window, through which the primary beam was originally admitted into the camera, has also been removed.

It should be pointed out, however, that the camera design is particularly suitable for vacuum operation, a feature which is essential to powder photography with longer wavelength radiation, such as  $\text{CrK}\alpha$ .

## 5. EXAMINATION OF POWDER SAMPLES IN THE GUINIER - HÄGG CAMERA

### 5.1. Specimen Treatment

Normally, powder patterns are obtained from specimens dusted onto an adhesive plastic tape stretched over a thin brass diaphragm. Care

should be taken to obtain a thin ( $<30 \mu$ ), uniform layer of powder to ensure X-ray transparency and the sharpest possible definition for the focused reflections. A simple rule of thumb is that, with the brass diaphragm held up against the light, the powder sample, crushed to  $>200 \#$ , should still transmit light without appearing unduly patchy in a 2 x 2 mm central region.

Due to the monochromatic character and focusing of the X-ray beam, uniformly smooth reflections are obtained with crystallites having sizes appreciably greater than those tolerated in a D - S specimen. This is clearly demonstrated in the patterns of  $\text{BaCl}_2 \cdot 2\text{H}_2\text{O}$  shown in plate II. The D - S pattern exhibits marked graininess due to diffraction from crystallites larger than  $20 \mu$ . For the same specimen treatment the G - H pattern is comprised of the customary sharp reflections. In this connection it has been possible to obtain sharp G - H patterns from thin alloy foil specimens which, after heat treatment demonstrated crystal sizes of 40 - 50  $\mu$ .

Crystalline samples in the form of well developed needles constitute the most serious hazard as regards irregularity of the specimen, since a fraction of the needles will tend to "hedgehog" from the surface of the tape producing streaky and uneven reflections. While smoothing the sample with a fine spatula achieves uniformity, the powder will tend to exhibit preferred orientation with a consequent weakening or even extinction of some reflections and artificial strengthening of others. A laborious but effective method of combating this phenomenon is to mix the powder with a small quantity of a plastic cement which becomes brittle on drying. Regular cleavage is not a property of such material and crushing in a mortar will reduce the brittle mass to irregularly shaped fragments.

A tape recommended for use in sample preparation is marketed by 3Ms under the trade name Magic Mending Tape. This has a base which retains its planarity on stretching and gives a low background, uniform over the whole  $\theta$  range even on prolonged (4 hour) X-ray exposures.

## 5.2. Encapsulated Materials

Materials sensitive to moisture or air (deliquescent, hygroscopic or pyrophoric compounds) or materials with which a health hazard is associated, can be handled in thin plastic envelopes, circularly shaped to fit the specimen holder.



Powder is first dusted over an area of tape and a circle of 3 mm radius is punched out. The circle is then inserted, with the help of forceps, into a bag of thin transparent plastic, the specimen being maintained in a planar condition by feeding it through a wide-bore, glass or perspex tube. The specimen is then sealed in with an annular weld, at least 3 mm wide, taking care not to heat the powder-coated area. (If HF heating is employed to make the weld, the specimen can be positioned between two recessed metal formers, the powder-coated area being located within the recess.) A disc of appropriate diameter can now be punched from the sealed envelope and mounted between two brass diaphragms for exposure in the focusing camera.

Guttagea foil, from which the envelopes can be prepared, is obtainable from Kalle AG, Wiesbaden-Blebrich, Germany. Plastic of thickness 0.08 mm, (grade T62 transparent, glossy) is sufficiently durable to be formed into large bags from which envelopes for a number of specimens may be prepared. Exposure times are roughly trebled with this material and, as might be expected, diffuse bands appear in the low-angle area of the diffraction pattern. General background scattering is not significantly increased, however.

The G - H method is not ideal for the most chemically unstable materials since it demands a specimen in the form of a thin film which implies the existence of a large surface area for the air- or moisture-sensitive powder. For this reason it is essential to preserve lengths of tape, stretched on perspex blocks, and small plastic bags, dilated on wire cages, in the dehydrating atmosphere of a vacuum desiccator.

### 5.3. Fluorescent Specimens

All materials fluoresce, to some extent, on irradiation with X-rays giving rise to a background continuum upon which the diffraction pattern is superimposed. Strict monochromatization affords almost complete elimination of this background except for materials containing elements excited by the chosen X-ray component. One solution to this problem is to replace the film with a scanning electronic detector fitted with a second monochromator. A simpler solution consists in screening the diffracted radiation through a thin aluminium foil inserted in the window of the film cassette, a narrow opening being left to permit passage of the primary, monochromatized beam. Foil of 0.03 mm thickness is completely effective with compounds of the rare-earth and actinide elements and even permits photography of patterns from iron- and cobalt-

containing compounds with  $\text{CuK}\alpha_1$ . Exposures are increased roughly two-fold and the high-angle reflections are disproportionately weakened by absorption in the foil.

## 6. EVALUATION OF THE GUINIER - HÄGG CAMERA AS AN ANALYTICAL INSTRUMENT

### 6.1. Exposure Times and General Sensitivity

A G - H camera, properly adjusted for the focusing of strictly monochromatic  $\text{CuK}\alpha_1$  radiation, gives high quality powder patterns over the full recording range up to  $45^\circ(\theta)$ . The photographs reproduced in plates I and II are representative of the patterns of well crystallised materials examined in these laboratories during the past three years. The D - S patterns of the same materials, reproduced for comparison purpose, were obtained using the line focus of the same type of fine focus X-ray tube.

It will be seen that even with  $\text{K}\alpha_1$  radiation alone the exposure time for a Guinier pattern is roughly one sixth of that for the corresponding D - S pattern. Moreover, the G - H pattern is roughly ten times more sensitive to the detection of weak reflections, owing to a combination of the greater intensity of the incident beam in relation to the area of sample irradiated, the focusing of the diffracted rays and the low rate at which the peak/background ratio falls with exposure time.

Independently of the type of camera employed, specimens with a high transparency to X-rays and a composition based on strongly scattering atoms can be expected to yield the shortest exposure times. This is the case so long as the available diffracted intensity is concentrated to a small number of reflections as in the cubic phases tungsten and the dioxides of uranium or thorium. With increasing pattern complexity, exposures lengthen and it may be necessary to overexpose the principal reflections in order to reveal the fainter lines, if these are of significance. This is often the case, for example, in phase analysis.

For X-ray film, the blackening curve is roughly linear, the intensity of a reflection increasing proportionally with time. If the first visible evidence of a reflection is taken to represent an intensity of one, the maximum registerable intensity is of the order of 180. Beyond this

point, the reflections only increase in width. Below are listed some typical minimum and maximum exposure times between which G - H patterns have been fully registered without demonstrating line broadening due to over-exposure. The film used was Ilford Industrial G which affords a good balance between speed and line definition. The patterns were obtained with  $\text{CuK}\alpha_1$  radiation.

Specimen	No. of reflections	Min. time (mins)	Max. time (mins)
Silicon	6	10	25
Black P	18	30	90
$\text{Pb}(\text{NO}_3)_2$	19	8	20
$\text{UO}_2$	9	<5	15

As an extension of this study, the sensitivity of the G - H camera in phase analysis was tested by photographing various mixtures of well crystallised  $\text{UO}_2$  and  $\text{ThO}_2$  which have comparable scattering properties for X-rays. The samples were made up by first ball milling the powders in a weight ratio for  $\text{UO}_2/\text{ThO}_2$  of 10/1. This mixture was successively diluted with further additions of  $\text{UO}_2$  and ball milled to ensure homogeneity. In this way 500 g mixtures of  $\text{ThO}_2$  in  $\text{UO}_2$  were obtained at dilutions of 1 %, 0.5 %, 0.1 %, 0.05 % and 0.01 %. The samples were exposed in the focusing camera and the times taken to register the 111 and 200 reflections of  $\text{ThO}_2$  were recorded. Specimens of these mixtures were also exposed in a powder diffractometer in order to provide a control of the peak heights of the 111 reflections from both  $\text{ThO}_2$  and  $\text{UO}_2$ . For this purpose the 111 peaks and the adjacent backgrounds at  $\pm 4^\circ$  ( $2\theta$ ) were also step-scanned using a step length of  $0.02^\circ$  ( $2\theta$ ).

Dilution  % $\text{ThO}_2$ in $\text{UO}_2$	Guinier-Hägg-patterns		Powder diffractometer			
	Exposure times (minutes) in which principal $\text{ThO}_2$ reflections are visible		Peak height counts for 111 reflections in		Peak ratios $\frac{111 \text{ ThO}_2}{111 \text{ UO}_2}$	Background counts
111	200	$\text{ThO}_2$	$\text{UO}_2$			
1	30	120	2150	22056	0.97	158
0.5	60	200	2325	45789	0.51	289
0.1	200	950	842	88956	0.9 <sub>5</sub>	589
0.05	950	Not visible	385	87601	0.4 <sub>3</sub>	600
0.01	Not visible	Not visible	Not visible	90010		610

From the above results it is clear that for phases of comparable scattering power, the detection of one component of a phase mixture is guaranteed at the 1 % level for a normal G - H pattern exposure. For prolonged exposures, detection is possible at the 0.1 - 0.05 % level. The sensitivity is in this respect comparable to that obtained in a powder diffractometer operated under step-scan conditions, with the difference that the diffractometer result is quantitative. In both instruments the 0.01 % dilution yields no visible trace of the weaker phase owing to interference from the background. These results are comparable to those obtained by Parrish and Taylor for diffractometer scans of silicon in LiF [15].

In less favourable cases where the minor phase scatters more weakly or is in a poorly crystalline condition the sensitivity of the X-ray method is clearly reduced and contents as high as 10 - 20 % may be undetectable.

## 6.2. Treatment of Diffracted Intensities

By comparison with the powder diffractometer, the G - H camera is a generally less satisfactory instrument for recording diffracted intensities, largely owing to the limitations of the photographic method. The sharpness of the focused reflections necessitates scanning by a microdensitometer which provides a light beam of 0.5 mm maximum width or even smaller. This requirement is in conflict with the need to employ as large a slit width and height as possible in order to minimize the effects of film graininess. Possible solutions to this problem are

- a) to defocus the X-ray beam slightly by displacing the specimen from the plane tangential to the film circle. The loss of resolution consequent upon the resultant broadening of the reflections could be compensated by using a film cassette of 50 % greater radius.
- b) to replace the film by a step-scanning proportional detector, fitted with a  $1^\circ$  receiving slit which moves along the focusing circle.

The correction of intensities recorded with monochromatic radiation must take account of the polarization of the incident beam by the monochromating crystal. The combined Lorenz, polarization, oblique

incidence and absorption corrections have been given by Hägg [16] as follows:

$$M = \frac{1 + \cos^2 2\theta_m \cos^2 2\theta}{\sin^2 \theta \cos \theta} \cdot \frac{1}{\cos(2\theta - \alpha)} \cdot \exp\left(-\frac{\mu t}{2\theta \cos(2\theta - \alpha)}\right) \\ \left[1 - \exp\left(\frac{-\mu_f h}{\cos(2\theta - \alpha)}\right)\right]$$

where

- $\theta$  = Bragg angle for reflection  $hkl$
- $\theta_m$  = glancing angle for monochromator crystal ( $13.21^\circ$  for  $\text{CuK}\alpha_1$  and quartz  $10\bar{1}1$  planes)
- $\alpha$  =  $90 - \zeta$  = angle between axis of monochromatic beam and normal to plane of specimen
- $\mu$  = absorption coefficient of specimen
- $\mu_f$  = absorption coefficient of film emulsion
- $t$  = thickness of specimen
- $h$  = thickness of emulsion layer

For thin specimens and high to medium X-ray transmission the above expression can be approximated to

$$M = \frac{1 + \cos^2 2\theta_m \cos 2\theta}{\sin^2 \theta \cos \theta} \cdot \frac{1}{\cos(2\theta - \alpha)}$$

The relationship between the observed Guinier intensity and the structure factor is in any case given by

$$I_{\text{Obs}} = C \cdot M \cdot p \cdot |F_{hkl}|^2$$

where

- $I_{\text{Obs}}$  = observed intensity
- $C$  = proportionality constant depending upon exposure time for a given specimen
- $M$  = trigonometrical factor defined above
- $p$  = multiplicity factor for the set of  $hkl$  planes
- $F_{hkl}$  = structure factor

An account of the solution of the  $\text{Sr}(\text{OH})_2 \cdot \text{OH}$  and  $\text{Sr}(\text{OH})_2$  crystal structures using G - H intensity data will be given separately.

### 6.3. Pattern Definition, Calibration and the Measurement of $\theta$

#### 6.3.1. Precision of Film Measurement

The G - H film cassette records the powder pattern only up to  $45 - 50^\circ$  ( $\theta$ ). Although, as indicated in section 2.4, this angular region is not ideal as regards the precision for obtaining  $d_{hkl}$ , the loss by comparison with high angle ( $>60^\circ$  ( $\theta$ )) D - S measurements is largely offset by the greater ease with which intensity maxima are located. Thus the film geometry of the G - H camera gives a relationship between the Bragg angle and the film measurement S of

$$(\theta/S)_{G-H} = 45/\pi R \text{ deg arc mm}^{-1}$$

For D - S film geometry

$$(\theta/S)_{D-S} = 90/\pi R \text{ deg arc mm}^{-1}$$

or a factor of two greater than that for the G - H camera with the same film radius. Furthermore the focusing action of the G - H camera limits the width of medium strength reflections to 0.04 - 0.05 mm; the intensity maximum can generally be located to within 0.01 mm. In the 80 mm diameter cassette this corresponds to a precision of  $0.0035^\circ$  ( $\theta$ ). In addition the use of strictly monochromatic radiation eliminates the risk of errors in  $\theta$  due to the overlap of peaks of different wavelength. Under these conditions it has proved possible to resolve the peaks of reflections which are separated by as little as  $0.03^\circ$  ( $\theta$ ).

The patterns reproduced in plates I and II demonstrate the difference in line definition to be expected as between D - S and G - H patterns. For simple materials in a well crystallised condition, such as silicon, the D - S patterns beyond  $60^\circ$  ( $\theta$ ) is well developed and a high precision in the measurement of  $\theta$  can be expected. For the majority of materials, however, such as minerals, alloys, complexes and other compounds with low symmetry structures or less favourable elastic properties,

the D - S patterns are as those represented by black phosphorous,  $U_3O_8$  or  $BaCl_2 \cdot 2H_2O$ . In these instances the high pattern definition and good resolution of the G - H films clearly offers the only real chance of obtaining reliable readings of  $\theta$ . It should be pointed out here that the width of the reflections in both types of pattern has been increased in the process of photographic reproduction.

6.3.2. The Camera Constant and the Origin of Systematic Errors in the Measurement of  $\theta$

The value of the camera constant

$$K = \theta/S$$

should be obtained as mentioned in section 4.5 f for a number of reflections using a specimen for which the cell dimension is known to within  $\pm 0.0001 \text{ \AA}$ . It will then be found that for the 80 mm diameter cassette, K departs in a systematic fashion from the expected value of 0.3581 over the whole angular range. The departures should be small (<1 %) for a well adjusted cassette and an average value of K can be used for most purposes. Thus a value of 0.3576 has been used in the present instance to construct a scale for the direct reading of interplanar spacings in G - H patterns. The values of d so obtained are of acceptable accuracy for use in phase identification with the ASTM Index to the Powder Diffraction File.

The variability of K with  $\theta$  is generally attributed to the approximation to ideal focusing geometry in the arrangement of specimen and film cassette. Thus a linear relationship between  $\theta$  and S in the focusing camera is only possible when the specimen corresponds over all its length with the recording circle. In practice, the specimen is at best at a tangent to the circle and may in fact be displaced from it. A major factor in producing variations in K is the departure from  $90^\circ$  in  $\zeta$ , the angle between the incident monochromatised beam and the plane of the specimen.

Möller [17] has analysed the effects of specimen displacement  $e$  from the tangential plane for different values of  $\zeta$  and derived a parameter E to describe the relative camera constant K, (see Fig. 8a).

$$E = \frac{\Delta K}{K \cdot K_0 \cdot \epsilon} = \frac{1}{\theta} \cdot \frac{\sin 2\theta}{\cos \zeta \cdot \cos(2\theta - \zeta)}$$

Variations in the camera constant K over the observable  $\theta$  range are shown in Fig. 12a for  $-0.67 \leq \epsilon \leq 0.04$ . Curves for E with  $\zeta = 70^\circ$ ,  $55^\circ$  and  $45^\circ$  are given in Fig. 12b. From these, it is seen that values of  $K_\theta$  over the diffraction range are most reliably interpolated from a set of calibration points when  $\zeta = 55^\circ$ . At  $\zeta = 45^\circ$  changes in E occur most rapidly at  $\theta < 20^\circ$  but are only small at  $35 < \theta < 50^\circ$ ; this inclination is therefore most appropriate if measurements at the higher Bragg angles are desired.

### 6.3.3. Calibration of G - H Patterns

There is considerable difficulty in measuring  $\epsilon$  and in maintaining a constant value for the specimen displacement from exposure to exposure. Accordingly, accurate values of  $\theta_{hkl}$  are most readily obtained from the Guinier patterns by including an internal calibrant in the X-ray specimen and referring all readings of  $S_{hkl}$  to the curve of  $K(\theta)$  obtained for calibrant reflections.

Requirements for the calibrant are as follows:

- a) It should give between five and eight reflections over the diffraction range, the last reflection lying within a few degrees of  $\theta_{max}$  for the film.
- b) The diffraction angles for the calibrant reflections should be known to within 10% of the standard deviation estimate for the film reading. This is most easily achieved if the calibrant is a cubic material which can be readily obtained in pure form.
- c) It should be chemically and physically stable and be hard and brittle so that crushing in a mortar and mixing with the specimen do not lead to detectable line broadening or other changes of pattern.

Semiconductor grade (>99.999% purity) crystals of silicon comply with these requirements, six calibration points being afforded with  $CuK\alpha$  radiation, the last at  $44.015^\circ(\theta)$ . The cell dimension of high purity silicon has been determined by a number of investigators to be  $5.43062 \pm 3 \text{ \AA}$



at 25°C [18]. The coefficient of linear expansion is  $22.5 \cdot 10^{-6} \text{ \AA deg}^{-1}$  so that variations in the quoted cell dimension at the  $\pm 0.0001 \text{ \AA}$  level can be ignored for a camera maintained at  $23 \pm 3^\circ\text{C}$ . Finally, silicon can be crushed to a powder with particle sizes less than  $50 \mu$  without evidence of line broadening. Calibration data for silicon with  $\text{CuK}\alpha_1$  radiation are given in Table 1.

#### 6.3.4. Film Measurement and Derivation of K

After the variability of K with  $\theta$ , the main systematic error associated with the measurement of G - H patterns results from film shrinkage on developing and fixing. According to Hägg, shrinkage errors are minimized by printing a 0.1 mm graduated scale on the exposed film before developing [19]. This has the advantage over the use of fiducial marks of eliminating errors due to non-uniform shrinkage. For measurement purposes the patterns and attendant scale are enlarged (X 30) and read with a 0.01 mm vernier. For a well defined pattern, with reflection widths of the order of 0.05 mm, the peak positions of silicon calibrant reflections can be estimated to within  $\pm 0.01 \text{ mm}$  in successive readings.

A calibration curve of K versus  $\theta$  can be constructed from the measured values of  $S_{\text{Si}}$  and the tabulated  $\theta_{\text{Si}}$  values and drawn on millimetre paper to facilitate the derivation of  $K_\theta$  for any interval S. Examples of some values of K for silicon in four different specimens are given in Table 2.

A more rapid and objective approach to obtaining K is afforded by computer methods. Thus a second degree Lagrange interpolation can be used to derive K for values of S between the calibration points. This is the basis of the programme MOTT which has been incorporated as a preliminary step in larger programmes for indexing powder patterns and refining cell dimensions from G - H pattern measurements.

The camera constant  $K_\theta$  at an interval XP from the trace of the primary reflection is obtained by a cumulative procedure which takes account of three, adjacent calibration points  $K_1, K_2, K_3$  at intervals  $X_1, X_2$  and  $X_3$ .

Then

$$K = K_1 \frac{(XP-X_2)(XP-X_3)}{(X_1-X_2)(X_1-X_3)} + K_2 \frac{(XP-X_1)(XP-X_3)}{(X_2-X_1)(X_2-X_3)} + K_3 \frac{(XP-X_1)(XP-X_2)}{(X_3-X_1)(X_3-X_2)}$$

Calculations show that for curves of the quality given in Table 2, the error in  $\theta$  resulting from this interpolation is less than 10 % of the random measurement error in  $\theta$ . A listing of the MOTT programme written in FORTRAN IV for the IBM 360/30 computer at Studsvik is given in the appendix.

General experience shows that observation of the following points serves to keep the influence of systematic errors to a level below that of the random measurement error.

- a) The graduations on the printed scale are aligned parallel to the X-ray reflections.
- b) Calibrant reflections should be sharp and clearly resolved, and for silicon, the last five reflections in patterns obtained with  $\text{CuK}\alpha$  radiation should not exceed medium intensity.
- c) The  $\text{CuK}\alpha_2$  component should be absent, particularly if the cassette is in the parallel position (section 3.1.).
- d) Background scattering should be less than one-tenth of the medium strength intensities.
- e) For broadened reflections,  $\theta$  is obtained from the averaged readings of the low and high angle edges of the line.
- f) The calibration curve should preferably be smooth and as nearly linear as possible ( $dK/d\theta < 10^{-4} \text{ mm}^{-1}$ ).
- g) If for any reason, remeasurement of reflections becomes necessary, the whole pattern should be remeasured.

#### 6.3.5. The Magnitude of Residual Systematic Errors in $\theta$

If it can be assumed that systematic errors in G - H film measurements can be reduced to negligible proportions by employing an internal calibrant and comparing the reflections with a scale printed on the film, the dominant error is the random error associated with the location of the reflection maxima. The total random error in a measurement at

$30^\circ(\theta)$  can be expected to produce at most an error of 0.01 % in the determination of  $d_{hkl}$ , or 0.005 Å in the measurement of a 5 Å cell dimension. For a D - S pattern, the accuracy obtainable at this angle is probably not better than 0.2 % owing to absorption in the specimen and eccentricity in the specimen/camera geometry. If the D - S pattern, for any of the reasons listed in 2.3 and 2.4, lacks definition beyond this angle, the removal of systematic errors is virtually impossible and the uncertainty in the final results is considerable. Evaluation of  $\theta$  from the G - H film, using the procedure described above, is therefore more consistently reliable, since it contains errors more closely related to the absolute error in  $\theta$  than is the case with the D - S pattern.

The systematic errors which remain in the G - H measurements are limited to the uncertainty in the wavelength of the radiation used and the cell dimension of the calibrant. The wavelength of  $\text{CuK}\alpha_1$  radiation is one of the most accurately determined X-ray constants. Quoted in Å units, however, it is given as  $1.54051 \pm 6$  [20] owing to the uncertainty in the factor relating the Å and KX units employed for the practical measurement of X-ray wavelengths. In order to avoid confusion, therefore, it is generally recommended that where values of  $d_{hkl}$  or cell dimensions are derived from measurements of  $\theta$ , the value of the wavelength used should be given. Similar practice extends to the quoting of the unit cell dimension of the compound used in calibrating the G - H pattern.

#### 6.4. Unit Cell Dimension from Guinier - Hagg Film Measurements

##### 6.4.1. Evaluation of Cell Dimensions and their Probable Errors

For powder reflections with known Miller indices values of  $\theta_{hkl}$ , obtained from film measurements as described above, can be used to derive the dimensions of the crystallographic unit cell. For this purpose the  $\theta$  values are converted to corresponding values of  $Q (= 4 \sin^2 \theta / \lambda)$  and employed in the linear equation appropriate to the cell symmetry given in Table 1. Where the evaluation of more than one coefficient from a number of different  $\theta_{hkl}$  is entailed, it is convenient to employ the method of least squares in accordance with the approach originally suggested by Cohen [9]. The function, R, to be minimized is formed from the

differences  $\Delta Q$  between observed values of  $Q$  and the values calculated from the coefficients. Then

$$R = \sum_{i=1}^n \omega_i (\Delta Q_i)^2$$

where  $\omega_i$  represents a weighting term for  $Q_i$ , based on the reliability of the measurement of  $\theta_i$ .

The advantage of G - H data in this context is that they are free from large scale systematic errors which reduce the value of least squares calculations. Measurement of all the reflections in the pattern can therefore be employed to obtain a statistical distribution of the measurement errors. In this way the probable error can be reduced to a level considerably below that for the single reflection measurement described in the preceding section.

It is assumed that the calibration procedure reduces the systematic error in  $\theta$  to a level below the random measurement error. The weighting scheme proposed by Hess [27]

$$\omega_i = 1/\sin^2 2\theta_i$$

based on the natural variation in the precision of  $d$  as a function of  $\theta$  (section 2.4.) can therefore be used with G - H data.

The least squares calculation is most conveniently performed with a computer and a programme MOTT-CELL has been devised for this purpose. In this programme the elements of the normal equations are formed from the linear expressions for  $Q$  by partial differentiation with respect to the parameters  $a_o$ ,  $b_o$ ,  $c_o$  etc. Values of the corrections  $\Delta a$ ,  $\Delta b$ ,  $\Delta c$  etc. are obtained iteratively, the process being carried out to convergence. Since the diagonal elements of the least square matrix contain the partial derivatives  $\partial Q/\partial a$ ,  $\partial Q/\partial b$ ,  $\partial Q/\partial c$  etc. standard deviations for the general cell parameter  $a_j$  can be calculated according to conventional statistical practice [22].

$$\sigma_{a_j} = R \cdot A'_{jj}/N$$

where

$N =$  number of degrees of freedom (number of  $Q_i$  employed ( $n$ )-

number of parameters to be determined (q)).

$$R = \sum_{i=1}^n \omega_i (\Delta Q_i)^2$$

$A'_{jj}$  = diagonal element of the inverted matrix corresponding to parameter  $a_j$ .

Computer print-outs of G - H diffraction data treated in this way are given in Appendix II by way of example. The compounds chosen range from cubic  $UO_2$  and  $ThO_2$  which afford patterns with only a few reflections to monoclinic  $BaCl_2 \cdot 2H_2O$  with a line-rich pattern of 132 measurable reflections. Inspection of the lists of  $\Delta \sin^2 \theta$  given in the print-outs shows that discrepancies are generally less than  $5 \cdot 10^{-5}$  while the standard deviations of the cell dimensions are 0.005 % or better.

#### 6. 4. 2. Significance Tests for Residual Systematic Errors

In order to test the correctness of the calibration and interpolation treatment for obtaining  $\theta$  from film measurements, significance calculations have been made on the Bragg-angle data used to calculate cell dimensions as described above.

The difference  $\Delta$  between the observed and calculated values of  $\sin^2 \theta$  is used in the least squares treatment as a measure of the approach to the probable cell dimensions. Measurement of n reflections in the powder pattern represents n independent estimates of the cell dimensions required to define the pattern. The self consistency of these n values of  $\Delta$  is accordingly an indication of the probable correctness of the dimensions; a transition from large negative values of  $\Delta$  for low  $\theta$  reflections to large positive values of  $\Delta$  for high  $\theta$  reflections should therefore signify the operation of a systematic error in the derivation of  $\theta$ . If the discrepancies  $\Delta$  are compared over the whole angular range of the pattern with an estimate of the random error in the measurement of  $\theta$ , a measure is obtained of the degree to which the angular dependent systematic errors are removed. This is the basis of the LRM or Likelihood Ratio Method developed by Beu [23] who uses the chi-squared distribution method for testing hypotheses, as follows.

The standard deviation estimate of the average  $\theta$  value for the ith reflection is calculated using the conventional expression

$$\sigma_{\theta}^2 = \frac{1}{p} \sum_{n=1}^p (\bar{\theta} - \theta_n)^2$$

where

- $\sigma_{\theta}$  = the standard deviation of  $\theta$
- $\theta_n$  = the nth measurement of  $\theta$  for the ith reflection
- $p$  = the total number of measurements of  $\theta_i$
- $\bar{\theta}$  = the average value  $\frac{1}{p} \sum_{n=1}^p \theta_n$  for  $p$  measurements of  $\theta$ .

A function  $W(a_o)$  has been derived to measure the probability of the cell dimensions from a comparison of the estimates of  $\sigma_{\theta}$  and the differences between observed and calculated values of  $\theta_i$  according to

$$W(a_o) = \sum_{i=1}^n p_i \ln [1 + (\Delta\theta/\sigma_{\theta})_i^2]$$

where  $n$  represents the number of  $\theta_i$  employed.

Calculation of  $W(a_o)$  for a range of cell dimensions in the neighbourhood of the values obtained by the least squares method leads to the realisation of a minimum  $W_m$  which corresponds to the most probable dimensions  $a_m, b_m, c_m$  etc.  $W_m$  is a statistical function used to determine whether or not systematic errors have been removed from the data within the precision of the measurement. For this purpose  $W_m$  is compared with  $W_{\epsilon}$ , a value of the chi-square distribution for  $N$  degrees of freedom at the 5% significance level [24]. If  $W_m < W_{\epsilon}$ ,  $\theta$  dependent systematic errors are assumed to be absent within the precision of the measurement. The values  $a_m, b_m, c_m$  etc. are accordingly cell dimensions which satisfy the hypothesis of "no remaining systematic errors".

A programme LIRIC for Likelihood Ratio Calculations has been devised by the writer to compute  $W(a_o)$  for symmetries up to and including orthorhombic. Values of the cell dimensions are taken at intervals of  $5 \cdot 10^{-5}$  Å on either side of the least squares results and  $W(a_o)$  is calculated at each interval with  $0.003^{\circ} < \sigma_{\theta} < 0.004^{\circ}$  for three readings of  $\theta_i$ . Table 4 gives a comparison of the LRM cell dimensions for  $UO_2$ ,  $Pb(NO_3)_2$ ,  $\alpha\text{-Fe}_2O_3$  and  $\alpha\text{-SiO}_2$  and the corresponding least squares values together with the  $W_{\epsilon}$  value taken at the 5% significance level and

the interpolated value of  $W_m$ . The standard deviations at the 95% confidence level of the dimensions are calculated in LIRIC using the expression

$$\sigma_{a_j} = 1.96 \cdot a_{m_j} / \left( \sum_{i=1}^n p_i \tan^2 \theta_{m_i} / \sigma_i^2 \right)$$

where

- $a_{m_j}$  = the LRM value for the jth parameter
- $\theta_{m_i}$  represents the calculated value of  $\theta_i$  for the ith reflection corresponding to parameters  $a_{m_j}$
- $p_i$  = the total number of measurements of  $\theta_i$
- $\sigma_i$  = the combined error for the ith reflection whose observed Bragg-angle is  $\theta$ :  $\sigma_i^2 = (\theta - \theta_m)^2 + \sigma_\theta^2$ .

The results in Table 4 are given for a cassette with the generally recommended  $\zeta = 55^\circ$  setting and also for a cassette with  $\zeta = 70^\circ$ . In the first of these settings differences between the least squares and LRM cell dimensions are insignificant, being roughly one-tenth of the standard deviations. In all cases the test  $W_m < W_\epsilon$  for the removal of  $\theta$ -dependent errors is satisfied at the 5% significance level.

For the second setting where only five silicon reflections are available to define the calibration curve (c.f. Table 3), the results are less satisfactory. The LRM values are consistently greater than the least squares values by  $3 - 5 \cdot 10^{-4}$  Å. These discrepancies are covered, however, by the standard deviations which are appreciably larger than those for the  $\zeta = 55^\circ$  setting. With the exception of  $UO_2$ , the values of  $W_m$  exceed  $W_\epsilon$  by more than a factor of two, indicating the presence in the data of residual systematic errors.

From the agreement between the least squares and LRM results for  $\zeta = 55^\circ$ , it is reasonable to assume that G - H patterns are capable of yielding cell dimensions with 0.005% accuracy. It is clear, however, that the effectiveness of calibration procedures should be tested before placing full confidence in the results of least squares calculations. In this connection the approach afforded by the LRM calculations appears to be an effective means of testing calibration reliability.

In order to demonstrate the reliability of the G - H powder data, cell dimensions for a number of the compounds listed in Appendix II are compared in Table 5 with values quoted in the literature. Only those materials with an acknowledged freedom from variations in stoichiometry were chosen for this comparison. Thus cubic  $\text{ThO}_2$  has been selected rather than  $\text{UO}_2$ ,  $\text{CeO}_2$  or  $\text{PuO}_2$ , each of which is a member of a binary solid solution.

The agreement between the G - H and literature results is significant, particularly in the case of the cubic phases where the errors are concentrated to a single parameter. In this connection, the value for  $\text{Pb}(\text{NO}_3)_2$  was remeasured using a D - S camera in view of the large  $\sigma_a$  of  $6.10^{-4}$  Å given in the literature. The D - S measurements were refined with the MOTT-CELL programme introducing additional terms in the linear equation for  $Q_{hkl}$  to account for specimen eccentricity and absorption [25]. The D - S results for black phosphorous were obtained using  $\text{CrK}\alpha$  radiation, the pattern with  $\text{CuK}\alpha$  radiation being indistinct beyond  $35^\circ(\theta)$  (see plate I). The graphical Nelson - Riley treatment of the data which led to the published results has since been checked using the MOTT-CELL programme. The revised values of the cell dimensions agree with the published values within the limits of the standard deviations.

The results obtained for  $\text{BaCl}_2 \cdot 2\text{H}_2\text{O}$  are particularly striking in view of the quality of the D - S film which is clearly quite unsuitable for measurement (Plate II). The literature values are based on the precise measurement of twelve  $hkl$  reflections using a single crystal diffractometer. The G - H pattern which contains 132 measurable reflections was indexed on a probability basis using the programme PIRUM devised by P. E. Werner of the Department of Inorganic and Physical Chemistry, University of Stockholm. Of the listed reflections only three yield differences  $\Delta \sin^2 \theta$ , which exceed  $2 \cdot 10^{-4}$ .

## 7. APPLICATIONS

The short exposure times (15 - 30 minutes), sharp line definition ( $< 0.05$  mm) and large effective film diameter (16 cm) make the G - H camera ideal as an instrument for rapid phase analysis of materials available as homogeneous powders. Since only microgramme quantities



of sample are required, the method is particularly suited to the analysis of small amounts of material. The D - S method is only superior when it becomes necessary to study, in situ, coatings on fragments of material or inclusions in transparent media such as glass.

The accuracies obtained for cell dimensions by routine treatment of the powder data facilitate the study of solid solubility effects in phases with low symmetry and/or large unit cells. The good resolution at low Bragg angles permits a high degree of sensitivity for the detection of line splitting, indicative of a reduction in crystal symmetry, which can accompany the formation of a solid solution or a defect compound. The level of accuracy, which is generally better than 0.01 %, is adequate for most analytical work involving the solubility of small amounts of material. Powder diffractometer and D - S results are only superior in the relatively limited context of detecting variations in lattice spacings at the 0.001 % level in well-crystallized materials with high symmetry.

Where powder patterns of hitherto unreported phases are recorded it is often desirable to determine the cell symmetry and space group in order to make possible a comparison with established compounds. For this purpose, it is necessary to determine the  $hkl$  indices of the constituent reflections of the pattern, a process which depends upon the occurrence of specific relationships between the values of  $\sin^2 \theta$  for the different symmetry classes. Since low-angle reflections have the simplest indices, often of the form 100, 010, 002 etc., the various trial-and-error indexing methods which have been devised are largely based on assumed values for the indices of these reflections. G - H powder data is particularly suited to this type of treatment in view of the close correlation between values obtained for the cell dimensions using low-angle data and those derived from data in the  $30 - 45^\circ(\theta)$  region. In this connection only diffractometer data is of comparable quality while measurements of D - S films have in the past led to many spurious indexings.

## ACKNOWLEDGEMENT

The author wishes to express his gratitude to Dr. Per Spiegelberg of the Institute of Metals Research, Stockholm, for his valuable instruction in the art of camera alignment. His generous assistance, given at the critical stage of camera reconstruction, guaranteed its subsequent reliability and stability in operation.

Thanks also go to Mr. Lennart Jacobsson of the Fuel Technology Section for his patient and painstaking measurement of the Guinier - Hägg patterns which forms the basis of the work reported here. His comments on the practical aspects of Guinier photography have given an insight into the needs of the camera user, and have thus so a useful background for the writing of this report.

Many thanks are also due to Prof. Gunnar Hägg, who introduced the author to the use of Guinier cameras, and who kindly read this manuscript.

REFERENCES

1. ARNDT, U. W. and WILLIS, B. T. M.  
Single crystal diffractometry.  
Cambridge Univ. Press, Cambridge, 1966. Chap. 3.
2. BOND, W. L.  
Precision lattice constant determination.  
Acta cryst. 13 (1960) p. 814.
3. DEBYE, P. J. W.  
The collected papers of Peter J. W. Debye.  
Interscience Publ. Inc. New York, 1954. p. 51.
4. VAND, V.  
The powder method in organic chemical research. Chap. 24 in  
X-ray diffraction by polycrystalline materials. Ed. by H. S.  
Peiser, H. P. Rooksby and A. J. C. Wilson.  
Chapman & Hall, London, 1960. p. 512.
5. PARRISH, W. and WILSON, A. J. C.  
Precision measurement of lattice parameters of polycrystalline  
specimens. Paper 10 in X-ray analysis papers.  
Ed. by W. Parrish. Centrex Publ. Co., Eindhoven, 1965, p. 142.
6. WILSON, A. J. C.  
Elements of X-ray crystallography.  
Addison-Wesley Publ. Co. Reading, Mass., 1970.
7. TAYLOR, A. and SINCLAIR, H.  
On the determination of lattice parameters by the Debye-Scherrer  
method.  
Proc. Phys. Soc. 57 (1945) p. 126.
8. NELSON, J. B. and RILEY, D. P.  
An experimental investigation of extrapolation methods in the de-  
rivation of accurate unit-cell dimensions of crystals.  
Proc. Phys. Soc. 57 (1945) p. 160.
9. COHEN, M. U.  
Precision lattice constants from X-ray powder photographs.  
Rev. Sci. Instr. 6 (1935) p. 68.
10. GUINIER, A.  
X-ray crystallographic technology.  
Hilger and Watts Ltd, London, 1952, Chap. 6.
11. ROBERTS, B. W. and PARRISH, W.  
Filter and crystal monochromator techniques. Chap. 2.3 in Inter-  
national tables for X-ray crystallography.  
The Kynoch Press, Birmingham, 1962, Vol. 3. p. 80.

12. WHITE, J. E.  
X-ray diffraction by elastically deformed crystals.  
J. Appl. Phys. 21 (1950) p. 855.
13. RENNINGER, R.  
Zwei Arten der Verzwilligung von Pentaerythrit.  
Acta Cryst. 7 (1954) p. 677.
14. GOULD, R. W., BATES, S. R. and SPARKS, C. J.  
Application of the graphite monochromator to light element X-ray spectroscopy.  
Appl. spectrosc. (Pt. 1), 22 (1968) p. 549.
15. PARRISH, W. and TAYLOR, J.  
Factors in the detection of low concentrations in X-ray diffractometry. Paper 9 in X-ray analysis papers.  
Ed. by W. Parrish. Centrex Publ. Co., Eindhoven, 1965, p. 137.
16. BERGER, S. G.  
The crystal structure of boron oxide.  
Acta Chem. Scand. 7 (1953) p. 611.
17. MÖLLER, M.  
On the calibration and accuracy of the Guinier camera for the determination of interplanar spacings. 1962.  
(AE-67).
18. KING, H. W. and RUSSEL, C. M.  
Double-scanning diffractometry in the back-reflection region.  
Advan. X-ray anal. Vol. 8. 1965.
19. HÄGG, G.  
Measurement of X-ray powder diffraction films with automatic correction for shrinkage.  
Rev. Sci. Instr. 18 (1947) p. 371.
20. RIECK, G. D.  
Tables relating to the production, wavelengths and intensities of X-rays. Chap. 2.2 in International tables for X-ray crystallography.  
The Kynoch Press, Birmingham 1962. Vol. 3, p. 60.
21. HESS, J. B.  
A modification of the Cohen procedure for computing precision lattice constants from powder data.  
Acta Cryst. 4 (1951) p. 209.
22. CRUICKSHANK, D. W. J.  
Statistics. Chap. 2.6. in International tables for X-ray crystallography.  
The Kynoch Press, Birmingham, 1959. Vol. 2, p. 92.
23. BEU, K. E., MUSIL, F. J. and WHITNEY, D. R.  
Precise and accurate lattice parameters by film powder methods. I. The likelihood ratio method.  
Acta Cryst. 15 (1962) p. 1292.

24. CRUICKSHANK, D. W. J.  
Statistics. Chap. 2.6 in International tables for X-ray crystallography.  
The Kynoch Press, Birmingham, 1959. Vol. 2, p. 95.
25. MUELLER, M. H. and HEATON, L.  
Determination of lattice parameters with the aid of a computer.  
1961.  
(ANL-6176).
26. OWEN, E. A. and WILLIAMS, G. I.  
A low-temperature X-ray camera.  
J. Sci. Instr. 31 (1954) p. 49.
27. MAUER, F. A. and BOLZ, L. H.  
Measurement of thermal expansion of cermet components of high temperature X-ray diffraction. 1955.  
(WADC-TR-55-473).
28. BROWN, A. and CHITTY, A.  
Thoria as a fertile component for a liquid metal breeder blanket.  
Reactor Techn. 1 (1959-61) p. 145.
29. STRAUMANIS, M. and IEVINS, A.  
Präzisionsaufnahmen nach dem Verfahren von Debye und Scherrer II.  
Z. Physik 98 (1936) p. 461.
30. BROWN, A.  
Structure data for some arsenic- and germanium-rich compounds of molybdenum.  
Nature 206 (1965) p. 502.
31. LEE, J. A. and RAYNOR, G. V.  
The lattice spacings of binary tin-rich alloys.  
Proc. Phys. Soc. 67B (1954) p. 737.
32. JAN, J. -P., STEINEMANN, S. and DINICHERT, P.  
The density and lattice parameters of ruby.  
Phys. Chem. Solids 12 (1959-60) p. 349.
33. ROOKSBY, H. P. and WILLIS, B. T. M.  
The low-temperature crystal structure of magnetite.  
Acta Cryst. 6 (1953) p. 565.
34. KEITH, H. D.  
Lattice spacings in clear crystalline quartz and their variability.  
Am. mineralogist 40 (1955) p. 530.
35. BROWN, A. and RUNDQVIST, S.  
Refinement of the crystal structure of black phosphorus.  
Acta Cryst. 19 (1965) p. 684.
36. BUSING, W. R.  
Quoted by U. W. Arndt and B. T. M. Willis in Single crystal diffractometry. Cambridge Univ. Press, Cambridge, 1966, p. 264.



TABLE 1

LINEAR EQUATIONS FOR THE RELATIONSHIP BETWEEN BRAGG ANGLE,  
MILLER INDICES AND UNIT CELL PARAMETERS  
FOR MONOCLINIC TO CUBIC SYMMETRIES

$\theta$  = Bragg angle;  $\lambda$  = radiation wavelength;  $hkl$  = Miller indices;  $a, b, c$  = cell dimensions;  $\beta$  = angle between  $a$  and  $c$  axes;  $Q_{hkl} = 4 \sin^2 \theta_{hkl} / \lambda^2$

MONOCLINIC $\alpha = \gamma = 90^\circ \neq \beta$ $a \neq b \neq c$	$Q_{hkl} = Ah^2 + Bk^2 + Cl^2 + Dh\ell$	$A = 1/a^2 \sin^2 \beta$	$B = 1/b^2$	$C = 1/c^2 \sin^2 \beta$	$D = -2 \cos \beta / ac \sin^2 \beta$
ORTHORHOMBIC $\alpha = \beta = \gamma = 90^\circ$ $a \neq b \neq c$	$Q_{hkl} = Ah^2 + Bk^2 + Cl^2$	$A = 1/a^2$	$B = 1/b^2$	$C = 1/c^2$	-
TETRAGONAL $\alpha = \beta = \gamma = 90^\circ$ $a = b \neq c$	$Q_{hkl} = A(h^2 + k^2) + Cl^2$	$A = 1/a^2$	-	$C = 1/c^2$	-
HEXAGONAL $\alpha = \beta = 90^\circ, \gamma = 120^\circ$ $a = b \neq c$	$Q_{hkl} = A(h^2 + hk + k^2) + Cl^2$	$A = 4/3a^2$	-	$C = 1/c^2$	-
CUBIC $\alpha = \beta = \gamma = 90^\circ$ $a = b = c$	$Q_{hkl} = A(h^2 + k^2 + \ell^2)$	$A = 1/a^2$	-	-	-

TABLE 2

CALIBRATION DATA FOR SILICON POWDER

$a_0 = 5.43062 \pm 5 \text{ \AA}$  at  $25^\circ\text{C}$ ;  $\alpha_T = 22.5 \cdot 10^{-6} \text{ \AA deg}^{-1} \text{ C}$ ;  
 $\lambda\text{CuK}\alpha_1 = 1.54051 \text{ \AA}$  (assumed as basis for calculation)

h	k	l	$\sin^2 \theta$	$\theta$
1	1	1	0.060352	14.2212
2	2	0	0.160939	23.6514
3	1	1	0.221291	28.0612
4	0	0	0.321877	34.5651
3	3	1	0.382229	38.1882
4	2	2	0.482816	44.0152
3	3	3	0.543168	47.4764



TABLE 3

CAMERA CONSTANTS AND THEIR DEVIATIONS OBTAINED WITH  
SILICON CALIBRANT FOR 80 MM DIAMETER CASSETTE

$\zeta$  is angle between axis of incident beam and plane of specimen;  
 $\sigma(s)$  is error in K produced by an error in film measurement  
of  $\pm 0.01$  mm  
 $\sigma(\theta)$  is error in K produced by error in silicon cell dimension  
of  $\pm 0.0001$  Å.

K							
$\zeta$ \ / \ $hkl$	111	220	311	400	331	422	333
70	0.35492	0.35498	0.35499	0.35514	0.35492	-	-
70	0.35518	0.35503	0.35499	0.35485	0.35475	-	-
55	0.35816	0.35809	0.35805	0.35812	0.35821	0.35830	-
55	0.35788	0.35769	0.35767	0.35765	0.35763	0.35764	-

$\sigma K$						
$\sigma(s)$	0.00011	0.00005	0.00004	0.00004	0.00003	0.00003
$\sigma(\theta)$	0.00008	0.00008	0.00007	0.00007	0.00007	0.00006

TABLE 4

COMPARISON OF CELL DIMENSION CALCULATIONS FROM  
GUINIER - HÄGG DATA USING LEAST-SQUARES AND  
LIKELIHOOD-RATIO METHODS

	UO <sub>2</sub>	Pb(NO <sub>3</sub> ) <sub>2</sub>	α-Fe <sub>2</sub> O <sub>3</sub>		α-SiO <sub>2</sub>		
	a <sub>o</sub>	a <sub>o</sub>	a <sub>o</sub>	c <sub>o</sub>	a <sub>o</sub>	c <sub>o</sub>	
ζ = 55°	Least squares Result	5.4706 ± 3	7.8552 ± 1	5.0351 ± 1	13.7515 ± 5	4.9124 ± 1	5.4045 ± 3
	LRM Result	5.4706 ± 3	7.8551 ± 3	5.0351 ± 2	13.7514 ± 5	4.9125 ± 2	5.4048 ± 2
	N	8	19	14		21	
	W <sub>m</sub>	4.54	17.58	13.13		30.02	
	W <sub>ε</sub>	15.51	30.14	23.68		32.67	
ζ = 70°	Least squares Result	5.4696 ± 3	7.8545 ± 8	5.0374 ± 4	13.757 ± 1	4.9147 ± 2	5.4040 ± 3
	LRM Result	5.4697 ± 4	7.8551 ± 6	5.0377 ± 3	13.758 ± 1	4.9149 ± 2	5.4043 ± 3
	N	7	16	11		20	
	W <sub>m</sub>	14.05	63.21	50.51		72.51	
	W <sub>ε</sub>	14.07	26.30	19.68		31.41	

Cell Dimensions in Å based on following assumptions:

$$\lambda_{\text{CuK}\alpha_1} = 1.540510 \text{ \AA}$$

$$a_o(S_i) = 5.43062 \text{ \AA at } 23^\circ\text{C.}$$

TABLE 5

COMPARISON OF CELL DIMENSIONS FROM GUINIER -  
HÄGG DATA WITH LITERATURE VALUES

Phase	No of reflections	Guinier-Hägg Data at $24 \pm 1^\circ\text{C}$	Literature Value in Å	Technique	Ref.
Cubic Symmetry					
$\alpha\text{-Fe}$	3	$a_o = 2.8659 \pm 4$	$2.86615 \pm 2$	D-S+N-R( $20^\circ\text{C}$ )	26
$\text{ThO}_2$	9	$a_o = 5.5971 \pm 2$	$5.5971 \pm 1$	Diffractionmeter ( $26^\circ\text{C}$ )	27
$\text{Pb}(\text{NO}_3)_2$	19	$a_o = 7.8552 \pm 1$	$5.5969 \pm 1$ $7.8561 \pm 6$ ( $7.8555 \pm 1^*$ )	D-S+N-R( $25^\circ\text{C}$ ) D-S+N-R( $23^\circ\text{C}$ )	28 29
$\text{Mo}_3\text{Sb}_7$	23	$a_o = 9.5688 \pm 2$	$9.5688 \pm 1$	D-S+N-R( $23^\circ\text{C}$ )	30
Tetragonal Symmetry					
$\alpha\text{-Sn}$	12	$a_o = 5.8312 \pm 2$ $c_o = 3.1808 \pm 2$	$5.8315 \pm 2$ $3.1812 \pm 2$	D-S+N-R( $25^\circ\text{C}$ )	31
Hexagonal Symmetry					
$\alpha\text{-Al}_2\text{O}_3$	20	$a_o = 4.7587 \pm 2$ $c_o = 12.991 \pm 1$	$4.7591 \pm 4$ $12.989 \pm 3$	D-S+N-R( $25^\circ\text{C}$ )	32
$\alpha\text{-Fe}_2\text{O}_3$	16	$a_o = 5.0351 \pm 1$ $c_o = 13.7515 \pm 5$	$5.0345 \pm 5$ $13.749 \pm 2$	D-S+N-R( $20^\circ\text{C}$ )	33
$\alpha\text{-Quartz}$ ( $\text{SiO}_2$ )	23	$a_o = 4.9125 \pm 1$ $c_o = 5.4044 \pm 3$	$4.9125 \pm 5$ $5.4042 \pm 5$	D-S+N-R( $18^\circ\text{C}$ )	34
Orthorhombic Symmetry					
Black P	18	$a_o = 3.3140 \pm 2$ $b_o = 10.479 \pm 1$ $c_o = 4.3769 \pm 4$	$3.3138 \pm 2$ $10.4776 \pm 6$ $4.3759 \pm 3$	D-S+N-R( $22^\circ\text{C}$ )	35
Monoclinic Symmetry					
$\text{BaCl}_2 \cdot 2\text{H}_2\text{O}$	132	$a_o = 6.7218 \pm 2$ $b_o = 10.9083 \pm 4$ $c_o = 7.1321 \pm 2$ $\beta = 91.102^\circ \pm 3$	$6.7215 \pm 2$ $10.9077 \pm 3$ $7.1315 \pm 3$ $91.102^\circ \pm 3$	Single crystal Diffractionmeter Least squares refinement of $12 \sin^2 \theta_{hkl}$	36

\* = This work.

D-S = Debye-Scherrer powder pattern.

N-R = Nelson-Riley extrapolation for data correction.



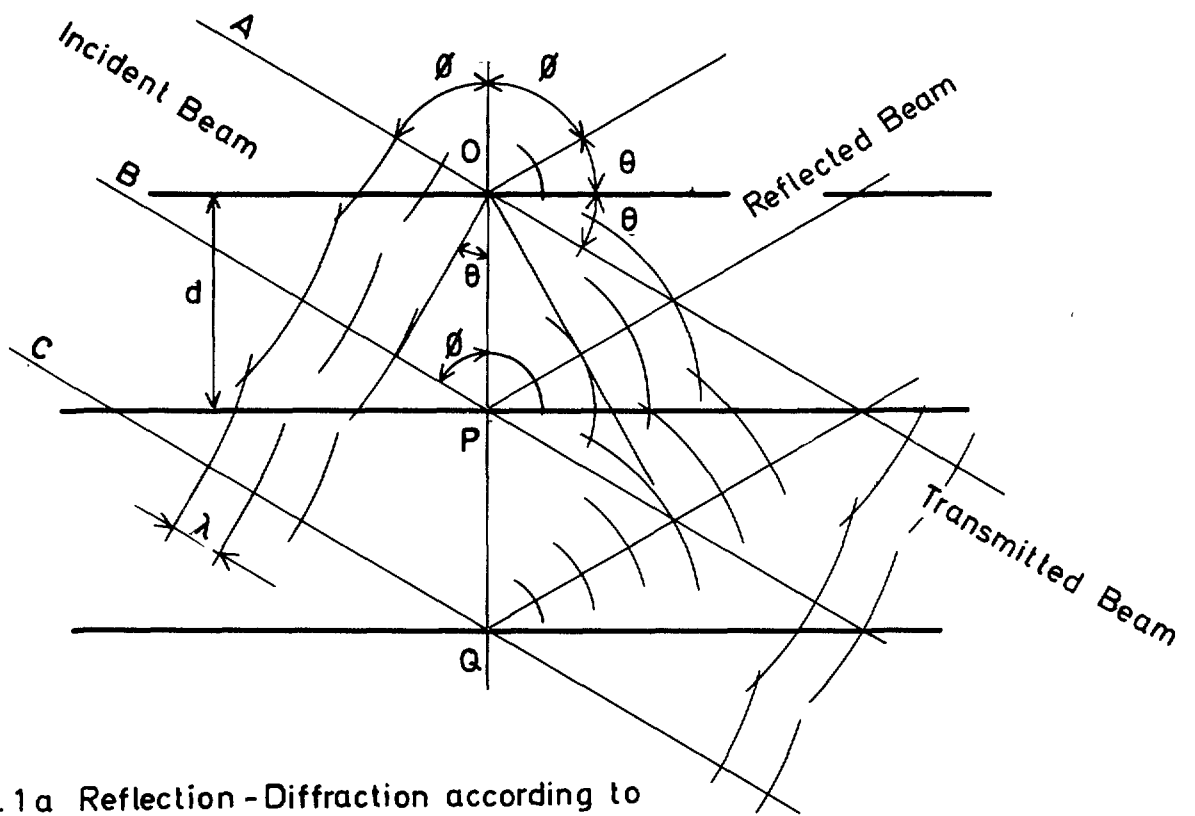


Fig.1a Reflection-Diffraction according to Bragg's Law

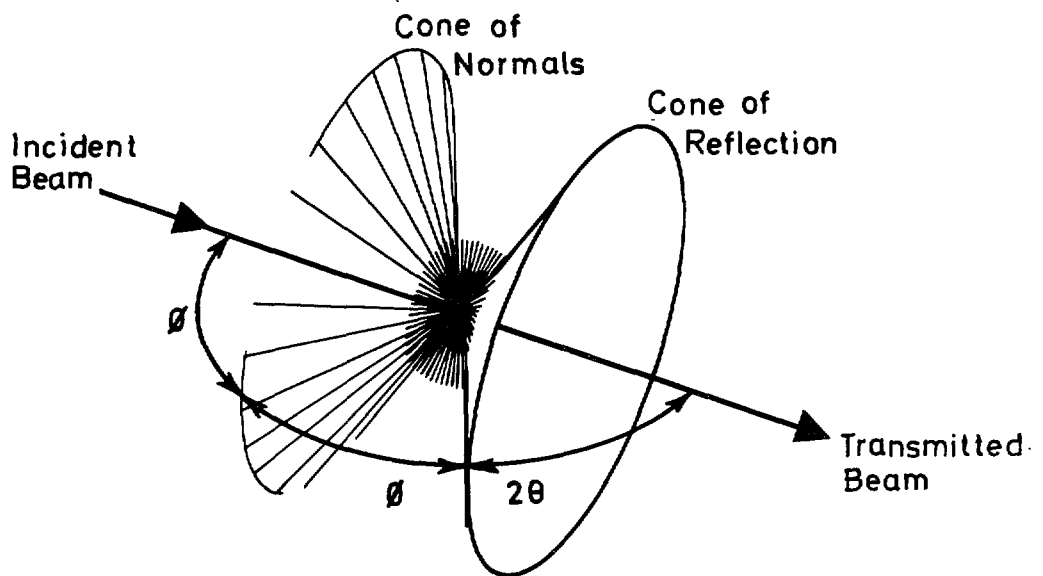


Fig.1b Generation of a cone of reflection in powder diffraction.

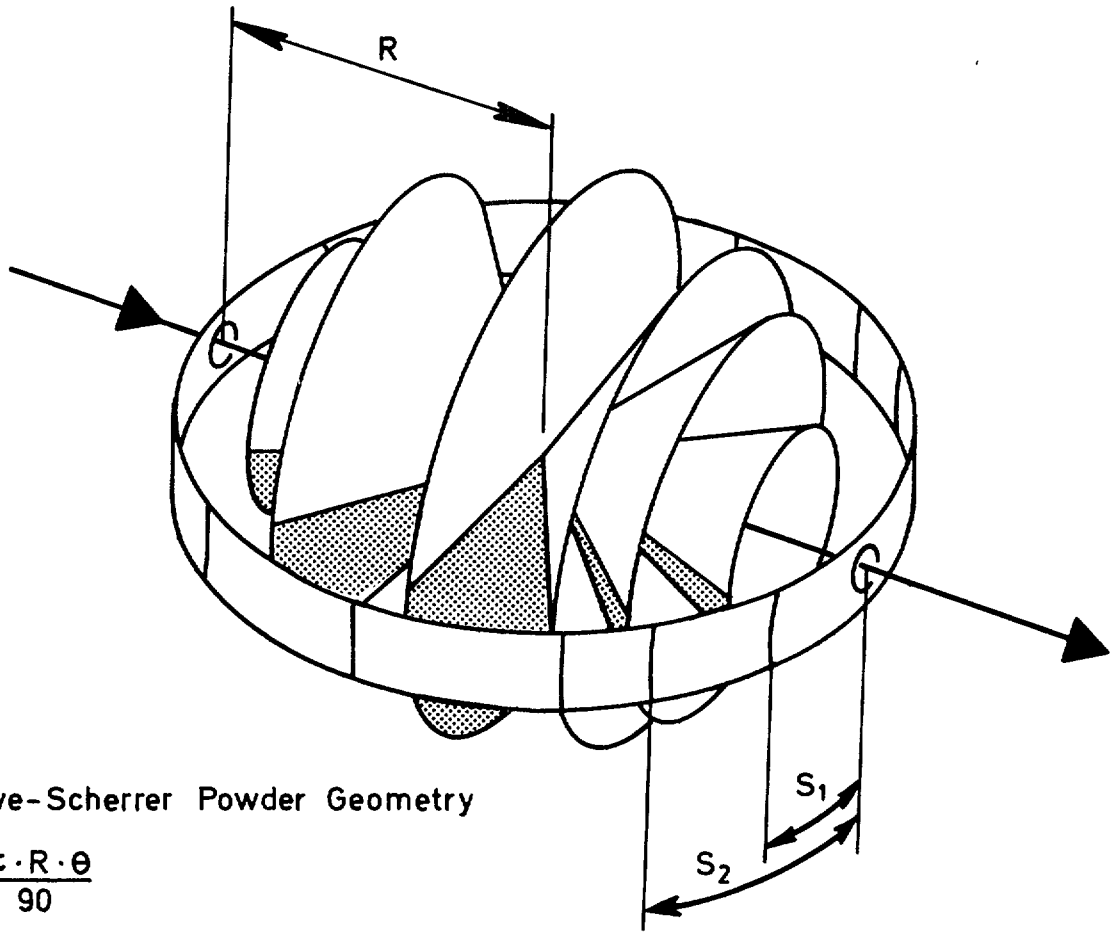


Fig. 2a Debye-Scherrer Powder Geometry

$$S = \frac{\pi \cdot R \cdot \theta}{90}$$

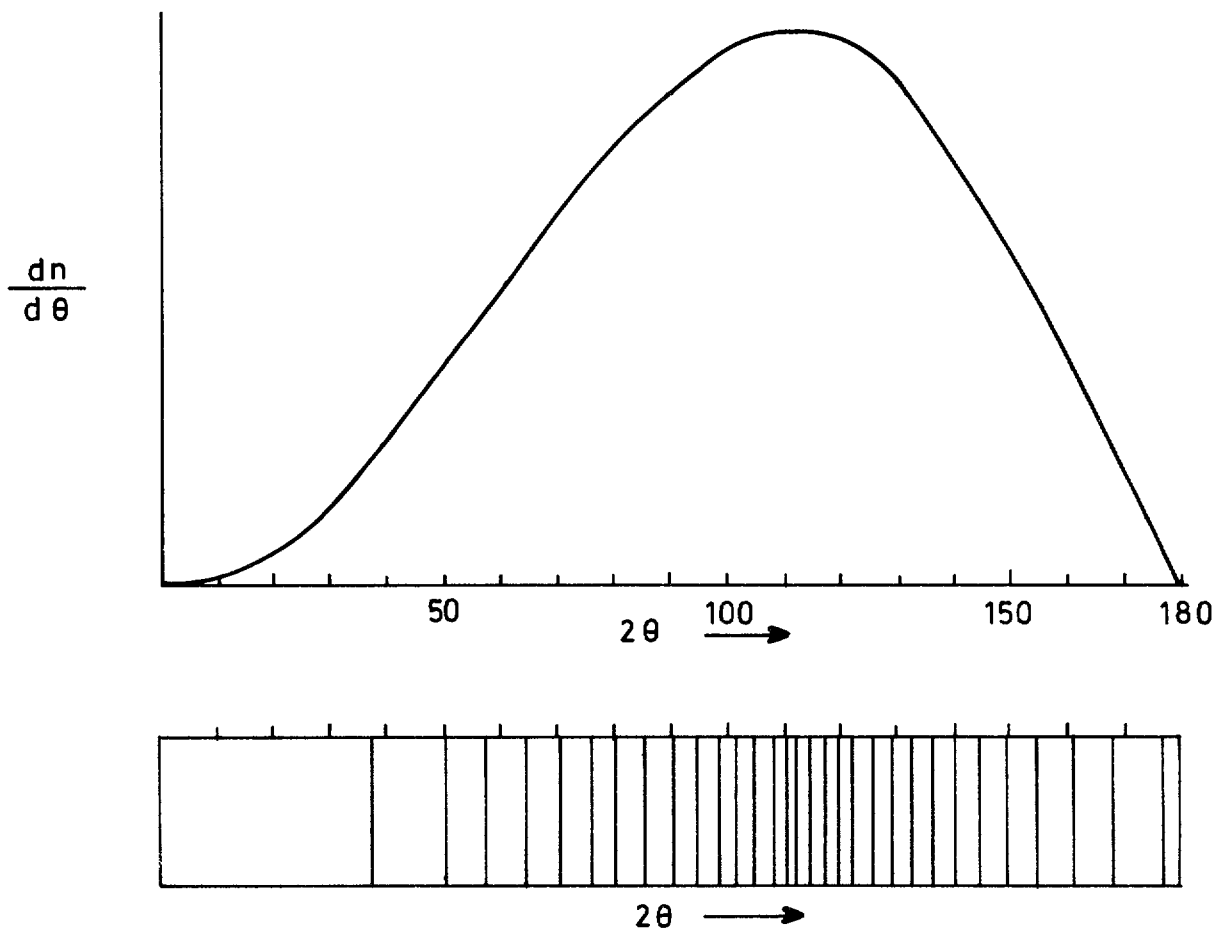


Fig. 2b. Average number of powder lines per unit of Bragg angle and schematic appearance of powder pattern.

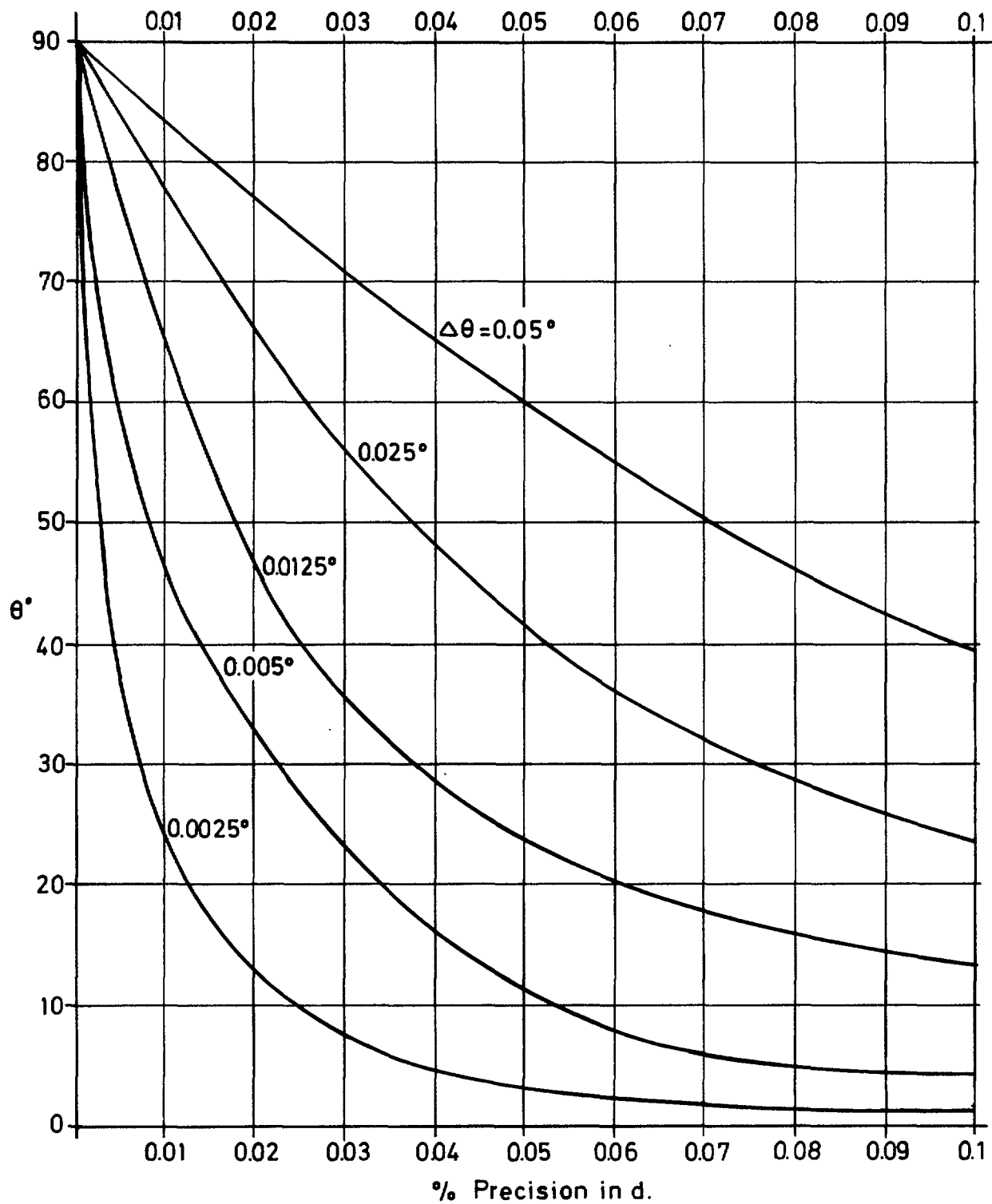


Fig.3 Percentage precision of  $d$  as a function of  $\theta$  for various errors  $\Delta\theta$

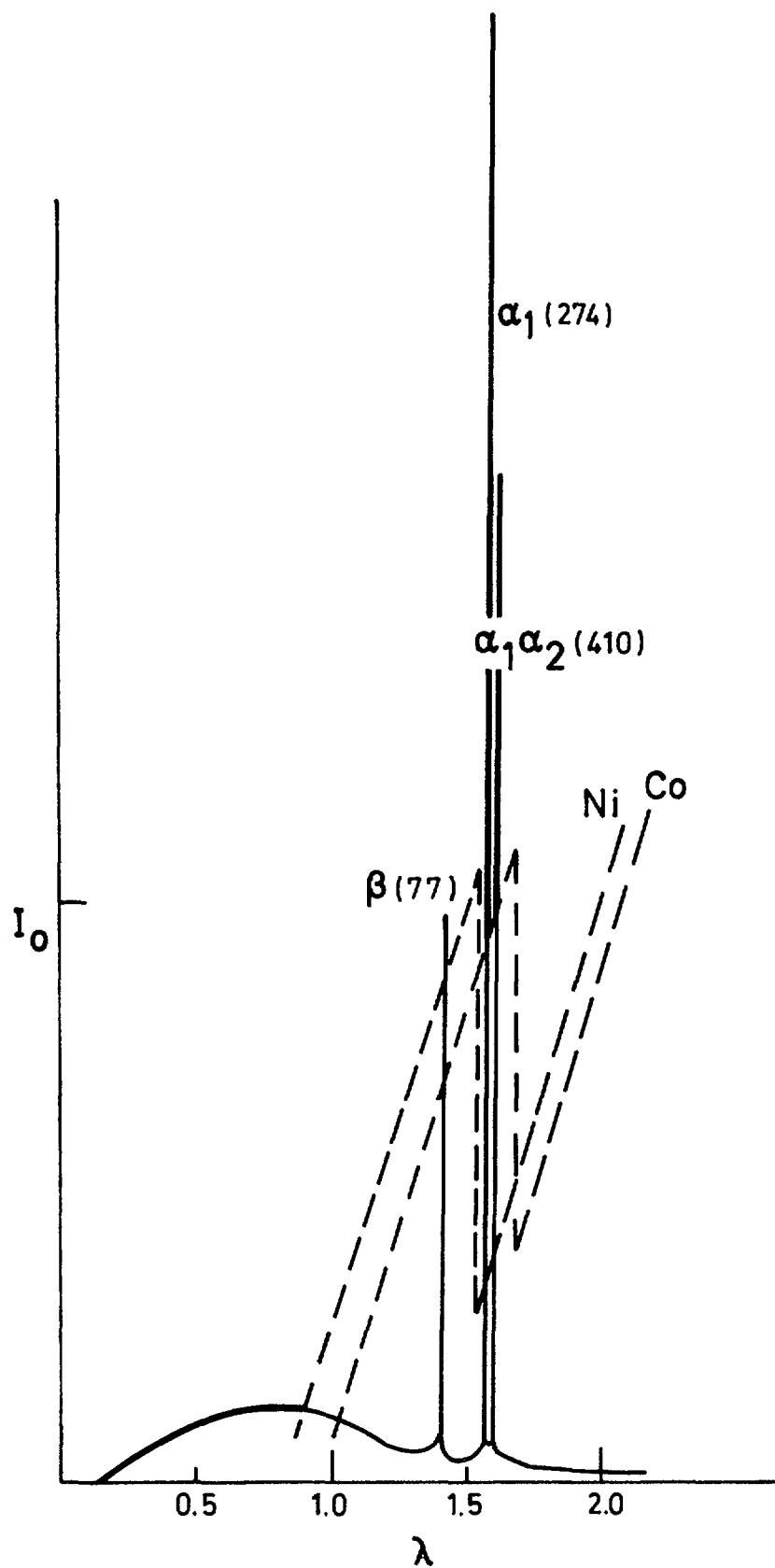
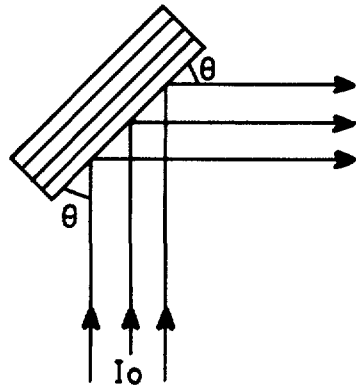
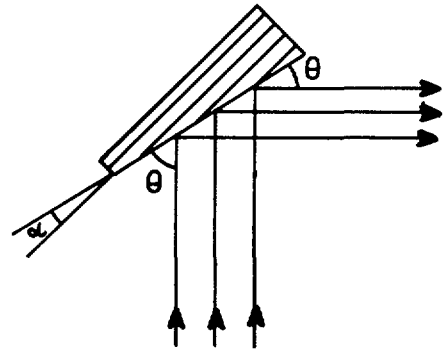


Fig.4 Intensity Distribution for CuK Radiation with superimposed Ni - Co Absorption Edges.

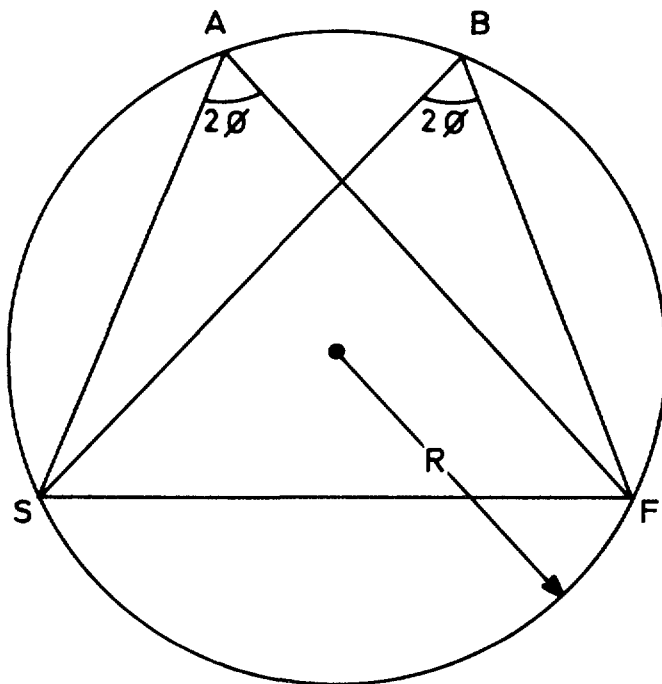




(a) Plane Parallel

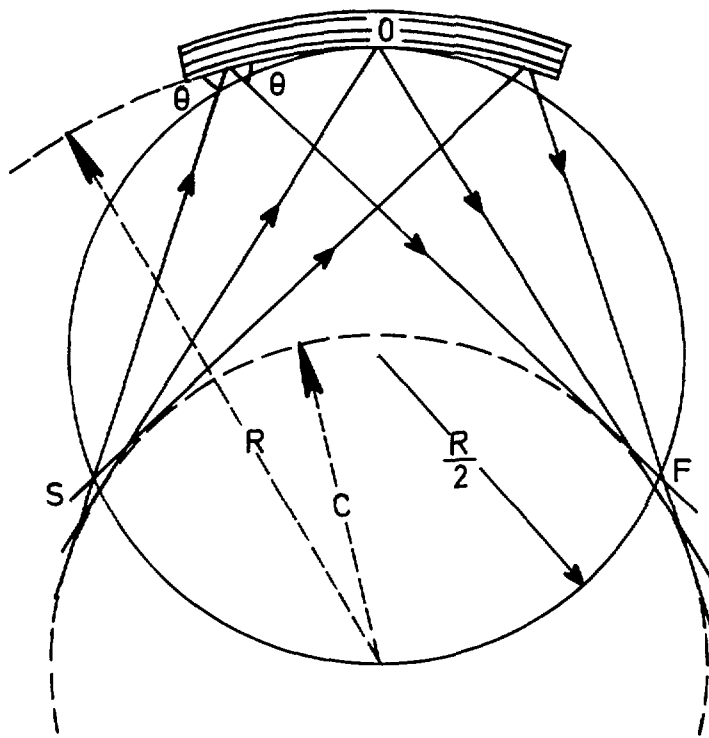


(b) Tilted Surface



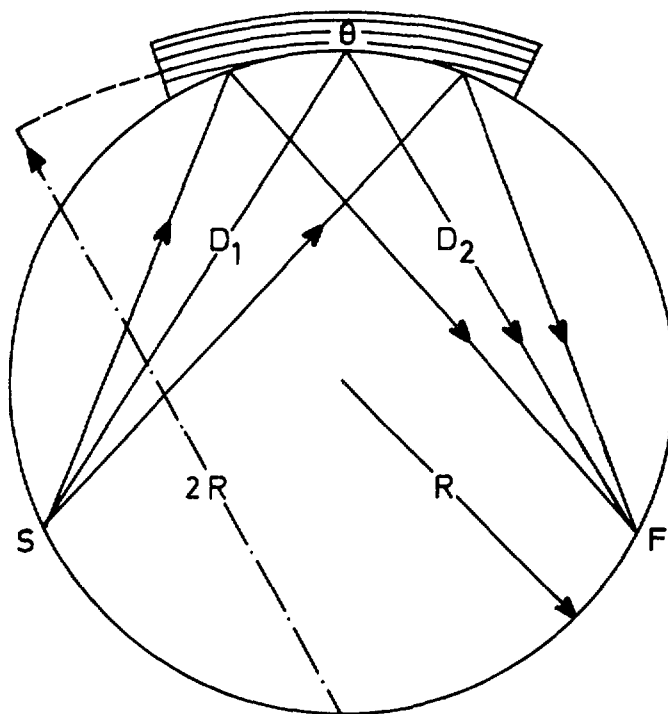
(c) Focusing Monochromator

Fig 5 Monochromator Geometries



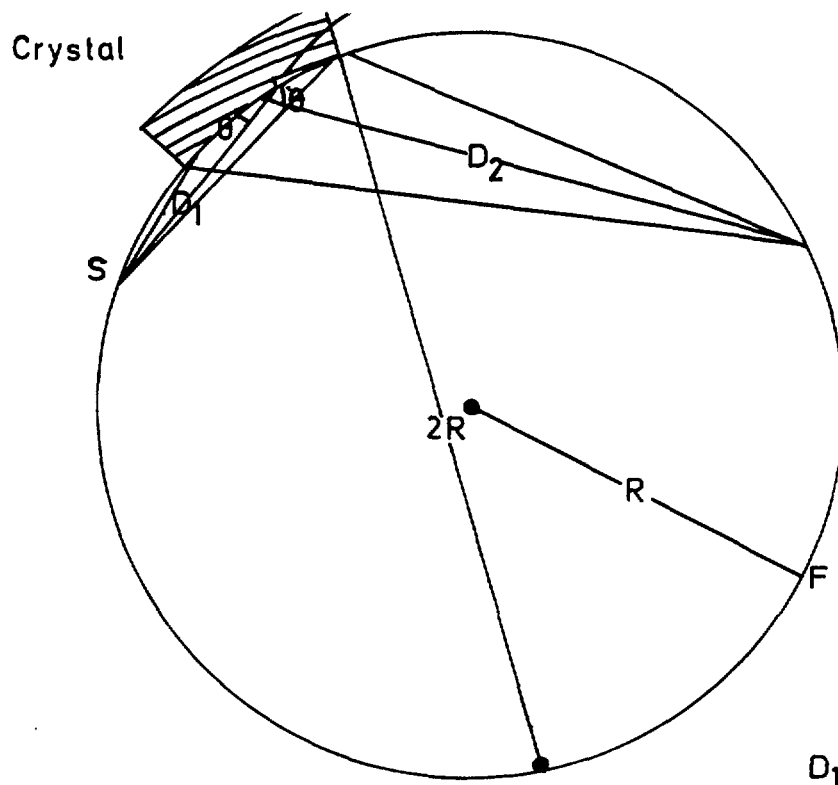
(a) Johann Bent Crystal

$\frac{R}{2}$  = Radius of focal circle  
 R Radius of crystal curvature  
 C Radius of caustic (error circle)



(b) Johannson Ground and Bent Crystal (Symmetrical)

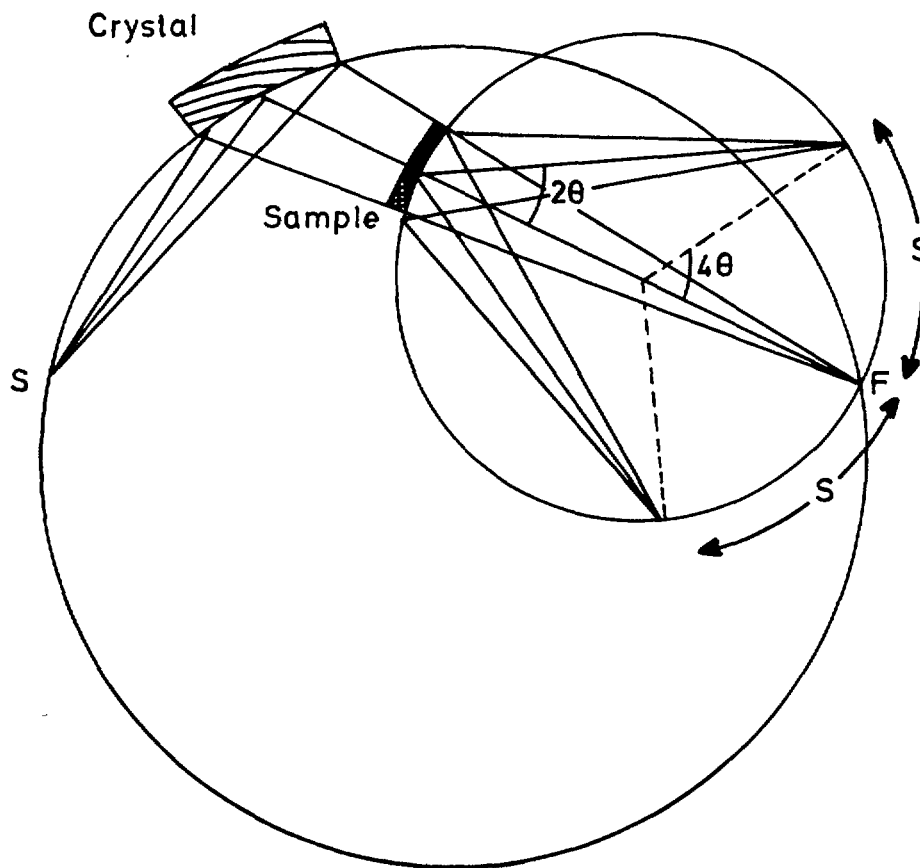
Fig 6. Practical Focusing Monochromators



$$D_1 = 2R \sin(\theta - \alpha)$$

$$D_2 = 2R \sin(\theta + \alpha)$$

a) Asymmetric monochromator



$$S = \frac{\pi \cdot R \cdot \theta}{45}$$

b) Asymmetric monochromator with symmetrical cassette

Fig 7. Guinier camera geometries for diffraction from monochromator and from sample

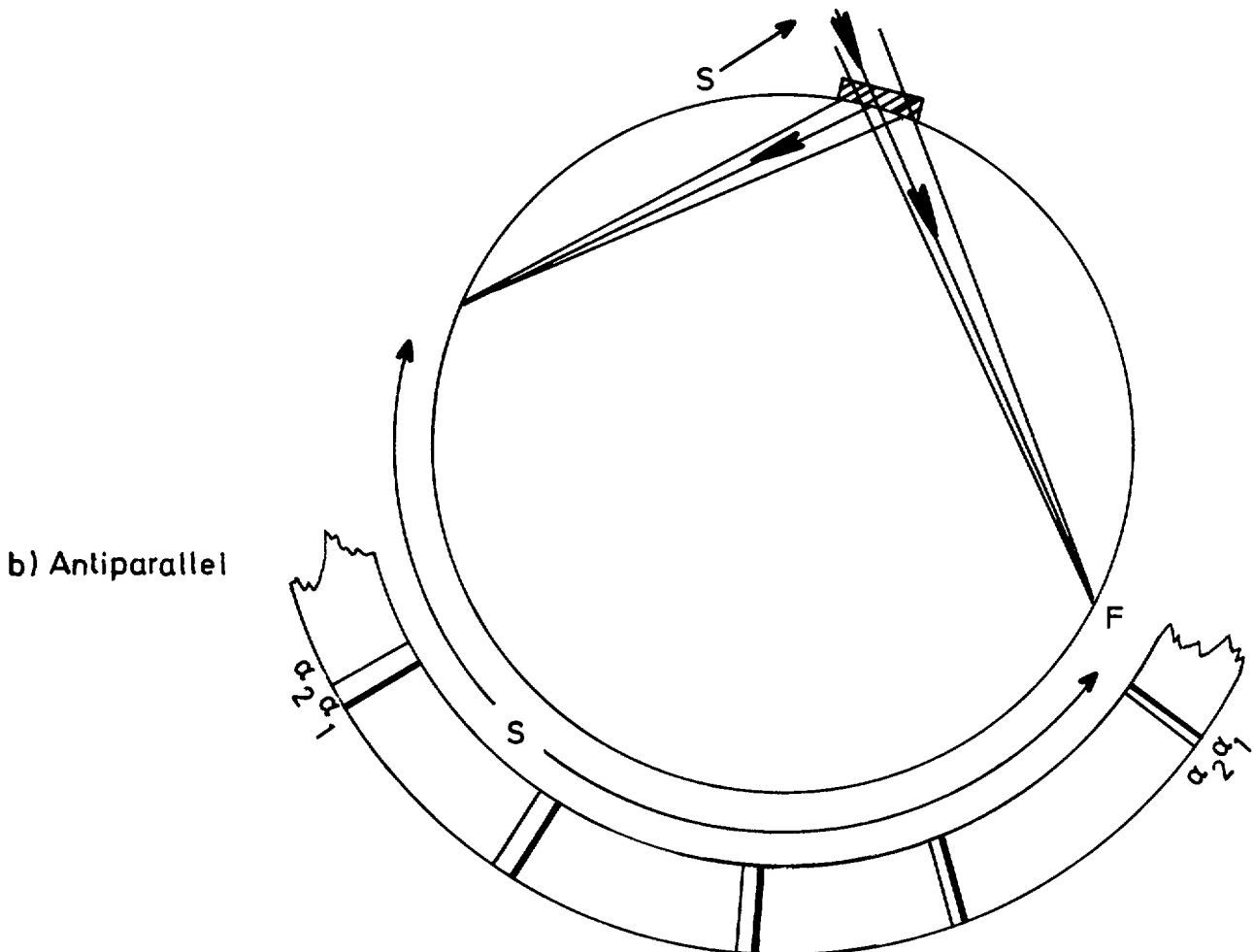
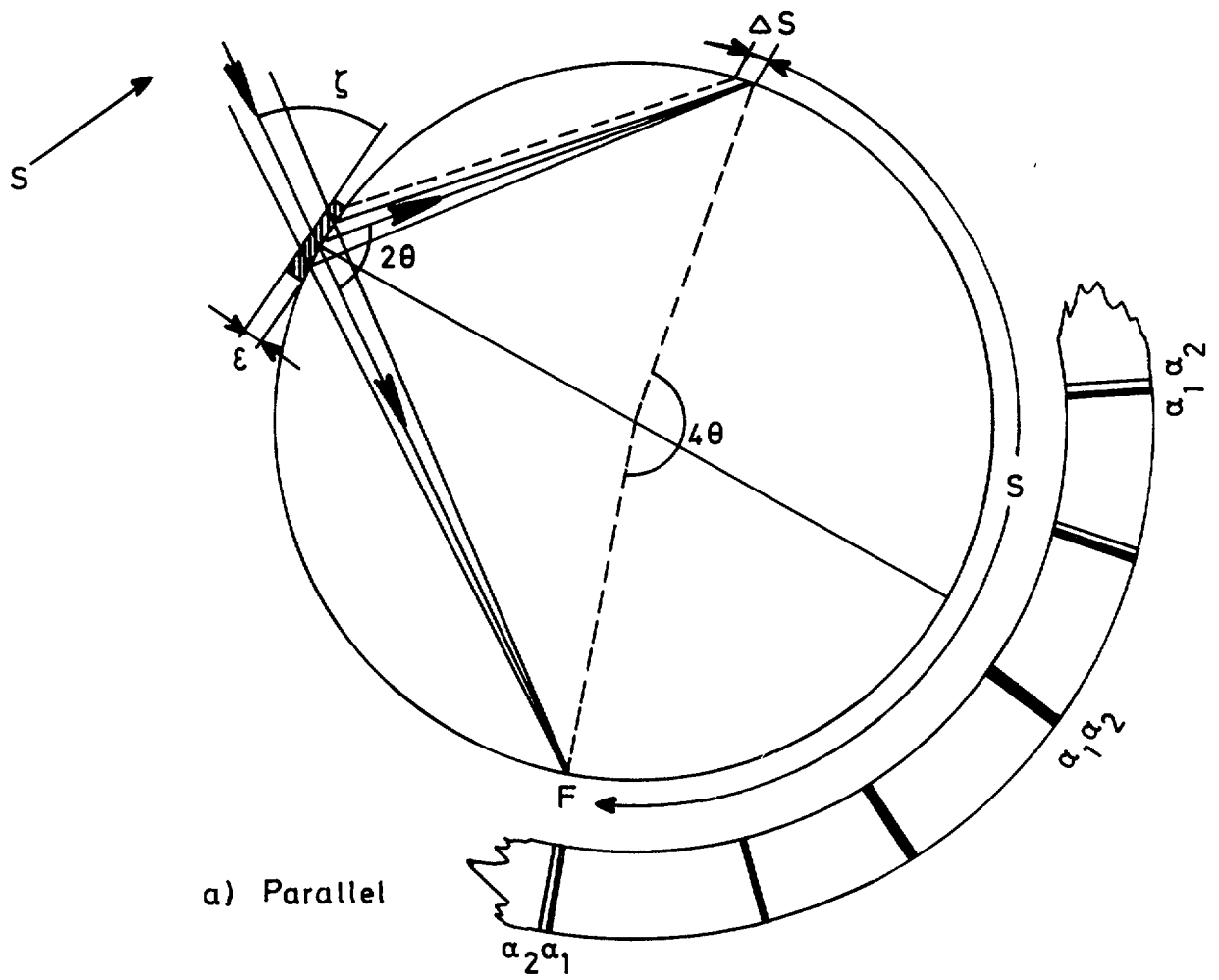
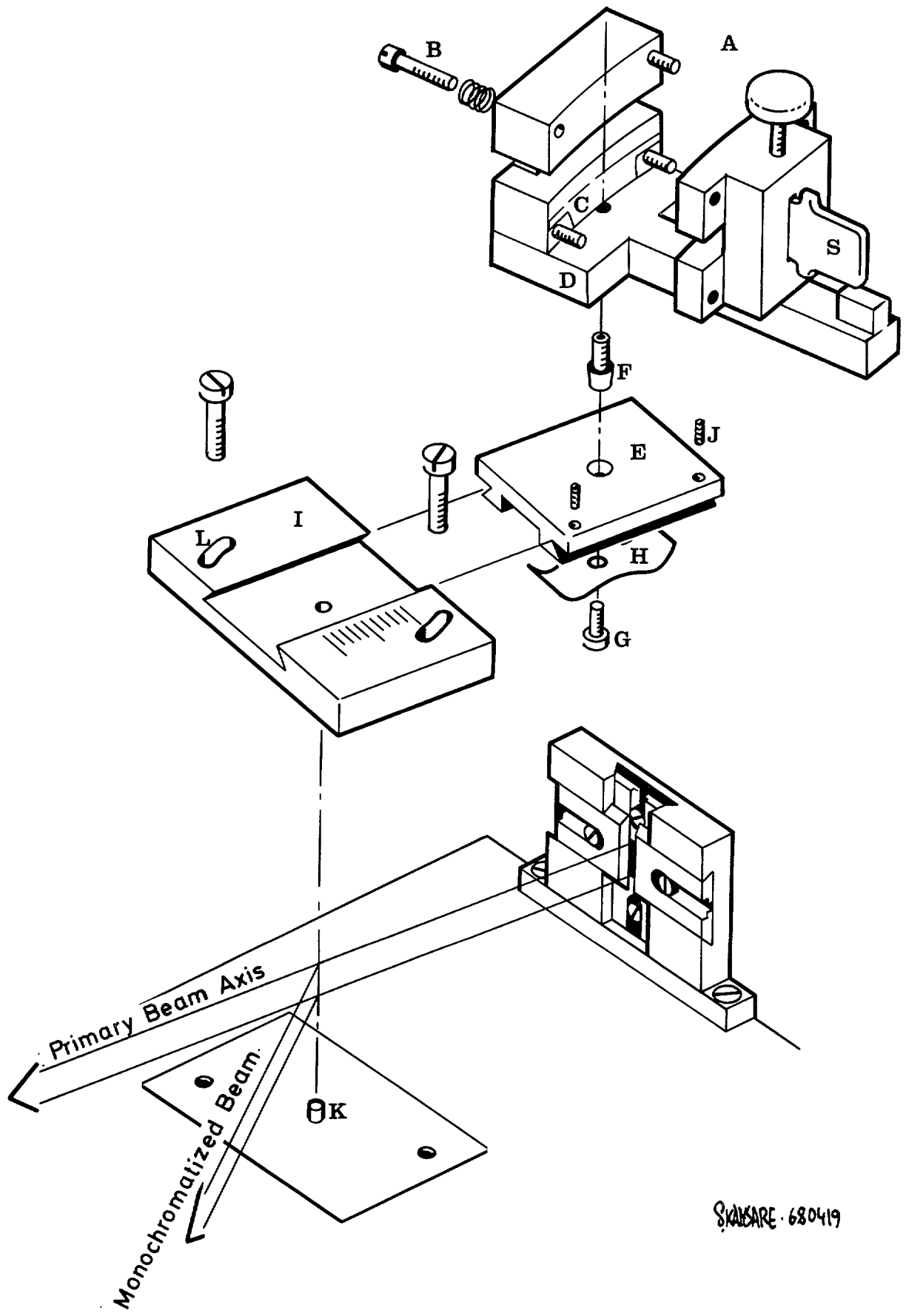


Fig. 8 Alternative placings of asymmetric cassette for operation at angles up to  $45^\circ$  ( $\theta$ ).



SIGMARE 680419

Fig. 9 Fully adjustable Crystal Monochromator for use with fine-focus sources

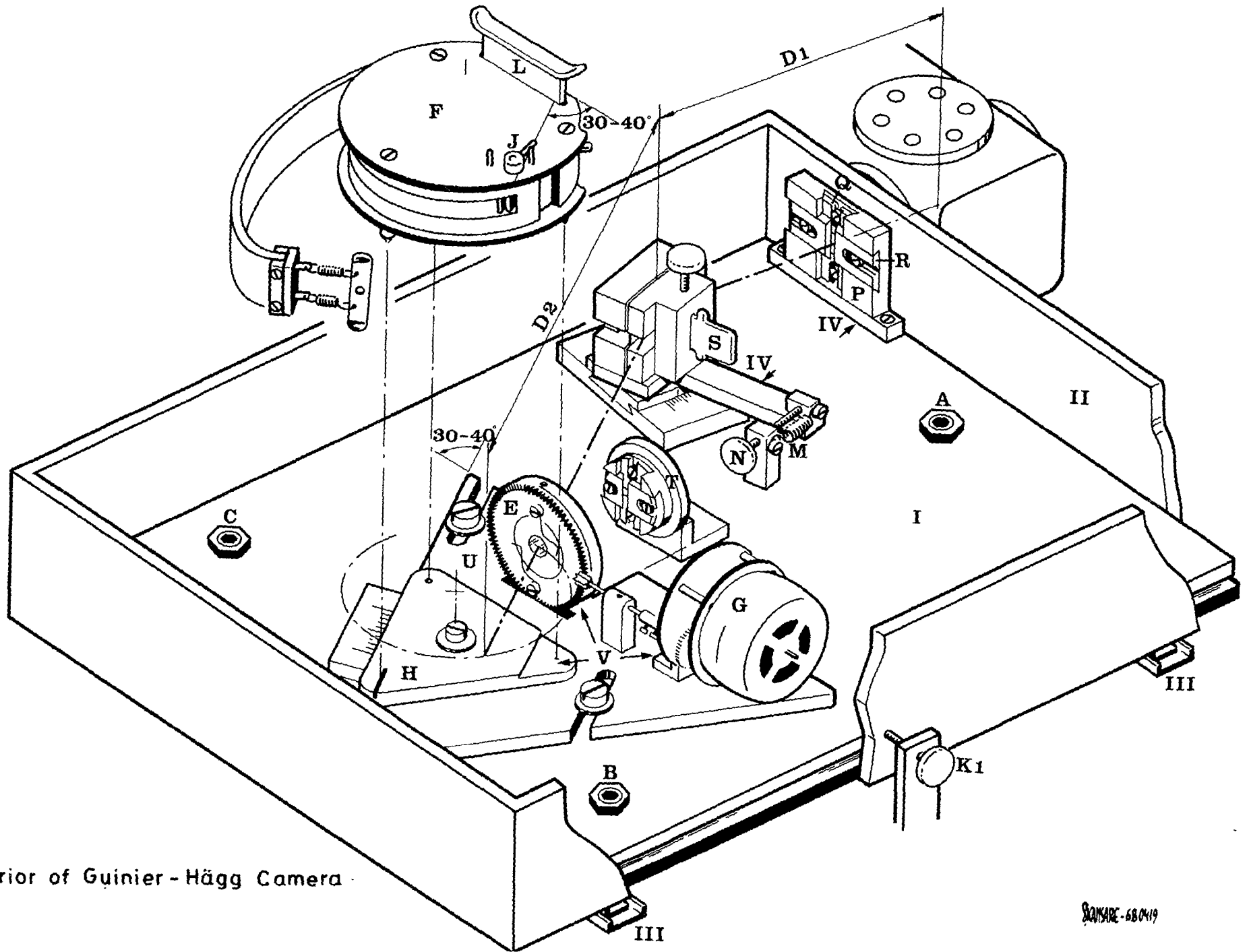
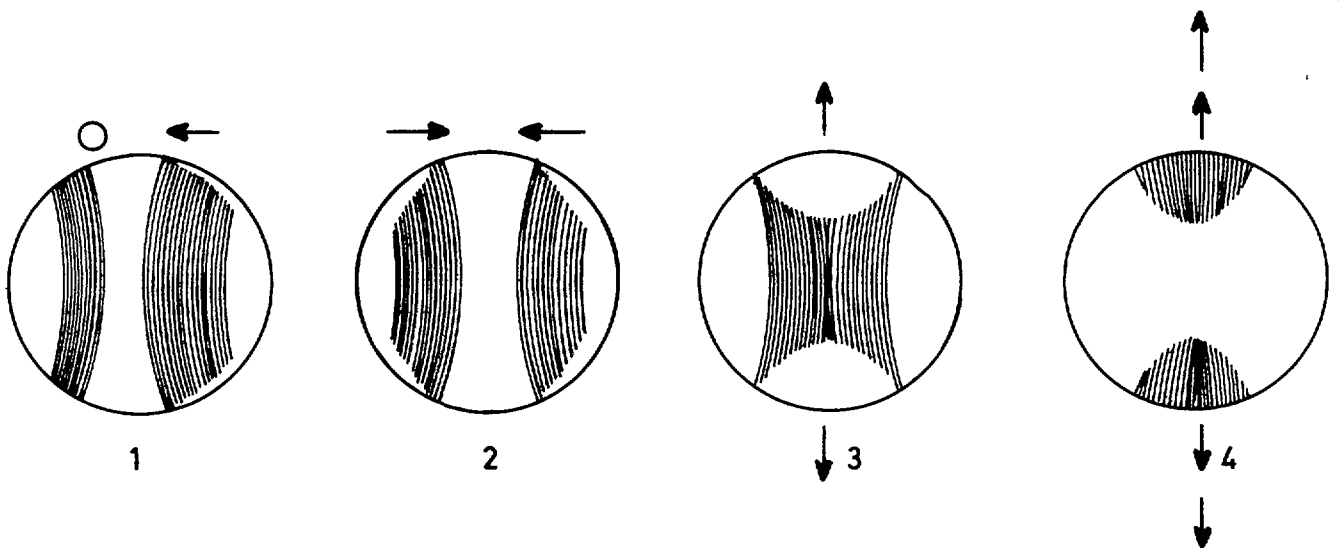
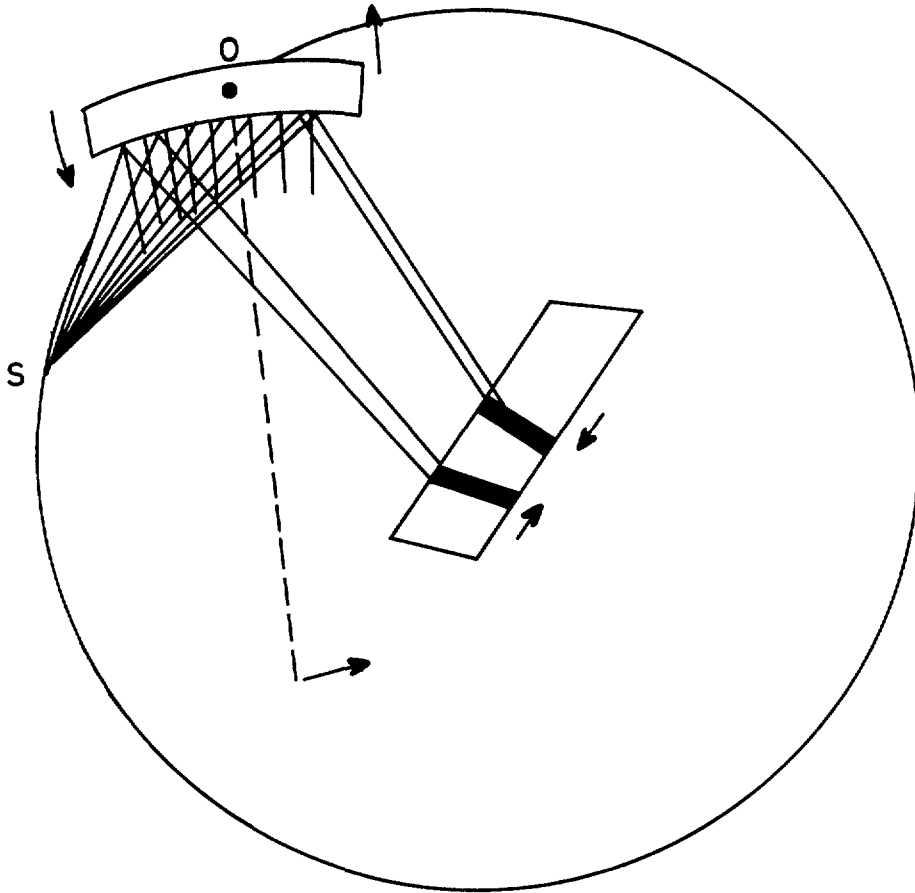


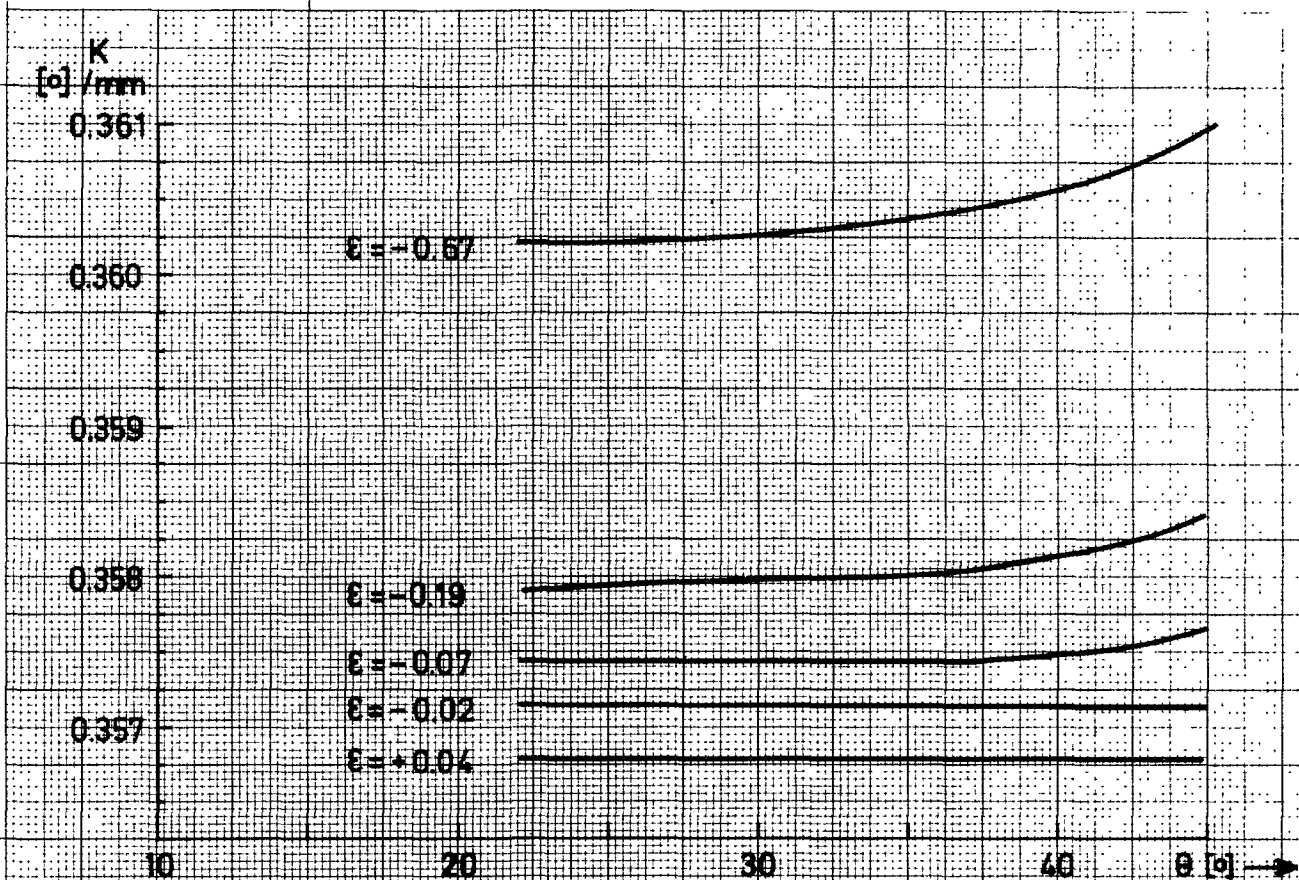
Fig.10 Interior of Guinier - Hägg Camera



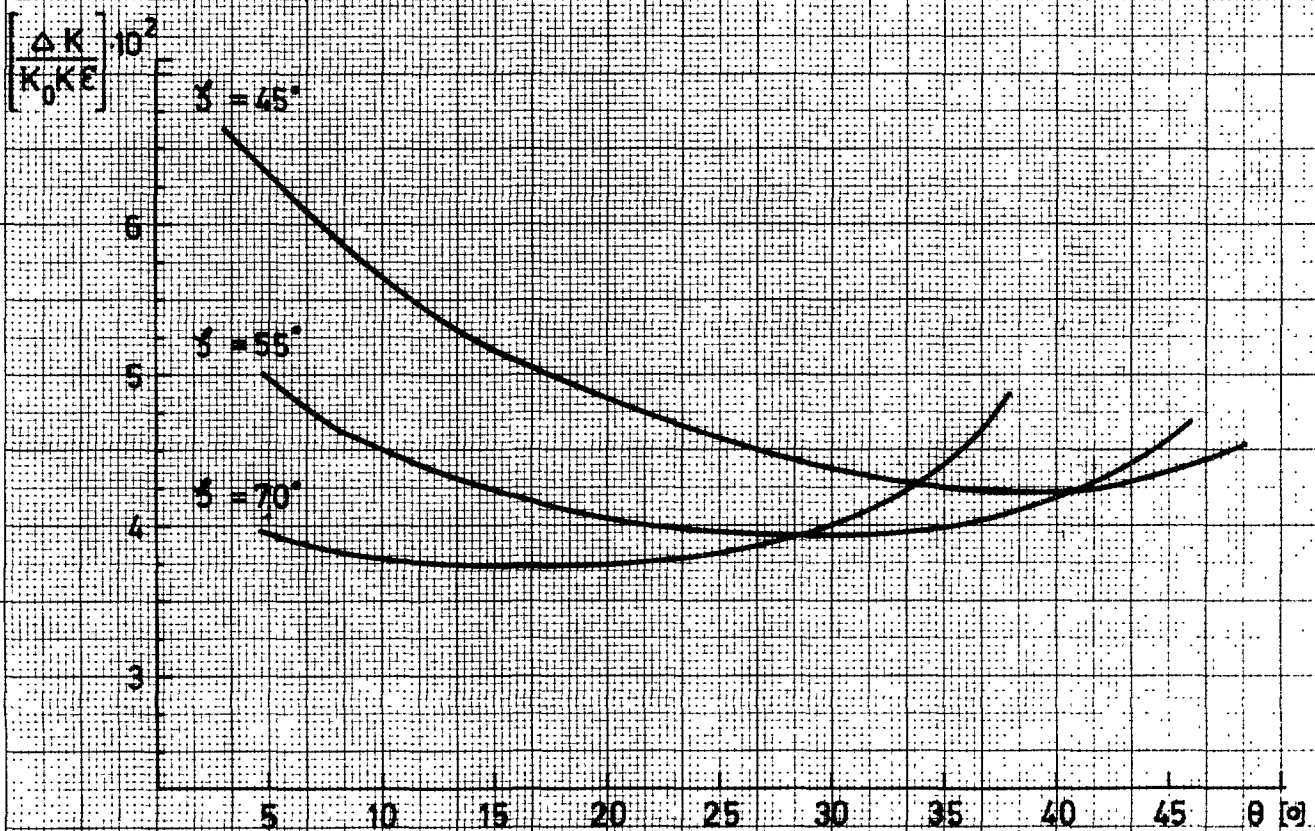
Fluorescent images of approach to focusing condition  
 (1) incorrect distance source to crystal  
 (2,3,&4) correct source-crystal distance for focusing

Fig.11 Alignment of the Monochromator Crystal.

Fig 12



Variation of camera constant,  $K$ , as a function of  $\theta$  for different settings of the sample relative to the recording circle.



(b) Relative change of camera constant  $\Delta K / K \cdot K_0 \cdot \epsilon$ , as a function of Bragg angle at different values of  $\psi$ .



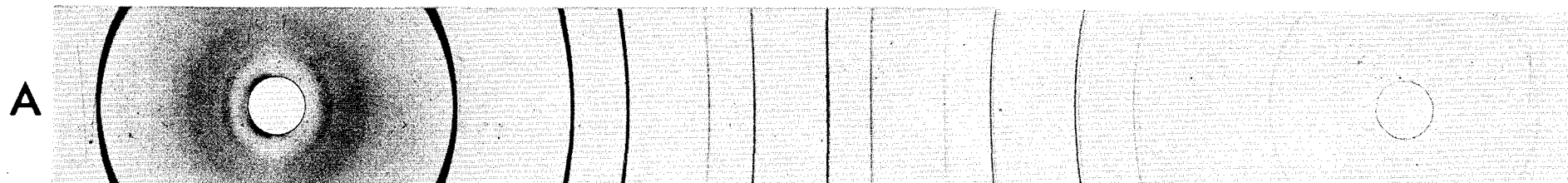
PLATES I & II

COMPARISON PHOTOGRAPHS OF POWDER PATTERNS

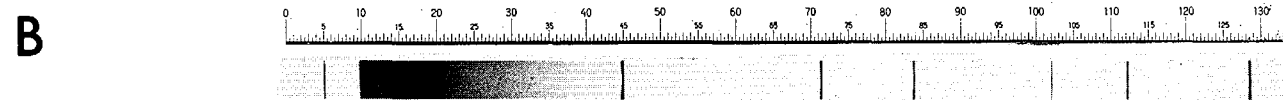
obtained with

- A. Debye - Scherrer camera of 11 · 46 cm diameter  
(2 mm = 1°  $\theta$ )                      CuK $\alpha_{1, 2}$  radiation
- B. Guinier - Hägg camera of 8 cm diameter  
(2 · 8 mm = 1°  $\theta$ )                      CuK $\alpha_1$  radiation



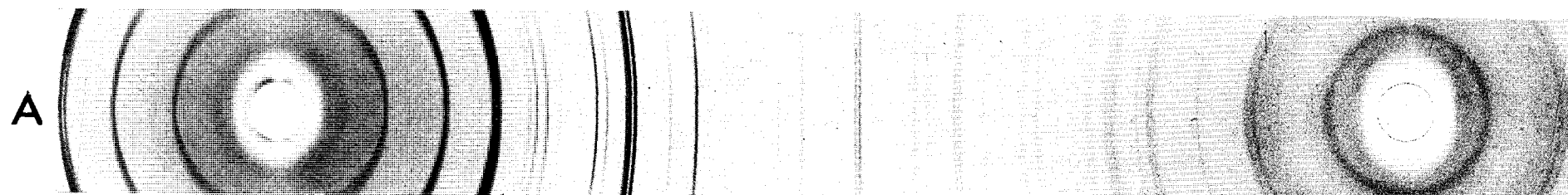


Exposure time 3 hours

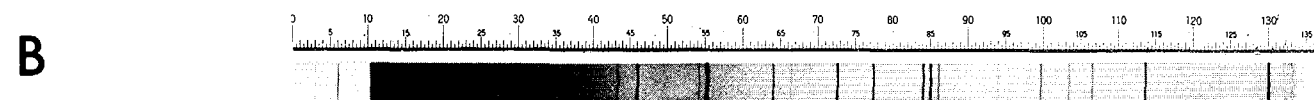


Exposure time 15 minutes

Silicon



Exposure time 8 hours



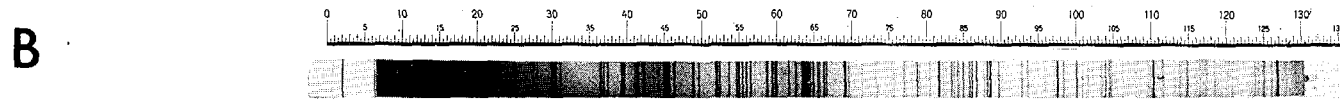
Exposure time 30 minutes

Black Phosphorous

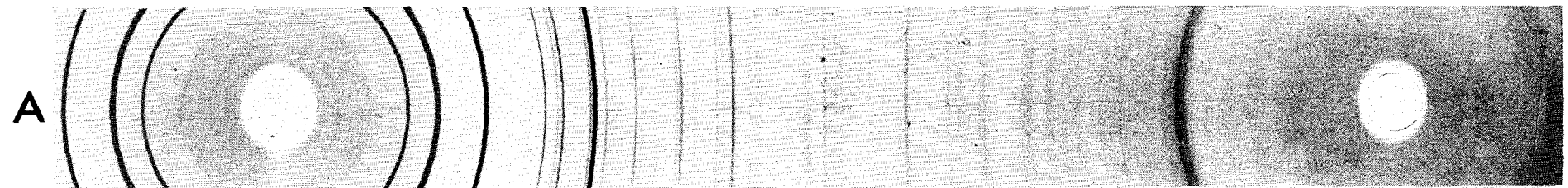
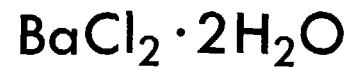




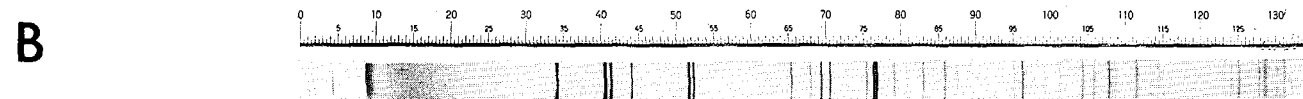
Exposure time 6 hours



Exposure time 90 minutes



Exposure time 4 hours



Exposure time 30 minutes





APPENDIX I

LISTING OF COMPUTER PROGRAMME MOTT







```

0001      DIMENSION IH(3),REFX(8),REFY(8),TIT(20)
0002      REAL LAMBDA
C
0003      100 FORMAT(2I5,2F10.5,45X,I5)
0004      101 FORMAT(8F10.6)
0005      102 FORMAT(3I5,2F10.5,I2)
0006      103 FORMAT(5F10.5,2X,3I5,I7,5X,F10.5)
0007      104 FORMAT('0',5X,'S',7X,'S-S0',8X,'CK',5X,'THETA',6X,'SINSQ',7X,'H',4
      *X,'K',4X,'L',6X,'N',10X,'D',/)
0008      105 FORMAT('1',20X,'THIS MOTT CALCULATION CONCERNS MEASURED GUINI
      *ER INTERVALS FOR',/)
0009      106 FORMAT('0',20A4,////////)
0010      107 FORMAT(20A4)
0011      108 FORMAT('0', 'THE FOLLOWING',I5,2X,'CALIBRATING POINTS HAVE BEEN
      * USED',//)
0012      109 FORMAT('0',20X,'S-S0(CAL) ',8F10.3)
0013      110 FORMAT('0',20X,'CK(CAL) ',8F10.6)
0014      111 FORMAT('0',20X,'S0 = 'F10.3,20X,'LAMBDA = ',F10.5,' Å',//)
C
0015      7 READ(5,107)(TIT(I),I=1,20)
0016      READ(5,100)NPUNCH,NREF,S0,LAMBDA,NEWCAL
0017      READ(5,101)(REFX(I),I=1,NREF)
0018      READ(5,101)(REFY(I),I=1,NREF)
0019      WRITE(6,105)
0020      WRITE(6,106)(TIT(I),I=1,20)
0021      WRITE(6,108)NREF
0022      WRITE(6,109)(REFX(I),I=1,NREF)
0023      WRITE(6,110)(REFY(I),I=1,NREF)
0024      WRITE(6,111)S0,LAMBDA
0025      WRITE(6,104)
0026      N=1
0027      1 READ(5,102)(IH(I),I=1,3),S,WI,IVL
0028      IF(IH(1)-10000)2,5,2
0029      2 SSO=S-S0
0030      CALL INTER(1,NREF,2,SSO,CK,REFX,REFY)
0031      THETA=SSO*CK
0032      THRAD=THETA/57.295795
0033      SINTH=SIN(THRAD)
0034      SINSQ=SINTH*SINTH
0035      D=0.5*LAMBDA/SINTH
0036      WRITE(6,103)S,SSO,CK,THETA,SINSQ,(IH(I),I=1,3),N,D
0037      IF(NPUNCH)4,3,4
0038      3 WRITE(7,102)(IH(I),I=1,3),SINSQ,WI,IVL
0039      4 N=N+1
0040      GO TO 1
0041      5 IF(NEWCAL)6,6,7
0042      6 CALL EXIT
0043      END

```

```

0001          SUBROUTINE INTER(JB,JE,L,XP,YP,X,Y)
0002          DIMENSION X(1),Y(1)
0003          100 FORMAT(51H0 TOO HIGH ORDER OF INTERPOLATION REQUESTED. ORDER=,I3,5
              1H USED)
0004          101 FORMAT(5H0 X =,1PE12.4,16H NOT IN INTERVAL)
0005          IF(L+JB-JE)2,2,1
0006          1 L=JE-JB
0007          WRITE(6,100)L
0008          2 IF(X(JB)-XP)4,9,3
0009          3 WRITE(6,101)XP
0010          GO TO 9
0011          4 IF(XP-X(JE))16,11,5
0012          5 WRITE(6,101)XP
0013          GO TO 11
0014          16 I=JB+1
0015          6 IF(XP-X(I))8,8,7
0016          7 I=I+1
0017          GO TO 6
0018          8 IR=I-L/2
0019          IS=I+(L+1)/2
0020          IF(IR-JB)9,12,10
0021          9 IR=JB
0022          IS=L+JB
0023          GO TO 12
0024          10 IF(JE-IS)11,12,12
0025          11 IR=JE-L
0026          IS=JE
0027          12 YP=0.
0028          DO 15 I=IR,IS
0029          A=Y(I)
0030          DO 14 K=IB,IS
0031          IF(I-K)13,14,13
0032          13 A=A*(XP-X(K))/(X(I)-X(K))
0033          14 CONTINUE
0034          15 YP=YP+A
0035          RETURN
0036          END

```



APPENDIX II

RESULTS OBTAINED FROM MEASUREMENTS OF SOME  
GUINIER - HÄGG PATTERNS OBTAINED IN ROUTINE STUDIES



REFINEMENT OF

CE O2 CUBIC

H K L SINSQ(O) SINSQ(C) OBS-CALC D OBS

WAVELENGTH = 1.54051

1	1	1	0.060771	0.060775	-0.000004	3.12453
2	0	0	0.081006	0.081033	-0.000027	2.70630
2	2	0	0.162093	0.162066	0.000026	1.91317
3	1	1	0.222802	0.222841	-0.000039	1.63183
2	2	2	0.243123	0.243099	0.000024	1.56215
4	0	0	0.324104	0.324133	-0.000028	1.35298
3	3	1	0.384852	0.384907	-0.000056	1.24162
4	2	0	0.405249	0.405166	0.000083	1.20997
4	2	2	0.486206	0.486199	0.000007	1.10465

NUMBER OF REFLECTIONS = 9

NUMBER OF REFLECTIONS USED = 9 FOR A GATE OF 0.00030

	PARAMETERS	STANDARD DEVIATIONS	LAST SHIFTS
A	= 5.411693	0.000134	0.000000

REFINEMENT OF

TH O2 CUBIC

H K L SINSQ(O) SINSQ(C) OBS-CALC D OBS

WAVELENGTH = 1.54051

1	1	1	0.056782	0.056815	-0.000033	3.23243
2	0	0	0.075752	0.075753	-0.000001	2.79858
2	2	0	0.151478	0.151506	-0.000028	1.97906
3	1	1	0.208330	0.208320	0.000010	1.68756
2	2	2	0.227271	0.227258	0.000012	1.61571
4	0	0	0.302915	0.303011	-0.000097	1.39950
3	3	1	0.359851	0.359826	0.000025	1.28402
4	2	0	0.378844	0.378764	0.000080	1.25142
4	2	2	0.454523	0.454517	0.000006	1.14250

NUMBER OF REFLECTIONS = 9

NUMBER OF REFLECTIONS USED = 9 FOR A GATE OF 0.00030

	PARAMETERS	STANDARD DEVIATIONS	LAST SHIFTS
A	= 5.597126	0.000173	0.000000



REFINEMENT OF

U O2 CUBIC

H	K	L	SINSQ(O)	SINSQ(C)	OBS-CALC	D OBS
---	---	---	----------	----------	----------	-------

WAVELENGTH = 1.54051

1	1	1	0.059465	0.059473	-0.000008	3.15867
2	0	0	0.079318	0.079298	0.000020	2.73495
2	2	0	0.158567	0.158595	-0.000028	1.93432
3	1	1	0.218091	0.218068	0.000023	1.64936
2	2	2	0.237939	0.237893	0.000046	1.57907
4	0	0	0.317226	0.317190	0.000035	1.36757
3	3	1	0.376660	0.376663	-0.000003	1.25505
4	2	0	0.396444	0.396488	-0.000043	1.22333
4	2	2	0.475762	0.475785	-0.000023	1.11671

NUMBER OF REFLECTIONS = 9

NUMBER OF REFLECTIONS USED = 9 FOR A GATE OF 0.00030

PARAMETERS STANDARD DEVIATIONS LAST SHIFTS

A = 5.470595 0.000107 -0.000000

## REFINEMENT OF

PU 02

CUBIC

H	K	L	SINSQ(O)	SINSQ(C)	OBS-CALC	D OBS
---	---	---	----------	----------	----------	-------

WAVELENGTH = 1.54051

1	1	1	0.061076	0.061150	-0.000074	3.11672
2	0	0	0.081603	0.081533	0.000070	2.69638
2	2	0	0.163009	0.163067	-0.000058	1.90778
3	1	1	0.224112	0.224217	-0.000105	1.62705
2	2	2	0.244489	0.244600	-0.000112	1.55778
4	0	0	0.326093	0.326134	-0.000041	1.34885
3	3	1	0.387298	0.387284	0.000015	1.23769
4	2	0	0.407643	0.407667	-0.000024	1.20641
4	2	2	0.489421	0.489200	0.000221	1.10101

NUMBER OF REFLECTIONS = 9

NUMBER OF REFLECTIONS USED = 9 FOR A GATE OF 0.00030

PARAMETERS STANDARD DEVIATIONS LAST SHIFTS

A = 5.395066 0.000357 0.000000

REFINEMENT OF

PB(NO3)2 CUBIC

H K L SINSQ(O) SINSQ(C) OBS-CALC D OBS

WAVELENGTH = 1.54051

1	1	1	0.028876	0.028845	0.000031	4.53281
2	0	0	0.038455	0.038460	-0.000005	3.92787
2	1	0	0.048090	0.048076	0.000014	3.51243
2	1	1	0.057729	0.057691	0.000039	3.20580
2	2	0	0.076935	0.076921	0.000014	2.77698
3	1	1	0.105782	0.105766	0.000016	2.36826
2	2	2	0.115395	0.115381	0.000014	2.26747
4	0	0	0.153857	0.153842	0.000015	1.96370
3	3	1	0.182708	0.182687	0.000021	1.80200
4	2	0	0.192310	0.192302	0.000007	1.75644
4	2	2	0.230772	0.230763	0.000009	1.60340
5	1	1	0.259544	0.259608	-0.000063	1.51192
4	4	0	0.307661	0.307683	-0.000022	1.38867
5	3	1	0.336595	0.336529	0.000066	1.32764
6	0	0	0.346090	0.346144	-0.000054	1.30930
6	2	0	0.384565	0.384604	-0.000039	1.24208
5	3	3	0.413534	0.413450	0.000084	1.19779
6	2	2	0.423049	0.423065	-0.000016	1.18424
7	1	1	0.490281	0.490371	-0.000089	1.10005
6	4	0	0.500051	0.499986	0.000065	1.08925

NUMBER OF REFLECTIONS = 20

NUMBER OF REFLECTIONS USED = 20 FOR A GATE OF 0.00030

PARAMETERS	STANDARD DEVIATIONS	LAST SHIFTS
A = 7.855203	0.000138	0.000000

## REFINEMENT OF

MO3 SB7

CUBIC

H	K	L	SINSQ(O)	SINSQ(C)	OBS-CALC	D CBS
---	---	---	----------	----------	----------	-------

WAVELENGTH = 1.54051

2	0	0	0.025921	0.025918	0.000002	4.78422
2	1	1	0.038885	0.038877	0.000008	3.90608
3	1	0	0.064801	0.064796	0.000005	3.02583
2	2	2	0.077771	0.077755	0.000017	2.76201
3	2	1	0.090701	0.090714	-0.000013	2.55758
4	0	0	0.103679	0.103673	0.000006	2.39216
4	1	1	0.116614	0.116632	-0.000018	2.25558
4	2	0	0.129575	0.129591	-0.000017	2.13981
4	4	0	0.207313	0.207346	-0.000033	1.69169
5	3	0	0.220313	0.220305	0.000008	1.64102
4	4	2	0.233277	0.233264	0.000013	1.59477
5	3	2	0.246228	0.246223	0.000005	1.55226
6	2	0	0.259196	0.259182	0.000013	1.51294
5	4	1	0.272156	0.272142	0.000015	1.47647
6	2	2	0.285089	0.285101	-0.000012	1.44259
7	2	1	0.349919	0.349896	0.000023	1.30212
7	3	0	0.375814	0.375815	-0.000001	1.25646
6	5	1	0.401699	0.401733	-0.000034	1.21530
8	0	0	0.414719	0.414692	0.000027	1.19607
8	1	1	0.427612	0.427651	-0.000039	1.17790
6	4	4	0.440616	0.440610	0.000006	1.16039
8	2	2	0.466549	0.466528	0.000020	1.12768
6	6	2	0.492445	0.492447	-0.000002	1.09763

NUMBER OF REFLECTIONS = 23

NUMBER OF REFLECTIONS USED = 23 FOR A GATE OF 0.00020

PARAMETERS STANDARD DEVIATIONS LAST SHIFTS

A = 9.568894 0.000071 0.000000

## REFINEMENT OF

SI O2 (ALPHA QUARTZ) HEXAGONAL

H	K	L	SINSQ(O)	SINSQ(C)	OBS-CALC	D OBS
WAVELENGTH = 1.54051						
1	0	0	0.032804	0.032779	0.000025	4.25279
1	0	1	0.053210	0.053092	0.000118	3.33916
1	1	0	0.098312	0.098337	-0.000025	2.45658
1	0	2	0.113985	0.114029	-0.000045	2.28145
1	1	1	0.118654	0.118650	0.000005	2.23611
2	0	0	0.131164	0.131116	0.000047	2.12681
2	0	1	0.151362	0.151429	-0.000067	1.97982
1	1	2	0.179485	0.179588	-0.000102	1.81811
2	0	2	0.212307	0.212367	-0.000060	1.67168
1	0	3	0.215630	0.215593	0.000037	1.65875
2	1	1	0.249655	0.249766	-0.000111	1.54157
1	1	3	0.281149	0.281151	-0.000002	1.45267
2	1	2	0.310691	0.310704	-0.000012	1.38188
2	0	3	0.313929	0.313930	-0.000001	1.37473
3	0	1	0.315319	0.315324	-0.000005	1.37170
1	0	4	0.357735	0.357781	-0.000046	1.28782
3	0	2	0.376249	0.376262	-0.000013	1.25573
2	2	0	0.393361	0.393348	0.000013	1.22811
2	1	3	0.412323	0.412267	0.000056	1.19954
2	2	1	0.413612	0.413661	-0.000049	1.19767
1	1	4	0.423394	0.423339	0.000056	1.18375
3	1	0	0.426168	0.426127	0.000041	1.17990
3	1	1	0.446515	0.446440	0.000075	1.15270

NUMBER OF REFLECTIONS = 23

NUMBER OF REFLECTIONS USED = 23 FOR A GATE OF 0.00020

	PARAMETERS	STANDARD DEVIATIONS	LAST SHIFTS
A	= 4.912537	0.000143	0.000000
C	= 5.404452	0.000270	0.000000

## REFINEMENT OF

AL2 O3

HEXAGONAL

H	K	L	SINSQ(O)	SINSQ(C)	OBS-CALC	D OBS
---	---	---	----------	----------	----------	-------

WAVELENGTH = 1.54051

1	0	2	0.048930	0.048995	-0.000065	3.48215
1	0	4	0.091080	0.091183	-0.000103	2.55225
1	1	0	0.104760	0.104796	-0.000036	2.37978
1	1	3	0.136400	0.136437	-0.000037	2.08558
2	0	2	0.153670	0.153790	-0.000120	1.96490
2	0	4	0.195890	0.195979	-0.000089	1.74032
1	1	6	0.231270	0.231361	-0.000091	1.60168
2	1	2	0.258540	0.258586	-0.000046	1.51485
1	0	8	0.259910	0.259938	-0.000028	1.51086
2	1	4	0.300780	0.300775	0.000005	1.40446
3	0	0	0.314260	0.314387	-0.000127	1.37401
2	0	8	0.364830	0.364733	0.000097	1.27523
1	0	10	0.386500	0.386503	-0.000004	1.23897
1	1	9	0.389540	0.389569	-0.000029	1.23412
2	2	0	0.419230	0.419182	0.000047	1.18962
3	0	6	0.441080	0.440953	0.000127	1.15978
2	2	3	0.450830	0.450824	0.000006	1.14717
3	1	2	0.468220	0.468177	0.000043	1.12567
2	1	8	0.469590	0.469529	0.000061	1.12402
2	0	10	0.491270	0.491299	-0.000029	1.09894

NUMBER OF REFLECTIONS = 20

NUMBER OF REFLECTIONS USED = 20 FOR A GATE OF 0.00025

PARAMETERS	STANDARD DEVIATIONS	LAST SHIFTS
A = 4.758751	0.000189	0.000000
C = 12.990552	0.000735	0.000000

## REFINEMENT OF

ALPHA-Fe<sub>2</sub>O<sub>3</sub> HEXAGONAL

H	K	L	SINSQ(O)	SINSQ(C)	OBS-CALC	D OBS
---	---	---	----------	----------	----------	-------

WAVELENGTH = 1.54051

1	0	2	0.043722	0.043753	-0.000031	3.68371
1	0	4	0.081464	0.081402	0.000062	2.69868
1	1	0	0.093655	0.093610	0.000045	2.51692
1	1	3	0.121902	0.121847	0.000056	2.20612
2	0	4	0.175000	0.175012	-0.000012	1.84126
1	1	6	0.206586	0.206558	0.000029	1.69466
1	0	8	0.232033	0.232000	0.000033	1.59904
2	1	4	0.268601	0.268622	-0.000020	1.48621
3	0	0	0.280789	0.280829	-0.000040	1.45360
1	0	10	0.344893	0.344948	-0.000054	1.31157
2	2	0	0.374420	0.374439	-0.000019	1.25880
3	0	6	0.393812	0.393777	0.000035	1.22741
2	1	8	0.419208	0.419219	-0.000011	1.18965
2	0	10	0.438541	0.438557	-0.000016	1.16313
3	1	4	0.455842	0.455841	0.000001	1.14085
2	2	6	0.487372	0.487387	-0.000014	1.10333

NUMBER OF REFLECTIONS = 16

NUMBER OF REFLECTIONS USED = 16 FOR A GATE OF 0.00050

	PARAMETERS	STANDARD DEVIATIONS	LAST SHIFTS
A	= 5.035054	0.000168	0.000000
C	= 13.751387	0.000696	0.000000

## REFINEMENT UF

CA5(OH)(PO4)3 HEXAGONAL

HYDROXY APETITE

H	K	L	SINSQ(O)	SINSQ(C)	OBS-CALC	D CBS
WAVELENGTH = 1.54051						
1	0	0	0.008890	0.008917	-0.000027	8.16928
1	0	1	0.021360	0.021440	-0.000080	5.27028
2	0	0	0.035540	0.035667	-0.000127	4.08579
1	1	1	0.039200	0.039274	-0.000074	3.89038
0	0	2	0.050020	0.050092	-0.000072	3.44400
1	0	2	0.058880	0.059009	-0.000129	3.17432
2	1	0	0.062360	0.062418	-0.000058	3.08448
2	1	1	0.074890	0.074941	-0.000051	2.81464
1	1	2	0.076840	0.076843	-0.000003	2.77869
3	0	0	0.080190	0.080252	-0.000062	2.72003
2	0	2	0.085730	0.085760	-0.000030	2.63068
3	0	1	0.092840	0.092775	0.000065	2.52794
2	1	2	0.112520	0.112510	0.000010	2.29625
3	1	0	0.115970	0.115919	0.000051	2.26184
2	2	1	0.119340	0.119525	-0.000185	2.22967
3	1	1	0.128450	0.128442	0.000008	2.14915
1	1	3	0.139470	0.139458	0.000012	2.06250
2	2	2	0.157090	0.157094	-0.000004	1.94339
3	1	2	0.166050	0.166011	0.000039	1.89023
3	2	0	0.169300	0.169420	-0.000120	1.87200
2	1	3	0.175170	0.175125	0.000045	1.84037
3	2	1	0.181970	0.181943	0.000027	1.80565
4	1	0	0.187380	0.187254	0.000126	1.77940
4	0	2	0.192790	0.192762	0.000028	1.75425
0	0	4	0.200400	0.200369	0.000031	1.72062
3	2	2	0.219480	0.219512	-0.000032	1.64413
3	1	3	0.228580	0.228626	-0.000046	1.61107
4	2	0	0.249740	0.249672	0.000068	1.54131
3	3	1	0.253420	0.253278	0.000142	1.53008
2	1	4	0.262640	0.262786	-0.000146	1.50298
5	0	2	0.273070	0.273013	0.000057	1.47400
3	0	4	0.280600	0.280620	-0.000020	1.45409
5	1	1	0.288930	0.288945	-0.000015	1.43297
4	2	2	0.299780	0.299764	0.000016	1.40680
5	1	2	0.326350	0.326514	-0.000164	1.34832
4	3	1	0.342580	0.342446	0.000134	1.31599
5	2	0	0.347970	0.347757	0.000213	1.30576
5	2	1	0.360300	0.360280	0.000020	1.28322
4	2	3	0.362270	0.362379	-0.000109	1.27973
2	1	5	0.375480	0.375494	-0.000014	1.25702
4	3	2	0.380010	0.380015	-0.000005	1.24950
6	1	0	0.383220	0.383424	-0.000204	1.24426
4	1	4	0.387820	0.387622	0.000198	1.23686
5	1	3	0.388980	0.389129	-0.000149	1.23501
5	2	2	0.397980	0.397849	0.000131	1.22097
4	4	0	0.428050	0.428008	0.000042	1.17730
4	3	3	0.442650	0.442630	0.000020	1.15772
4	2	4	0.449970	0.450040	-0.000070	1.14827
1	1	6	0.477730	0.477580	0.000150	1.11441
3	2	5	0.482600	0.482496	0.000104	1.10877

NUMBER OF REFLECTIONS = 50

NUMBER OF REFLECTIONS USED = 50 FOR A GATE OF 0.00030

PARAMETERS	STANDARD DEVIATIONS	LAST SHIFTS
A = 9.418860	0.000456	0.000000
C = 6.883031	0.000556	0.000000



## REFINEMENT OF

TH AU3

HEXAGONAL

P6(3)

H	K	L	SINSQ(O)	SINSQ(C)	OBS-CALC	D OBS
---	---	---	----------	----------	----------	-------

WAVELENGTH = 1.54051

0	0	2	0.027890	0.027858	0.000032	4.61222
2	1	2	0.061610	0.061570	0.000040	3.10319
3	1	0	0.062660	0.062606	0.000054	3.07708
2	2	1	0.064830	0.064755	0.000075	3.02515
3	1	1	0.069510	0.069571	-0.000061	2.92153
3	0	2	0.071170	0.071201	-0.000031	2.88726
1	1	3	0.077120	0.077129	-0.000009	2.77365
4	0	1	0.084040	0.084019	0.000021	2.65700
2	2	2	0.085680	0.085649	0.000031	2.63145
3	1	2	0.090450	0.090465	-0.000015	2.56112
3	2	0	0.091530	0.091502	0.000028	2.54597
2	1	3	0.096330	0.096393	-0.000063	2.48173
3	2	1	0.098620	0.098466	0.000154	2.45274
4	1	0	0.101170	0.101133	0.000037	2.42163
3	0	3	0.105880	0.106024	-0.000144	2.36716
4	1	1	0.108160	0.108098	0.000062	2.34208
0	0	4	0.111390	0.111434	-0.000044	2.30787
1	0	4	0.116220	0.116249	-0.000030	2.25941
3	2	2	0.119280	0.119360	-0.000080	2.23024
5	0	0	0.120410	0.120397	0.000013	2.21975
3	1	3	0.125240	0.125288	-0.000048	2.17652
4	1	2	0.129070	0.128992	0.000078	2.14399
2	0	4	0.130660	0.130697	-0.000037	2.13090
4	0	3	0.139740	0.139735	0.000005	2.06051
4	2	1	0.141780	0.141809	-0.000029	2.04563
2	1	4	0.145230	0.145145	0.000085	2.02119
5	1	0	0.149300	0.149292	0.000008	1.99345
3	2	3	0.154130	0.154183	-0.000053	1.96196
4	2	2	0.162640	0.162703	-0.000063	1.90994
4	1	3	0.163650	0.163815	-0.000165	1.90404
2	2	4	0.169220	0.169224	-0.000004	1.87244
3	1	4	0.173970	0.174040	-0.000070	1.84670
4	3	0	0.178150	0.178188	-0.000038	1.82491
6	0	1	0.180200	0.180336	-0.000136	1.81450
1	1	5	0.188560	0.188563	-0.000003	1.77382
5	2	1	0.194990	0.194784	0.000206	1.74433
4	2	3	0.197410	0.197526	-0.000116	1.73360
3	2	4	0.203050	0.202935	0.000115	1.70936
2	1	5	0.207630	0.207826	-0.000196	1.69040
4	1	4	0.212360	0.212567	-0.000207	1.67147
6	1	2	0.234790	0.234941	-0.000151	1.58963
3	1	5	0.236640	0.236721	-0.000081	1.58340
4	3	3	0.240840	0.240869	-0.000029	1.56953
4	2	4	0.246190	0.246278	-0.000088	1.55238
5	2	3	0.250550	0.250501	0.000049	1.53882
5	1	4	0.260830	0.260726	0.000104	1.50819
7	0	2	0.263910	0.263837	0.000073	1.49936
6	1	3	0.269700	0.269764	-0.000064	1.48318
4	1	5	0.275090	0.275248	-0.000159	1.46858
6	2	2	0.278320	0.278284	0.000036	1.46003
6	0	4	0.284660	0.284805	-0.000145	1.44368
4	3	4	0.289630	0.289621	0.000009	1.43124

5	4	0	0.293770	0.293769	0.000001	1.42112
5	2	4	0.299130	0.299253	-0.000123	1.40833
6	3	0	0.303430	0.303400	0.000030	1.39832
2	2	6	0.308490	0.308516	-0.000026	1.38680
6	3	1	0.310330	0.310365	-0.000035	1.38268
6	2	3	0.313170	0.313107	0.000063	1.37640
8	0	1	0.315430	0.315181	0.000249	1.37146
6	1	4	0.318570	0.318516	0.000054	1.36468
4	0	6	0.327690	0.327780	-0.000090	1.34556
7	1	3	0.337120	0.337187	-0.000067	1.32661
6	0	5	0.347490	0.347487	0.000003	1.30666
4	1	6	0.351840	0.351859	-0.000019	1.29856
5	0	6	0.371170	0.371123	0.000047	1.26429
3	3	6	0.380850	0.380754	0.000096	1.24812
5	1	6	0.400270	0.400018	0.000252	1.21747
8	2	0	0.404310	0.404534	-0.000224	1.21137
4	4	5	0.405290	0.405277	0.000013	1.20991
7	3	2	0.408360	0.408313	0.000047	1.20535
6	3	4	0.414740	0.414834	-0.000094	1.19604
6	2	5	0.424590	0.424541	0.000049	1.18209
4	3	6	0.429210	0.428913	0.000297	1.17571
3	2	7	0.432980	0.432767	0.000213	1.17058
9	1	0	0.438230	0.438245	-0.000015	1.16355
4	1	7	0.442500	0.442399	0.000101	1.15792
0	0	8	0.445720	0.445734	-0.000014	1.15373
9	0	3	0.453090	0.452768	0.000322*	1.14431
6	1	6	0.457800	0.457808	-0.000009	1.13840

NUMBER OF REFLECTIONS = 79

NUMBER OF REFLECTIONS USED = 78 FOR A GATE OF 0.00030

	PARAMETERS	STANDARD DEVIATIONS	LAST SHIFTS
A	= 12.816400	0.000535	0.000000
C	= 9.229675	0.000499	0.000000

REFINEMENT OF

ALPHA-TIN TETRAGONAL

H K L SINSQ(O) SINSQ(C) OBS-CALC D OBS

WAVELENGTH = 1.54051

2	0	0	0.069770	0.069792	-0.000023	2.91609
1	0	1	0.076097	0.076090	0.000007	2.79222
2	2	0	0.139628	0.139585	0.000043	2.06134
2	1	1	0.145950	0.145883	0.000067	2.01620
3	0	1	0.215641	0.215675	-0.000034	1.65870
1	1	2	0.269478	0.269464	0.000014	1.48379
4	0	0	0.279197	0.279170	0.000027	1.45774
3	2	1	0.285417	0.285468	-0.000050	1.44176
4	2	0	0.348982	0.348962	0.000020	1.30387
4	1	1	0.355297	0.355260	0.000037	1.29223
3	1	2	0.409038	0.409049	-0.000011	1.20435
4	3	1	0.494805	0.494845	-0.000040	1.09501

NUMBER OF REFLECTIONS = 12

NUMBER OF REFLECTIONS USED = 12 FOR A GATE OF 0.00020

	PARAMETERS	STANDARD DEVIATIONS	LAST SHIFTS
A	= 5.831230	0.000159	0.000000
C	= 3.180755	0.000189	0.000000

## REFINEMENT OF

MN3 O4

TETRAGONAL

H	K	L	SINSQ(O)	SINSQ(C)	OBS-CALC	D OBS
---	---	---	----------	----------	----------	-------

WAVELENGTH = 1.54051

1	0	1	0.024437	0.024513	-0.000076	4.92735
1	1	2	0.062242	0.062266	-0.000024	3.08740
2	0	0	0.071503	0.071571	-0.000068	2.88053
1	0	3	0.077436	0.077474	-0.000037	2.76797
2	1	1	0.096112	0.096084	0.000028	2.48454
2	0	2	0.097997	0.098052	-0.000055	2.46053
0	0	4	0.105968	0.105922	0.000046	2.36618
2	2	0	0.143082	0.143142	-0.000060	2.03630
2	0	4	0.177480	0.177493	-0.000013	1.82835
1	0	5	0.183374	0.183395	-0.000021	1.79873
3	1	2	0.205314	0.205408	-0.000095	1.69991
3	2	1	0.239156	0.239226	-0.000071	1.57505
2	2	4	0.248965	0.249064	-0.000099	1.54371
4	0	0	0.286355	0.286284	0.000071	1.43940
3	0	5	0.326620	0.326538	0.000082	1.34776
4	1	3	0.363825	0.363758	0.000067	1.27699
4	2	2	0.384365	0.384336	0.000029	1.24240
4	0	4	0.392214	0.392206	0.000008	1.22991
2	1	7	0.413831	0.413849	-0.000018	1.19735
3	1	6	0.417277	0.417252	0.000026	1.19240
4	1	5	0.469670	0.469680	-0.000010	1.12393

NUMBER OF REFLECTIONS = 21

NUMBER OF REFLECTIONS USED = 21 FOR A GATE OF 0.00020

	PARAMETERS	STANDARD DEVIATIONS	LAST SHIFTS
A	= 5.758319	0.000237	-0.000000
C	= 9.466774	0.000595	-0.000000

REFINEMENT OF SR(DH)2.8H2 O TETRAGONAL P4/NCC

H	K	L	SINSQ(O)	SINSQ(C)	OBS-CALC	D OBS
WAVELENGTH = 1.54051						
1	1	0	0.014560	0.014597	-0.000037	6.38348
0	0	2	0.017587	0.017613	-0.000026	5.80820
2	0	0	0.029177	0.029193	-0.000016	4.50933
1	1	2	0.032192	0.032209	-0.000018	4.29301
2	0	2	0.046824	0.046806	0.000018	3.55958
2	2	0	0.058406	0.058386	0.000020	3.18716
0	0	4	0.070506	0.070451	0.000055	2.90082
2	2	2	0.076037	0.075999	0.000038	2.79334
3	1	1	0.077366	0.077386	-0.000020	2.76924
1	1	4	0.085036	0.085048	-0.000012	2.64139
3	1	2	0.090655	0.090595	0.000059	2.55823
2	0	4	0.099700	0.099644	0.000055	2.43942
2	1	4	0.106993	0.106943	0.000050	2.35481
3	1	3	0.112650	0.112612	0.000039	2.29492
4	0	0	0.116866	0.116772	0.000093	2.25316
2	2	4	0.128904	0.128838	0.000066	2.14537
3	3	0	0.131380	0.131369	0.000011	2.12505
4	0	2	0.134428	0.134385	0.000043	2.10082
3	1	4	0.143486	0.143434	0.000052	2.03343
4	2	0	0.146031	0.145965	0.000066	2.01564
3	3	2	0.149037	0.148981	0.000056	1.99520
4	2	1	0.150416	0.150368	0.000048	1.98603
0	0	6	0.158616	0.158516	0.000100	1.93402
4	2	2	0.163607	0.163578	0.000029	1.90429
1	1	6	0.173062	0.173112	-0.000051	1.85154
3	1	5	0.183015	0.183063	-0.000048	1.80049
4	3	1	0.186980	0.186860	0.000120	1.78130
4	0	4	0.187223	0.187224	-0.000001	1.78015
2	0	6	0.187660	0.187709	-0.000049	1.77807
5	1	0	0.189755	0.189755	0.000000	1.76823
3	3	4	0.201862	0.201820	0.000042	1.71438
5	1	2	0.207390	0.207368	0.000023	1.69138
2	2	6	0.216812	0.216902	-0.000090	1.65422
3	1	6	0.231479	0.231498	-0.000019	1.60095
5	3	0	0.248048	0.248141	-0.000093	1.54656
4	4	2	0.251126	0.251157	-0.000031	1.53705
5	3	1	0.252480	0.252544	-0.000063	1.53292
4	2	5	0.256013	0.256046	-0.000032	1.52231
5	1	4	0.260109	0.260206	-0.000097	1.51028
5	3	2	0.265713	0.265754	-0.000041	1.49427
4	0	6	0.275193	0.275288	-0.000095	1.46830
6	0	2	0.280280	0.280350	-0.000070	1.45492
0	0	8	0.281851	0.281806	0.000045	1.45086
3	1	7	0.288614	0.288740	-0.000126	1.43376
3	3	6	0.289916	0.289884	0.000031	1.43054
6	2	0	0.291843	0.291930	-0.000087	1.42580
6	2	1	0.296222	0.296334	-0.000112	1.41523
4	4	4	0.304002	0.303996	0.000006	1.39700
4	2	6	0.304404	0.304481	-0.000077	1.39608
6	2	2	0.309471	0.309543	-0.000073	1.38460
5	3	4	0.318508	0.318592	-0.000084	1.36482
6	0	4	0.333194	0.333189	0.000006	1.33440
5	1	6	0.348223	0.348270	-0.000047	1.30529
3	1	8	0.354840	0.354788	0.000052	1.29306
6	2	4	0.362385	0.362382	0.000003	1.27953
6	4	0	0.379573	0.379509	0.000064	1.25022
4	4	6	0.392093	0.392060	0.000033	1.23010
6	4	2	0.397158	0.397122	0.000036	1.22223
6	3	4	0.398931	0.398873	0.000058	1.21951
5	3	6	0.406708	0.406657	0.000052	1.20779
3	3	8	0.413217	0.413175	0.000043	1.19824
6	0	6	0.421283	0.421253	0.000030	1.18672
7	3	0	0.423318	0.423299	0.000019	1.18386
4	2	8	0.427763	0.427771	-0.000008	1.17769
7	1	4	0.435432	0.435364	0.000068	1.16728
7	3	2	0.440946	0.440912	0.000034	1.15996
6	2	6	0.450317	0.450446	-0.000129	1.14782
1	1	10	0.454916	0.454918	-0.000002	1.14201
5	1	8	0.471603	0.471561	0.000042	1.12162

NUMBER OF REFLECTIONS = 69

NUMBER OF REFLECTIONS USED = 69 FOR A GATE OF 0.00020

PARAMETERS	STANDARD DEVIATIONS	LAST SHIFTS
A = 9.016229	0.000215	0.000000
C = 11.607788	0.000426	-0.000000

## REFINEMENT OF

SR(OH)2.H2O

ORTHOROMBIC

PMMA

H	K	L	SINSQ(O)	SINSQ(C)	OBS-CALC	D OBS
---	---	---	----------	----------	----------	-------

WAVELENGTH = 1.54051

0	0	1	0.015390	0.015438	-0.000048	6.20891
1	0	1	0.028570	0.028597	-0.000027	4.55700
0	1	0	0.044560	0.044577	-0.000017	3.64890
2	0	0	0.052640	0.052635	0.000005	3.35719
0	1	1	0.060030	0.060015	0.000015	3.14377
2	0	1	0.068110	0.068073	0.000037	2.95141
1	1	1	0.073190	0.073174	0.000016	2.84714
1	0	2	0.074920	0.074911	0.000009	2.81407
2	1	0	0.097180	0.097212	-0.000032	2.47085
0	1	2	0.106330	0.106329	0.000001	2.36215
2	1	1	0.112680	0.112650	0.000030	2.29462
1	1	2	0.119500	0.119488	0.000012	2.22818
3	0	1	0.133930	0.133867	0.000062	2.10473
0	0	3	0.138980	0.138943	0.000037	2.06613
1	0	3	0.152070	0.152102	-0.000032	1.97521
0	2	0	0.178290	0.178306	-0.000016	1.82419
3	0	2	0.180110	0.180182	-0.000072	1.81495
0	1	3	0.183470	0.183520	-0.000050	1.79826
2	0	3	0.191500	0.191578	-0.000078	1.76015
0	2	1	0.193760	0.193745	0.000015	1.74986
1	1	3	0.196680	0.196678	0.000002	1.73682
1	2	1	0.206830	0.206903	-0.000073	1.69367
4	0	0	0.210530	0.210541	-0.000011	1.67872
3	1	2	0.224770	0.224758	0.000012	1.62467
4	0	1	0.226020	0.225979	0.000041	1.62017
2	2	0	0.230940	0.230942	-0.000002	1.60282
2	1	3	0.236160	0.236155	0.000005	1.58501
2	2	1	0.246290	0.246380	-0.000090	1.55207
0	0	4	0.246990	0.247010	-0.000020	1.54987
1	2	2	0.253250	0.253218	0.000032	1.53059
4	1	0	0.255040	0.255118	-0.000078	1.52521
3	0	3	0.257320	0.257372	-0.000052	1.51844
4	1	1	0.270510	0.270556	-0.000046	1.48096
0	1	4	0.291580	0.291586	-0.000006	1.42645
2	0	4	0.299600	0.299645	-0.000045	1.40722
3	1	3	0.301890	0.301949	-0.000059	1.40188
3	2	1	0.312130	0.312174	-0.000044	1.37869
0	2	3	0.317230	0.317249	-0.000019	1.36756
1	2	3	0.330320	0.330408	-0.000088	1.34019
5	0	1	0.344430	0.344409	0.000021	1.31245
4	0	3	0.349480	0.349484	-0.000004	1.30294
3	2	2	0.358430	0.358488	-0.000058	1.28657
2	2	3	0.369970	0.369885	0.000085	1.26634
5	1	1	0.388980	0.388985	-0.000005	1.23501
5	0	2	0.390870	0.390723	0.000147	1.23202
4	1	3	0.394100	0.394061	0.000039	1.22696
1	0	5	0.398980	0.399112	-0.000132	1.21944
0	3	0	0.401120	0.401189	-0.000069	1.21618
4	2	1	0.404240	0.404286	-0.000046	1.21148
0	3	1	0.416640	0.416628	0.000012	1.19331
0	2	4	0.425380	0.425316	0.000064	1.18099
1	3	1	0.429830	0.429786	0.000044	1.17486
3	2	3	0.435570	0.435679	-0.000109	1.16709
2	0	5	0.438670	0.438588	0.000082	1.16296
1	1	5	0.443870	0.443688	0.000182	1.15613
2	3	0	0.453790	0.453825	-0.000035	1.14342
4	0	4	0.457510	0.457551	-0.000041	1.13877
2	3	1	0.469320	0.469263	0.000057	1.12435
6	0	0	0.473740	0.473718	0.000022	1.11909
1	3	2	0.476230	0.476101	0.000129	1.11616
2	2	4	0.478100	0.477952	0.000148	1.11397
6	0	1	0.489180	0.489156	0.000024	1.10129
4	1	4	0.502070	0.502128	-0.000058	1.08706

NUMBER OF REFLECTIONS = 63

NUMBER OF REFLECTIONS USED = 63 FOR A GATE OF 0.00030

PARAMETERS	STANDARD DEVIATIONS	LAST SHIFTS
A =	6.714691	0.000212
B =	3.648220	0.000109
C =	6.199225	0.000207

## REFINEMENT OF

SR(OH)2

ORTHORHOMBIC

PNMA

H	K	L	SINSQ(O)	SINSQ(C)	OBS-CALC	D OBS
---	---	---	----------	----------	----------	-------

WAVELENGTH = 1.54051

1	0	1	0.021910	0.021920	-0.000010	5.20372
2	0	0	0.024240	0.024268	-0.000028	4.94730
2	0	1	0.040100	0.040121	-0.000021	3.84647
0	1	1	0.054470	0.054489	-0.000019	3.30032
2	1	0	0.062890	0.062904	-0.000014	3.07145
0	0	2	0.063370	0.063413	-0.000043	3.05980
1	0	2	0.069410	0.069480	-0.000070	2.92364
3	0	1	0.070490	0.070456	0.000034	2.90115
2	1	1	0.078750	0.078757	-0.000007	2.74479
2	0	2	0.087680	0.087681	-0.000001	2.60126
4	0	0	0.097110	0.097071	0.000039	2.47174
1	1	2	0.108090	0.108116	-0.000026	2.34284
4	0	1	0.112970	0.112924	0.000046	2.29167
3	0	2	0.118090	0.118016	0.000074	2.24144
2	1	2	0.126280	0.126317	-0.000037	2.16754
4	1	0	0.135720	0.135707	0.000013	2.09080
1	0	3	0.148660	0.148747	-0.000087	1.99773
4	1	1	0.151600	0.151560	0.000040	1.97827
0	2	0	0.154510	0.154544	-0.000034	1.95955
3	1	2	0.156720	0.156652	0.000068	1.94568
2	0	3	0.166980	0.166948	0.000032	1.88496
1	2	1	0.176460	0.176465	-0.000005	1.83363
2	2	0	0.178840	0.178812	0.000028	1.82139
0	1	3	0.181370	0.181316	0.000054	1.80864
1	1	3	0.187500	0.187383	0.000117	1.77883
2	2	1	0.194740	0.194665	0.000075	1.74545
4	1	2	0.199140	0.199120	0.000020	1.72606
2	1	3	0.205690	0.205584	0.000106	1.69835
5	1	1	0.206290	0.206163	0.000127	1.69588
5	0	2	0.215170	0.215086	0.000084	1.66052
6	0	0	0.218500	0.218409	0.000091	1.64782
1	2	2	0.224020	0.224025	-0.000005	1.62739
3	2	1	0.224950	0.225000	-0.000050	1.62402
4	0	3	0.239850	0.239751	0.000099	1.57277
2	2	2	0.242190	0.242225	-0.000035	1.56515
4	2	0	0.251720	0.251615	0.000105	1.53524
0	0	4	0.253560	0.253653	-0.000093	1.52966
1	0	4	0.259800	0.259720	0.000080	1.51118
4	2	1	0.267620	0.267469	0.000151	1.48893
6	1	1	0.272970	0.272899	0.000071	1.47427
4	1	3	0.278520	0.278387	0.000133	1.45951
6	0	2	0.281860	0.281823	0.000037	1.45083
1	1	4	0.298370	0.298356	0.000014	1.41012
1	2	3	0.303440	0.303291	0.000149	1.39829
7	0	1	0.313130	0.313133	-0.000003	1.37649
2	1	4	0.316580	0.316557	0.000023	1.36897
5	1	3	0.332850	0.332989	-0.000139	1.33509
3	1	4	0.346890	0.346892	-0.000002	1.30779
4	0	4	0.350670	0.350724	-0.000054	1.30072
3	2	3	0.351850	0.351827	0.000023	1.29854
7	0	2	0.360710	0.360693	0.000017	1.28249
0	3	1	0.363510	0.363578	-0.000068	1.27754
5	2	2	0.369550	0.369631	-0.000081	1.26706
2	3	0	0.371770	0.371993	-0.000223	1.26327
6	2	0	0.372850	0.372954	-0.000104	1.26144
4	1	4	0.389250	0.389360	-0.000110	1.23458
4	2	3	0.394220	0.394295	-0.000075	1.22678
6	1	3	0.399570	0.399725	-0.000155	1.21853
1	0	5	0.402310	0.402400	-0.000090	1.21438
8	0	1	0.404020	0.404137	-0.000117	1.21181
5	0	4	0.405180	0.405326	-0.000146	1.21007
0	2	4	0.408110	0.408198	-0.000088	1.20572
1	2	4	0.414350	0.414265	0.000085	1.19660
1	3	2	0.417170	0.417205	-0.000035	1.19255
8	1	0	0.426930	0.426919	0.000011	1.17884
2	2	4	0.432530	0.432465	0.000065	1.17119
2	3	2	0.435310	0.435406	-0.000096	1.16744
6	2	2	0.436110	0.436367	-0.000257	1.16637
1	1	5	0.441050	0.441036	0.000014	1.15982
4	3	0	0.444820	0.444796	0.000024	1.15489
3	0	5	0.450950	0.450936	0.000014	1.14702
4	3	1	0.460620	0.460649	-0.000029	1.13491
3	3	2	0.465840	0.465741	0.000099	1.12854
7	2	1	0.467710	0.467677	0.000033	1.12628
6	0	4	0.472120	0.472063	0.000057	1.12101
0	3	3	0.490680	0.490405	0.000275	1.09960

NUMBER OF REFLECTIONS = 76

NUMBER OF REFLECTIONS USED = 76 FOR A GATE OF 0.00030

	PARAMETERS	STANDARD DEVIATIONS	LAST SHIFTS
A	= 9.888949	0.000452	-0.000000
B	= 3.918662	0.000164	0.000000
C	= 6.117504	0.000243	0.000000

## REFINEMENT OF

U3 O8

ORTHORHOMBIC

H	K	L	SINSQ(O)	SINSQ(C)	OBS-CALC	D OBS
WAVELENGTH = 1.54051						
1	1	0	0.017300	0.017306	-0.000006	5.85614
0	0	1	0.034510	0.034508	0.000002	4.14631
1	3	0	0.050460	0.050471	-0.000011	3.42895
2	2	0	0.069230	0.069223	0.000007	2.92744
1	3	1	0.085020	0.084979	0.000041	2.64164
2	0	1	0.087120	0.087148	-0.000028	2.60961
2	2	1	0.103760	0.103730	0.000030	2.39122
1	5	0	0.116650	0.116801	-0.000151	2.25524
2	4	0	0.119060	0.118971	0.000089	2.23230
3	1	0	0.122600	0.122586	0.000014	2.19983
0	0	2	0.138090	0.138030	0.000060	2.07278
0	6	0	0.149290	0.149243	0.000047	1.99351
1	5	1	0.151350	0.151309	0.000041	1.97990
2	4	1	0.153590	0.153478	0.000112	1.96541
3	3	0	0.155840	0.155751	0.000089	1.95117
3	1	1	0.157110	0.157094	0.000016	1.94327
0	6	1	0.183880	0.183751	0.000129	1.79625
1	3	2	0.188540	0.188501	0.000039	1.77391
3	3	1	0.190350	0.190259	0.000091	1.76546
2	6	0	0.201940	0.201884	0.000056	1.71405
4	0	0	0.210470	0.210561	-0.000091	1.67896
4	2	0	0.227130	0.227143	-0.000013	1.61621
2	6	1	0.236350	0.236391	-0.000041	1.58437
4	0	1	0.245050	0.245068	-0.000018	1.55599
1	7	1	0.250820	0.250805	0.000015	1.53799
1	5	2	0.254680	0.254832	-0.000152	1.52629
3	5	1	0.256690	0.256589	0.000101	1.52030
3	1	2	0.260790	0.260617	0.000173	1.50830
4	2	1	0.261560	0.261651	-0.000091	1.50608
0	6	2	0.287280	0.287274	0.000006	1.43708
3	3	2	0.293740	0.293782	-0.000042	1.42119
0	0	3	0.310580	0.310569	0.000011	1.38213
5	1	0	0.333280	0.333147	0.000133	1.33423
2	6	2	0.339940	0.339914	0.000026	1.32109
4	0	2	0.348700	0.348591	0.000109	1.30439
1	3	3	0.360980	0.361039	-0.000059	1.28201
2	0	3	0.363130	0.363209	-0.000079	1.27821
5	3	0	0.366190	0.366312	-0.000122	1.27286
1	9	1	0.383330	0.383465	-0.000135	1.24408
4	6	1	0.394270	0.394312	-0.000042	1.22670
5	3	1	0.400680	0.400820	-0.000140	1.21685
3	1	3	0.433100	0.433155	-0.000055	1.17042

NUMBER OF REFLECTIONS = 42

NUMBER OF REFLECTIONS USED = 42 FOR A GATE OF 0.00020

	PARAMETERS	STANDARD DEVIATIONS	LAST SHIFTS
A	= 6.714377	0.000379	0.000000
B	= 11.962947	0.000902	0.000000
C	= 4.146456	0.000276	0.000000



## REFINEMENT OF

U SI

ORTHORHOMBIC

H	K	L	SINSQ(O)	SINSQ(C)	OBS-CALC	D OBS
---	---	---	----------	----------	----------	-------

WAVELENGTH = 1.54051

1	0	1	0.028658	0.028595	0.000063	4.55002
2	0	0	0.040369	0.040380	-0.000010	3.83361
0	1	1	0.057505	0.057549	-0.000045	3.21206
2	0	1	0.058877	0.058880	-0.000002	3.17439
1	1	1	0.067618	0.067644	-0.000026	2.96213
2	1	0	0.079427	0.079429	-0.000002	2.73306
1	0	2	0.084110	0.084095	0.000015	2.65590
2	1	1	0.097913	0.097929	-0.000015	2.46158
3	0	1	0.109431	0.109354	0.000077	2.32844
1	1	2	0.123263	0.123144	0.000119	2.19391
3	1	1	0.148409	0.148403	0.000006	1.99942
0	2	0	0.156207	0.156197	0.000010	1.94888
4	0	1	0.179937	0.180018	-0.000081	1.81583
1	2	1	0.184705	0.184792	-0.000086	1.79223
2	2	0	0.196512	0.196576	-0.000064	1.73756
4	1	0	0.200442	0.200567	-0.000125	1.72044
3	1	2	0.203899	0.203903	-0.000005	1.70580
2	0	3	0.206972	0.206880	0.000093	1.69308
2	2	1	0.214910	0.215076	-0.000166	1.66152
1	1	3	0.215628	0.215644	-0.000016	1.65875
1	2	2	0.240291	0.240292	-0.000000	1.57132
2	1	3	0.245903	0.245929	-0.000026	1.55329
3	0	3	0.257421	0.257354	0.000067	1.51814
3	2	1	0.265527	0.265551	-0.000024	1.49479
5	0	1	0.271050	0.270872	0.000178	1.47948
0	0	4	0.296057	0.296000	0.000057	1.41562
1	0	4	0.305958	0.306095	-0.000137	1.39253
5	1	1	0.310048	0.309921	0.000127	1.38331
5	0	2	0.326274	0.326372	-0.000098	1.34848
4	0	3	0.328034	0.328018	0.000015	1.34485
4	2	1	0.336098	0.336215	-0.000117	1.32862
2	2	3	0.363210	0.363076	0.000134	1.27807
5	1	2	0.365315	0.365422	-0.000106	1.27438
0	3	1	0.369773	0.369943	-0.000169	1.26668
1	3	1	0.380056	0.380038	0.000019	1.24943
2	3	0	0.391977	0.391822	0.000155	1.23028
6	1	0	0.402368	0.402465	-0.000097	1.21429
2	3	1	0.410344	0.410322	0.000021	1.20243
3	2	3	0.413602	0.413551	0.000051	1.19769
6	1	1	0.421054	0.420965	0.000088	1.18704
5	2	1	0.427164	0.427069	0.000095	1.17852
1	3	2	0.435636	0.435538	0.000098	1.16700
0	2	4	0.452135	0.452197	-0.000062	1.14551
5	1	3	0.457854	0.457922	-0.000068	1.13834

NUMBER OF REFLECTIONS = 44

NUMBER OF REFLECTIONS USED = 44 FOR A GATE OF 0.00020

PARAMETERS STANDARD DEVIATIONS LAST SHIFTS

A	=	7.666263	0.000405	-0.000000
B	=	3.897880	0.000194	0.000000
C	=	5.663025	0.000375	0.000000

## REFINEMENT OF

P

ORTHORHOMBIC

H	K	L	SINSQ(O)	SINSQ(C)	OBS-CALC	D OBS
WAVELENGTH = 1.54051						
0	2	0	0.021590	0.021610	-0.000020	5.24214
0	2	1	0.052520	0.052580	-0.000060	3.36103
0	4	0	0.086430	0.086440	-0.000010	2.62001
1	1	1	0.090360	0.090393	-0.000033	2.56240
0	0	2	0.123840	0.123879	-0.000039	2.18879
1	3	1	0.133650	0.133613	0.000037	2.10693
1	1	2	0.183330	0.183303	0.000027	1.79894
2	0	0	0.215990	0.216084	-0.000094	1.65736
1	5	1	0.220000	0.220053	-0.000053	1.64219
1	3	2	0.226550	0.226523	0.000027	1.61828
2	2	0	0.237660	0.237694	-0.000034	1.58000
2	2	1	0.268630	0.268664	-0.000034	1.48613
0	2	3	0.300320	0.300338	-0.000018	1.40554
2	4	0	0.302440	0.302524	-0.000084	1.40060
2	0	2	0.340060	0.339963	0.000097	1.32086
2	6	0	0.410720	0.410574	0.000146	1.20188
2	4	2	0.426480	0.426403	0.000077	1.17947
1	7	2	0.442600	0.442622	-0.000022	1.15779

NUMBER OF REFLECTIONS = 18

NUMBER OF REFLECTIONS USED = 18 FOR A GATE OF 0.00030

	PARAMETERS	STANDARD DEVIATIONS	LAST SHIFTS
A	= 3.314005	0.000242	0.000000
B	= 10.479428	0.001141	0.000000
C	= 4.376888	0.000407	0.000000

## REFINEMENT OF

RE3 GE7

ORTHOROMBIC

CMCM

H	K	L	SINSQ(O)	SINSQ(C)	OBS-CALC	D CBS
WAVELENGTH = 1.54051						
0	0	2	0.004870	0.004920	-0.000050	11.03748
0	0	4	0.019590	0.019678	-0.000088	5.50323
0	2	0	0.028980	0.029012	-0.000032	4.52466
0	2	1	0.030200	0.030242	-0.000042	4.43232
0	2	3	0.040010	0.040081	-0.000071	3.85079
0	0	6	0.044260	0.044276	-0.000016	3.66125
0	2	4	0.048670	0.048691	-0.000021	3.49143
0	2	5	0.059670	0.059760	-0.000090	3.15324
1	1	0	0.064150	0.064218	-0.000068	3.04114
1	1	2	0.069130	0.069137	-0.000007	2.92955
0	2	6	0.073270	0.073289	-0.000019	2.84558
1	1	3	0.075230	0.075287	-0.000057	2.80827
1	1	4	0.083900	0.083896	0.000004	2.65921
0	2	7	0.089230	0.089277	-0.000047	2.57857
1	1	5	0.094970	0.094965	0.000005	2.49943
0	2	8	0.107680	0.107726	-0.000046	2.34729
0	4	2	0.120890	0.120969	-0.000079	2.21533
1	3	0	0.122200	0.122243	-0.000043	2.20343
0	0	10	0.122890	0.122990	-0.000100	2.19723
1	1	7	0.124410	0.124483	-0.000073	2.18377
0	4	3	0.127020	0.127119	-0.000099	2.16122
0	4	4	0.135700	0.135728	-0.000028	2.09095
1	3	4	0.141910	0.141921	-0.000011	2.04469
1	1	8	0.142950	0.142931	0.000019	2.03724
0	4	5	0.146820	0.146797	0.000023	2.01021
0	2	10	0.151930	0.152002	-0.000072	1.97612
1	3	5	0.152920	0.152990	-0.000070	1.96971
1	3	6	0.166440	0.166519	-0.000079	1.88802
0	4	7	0.176260	0.176315	-0.000055	1.83467
0	2	11	0.177790	0.177830	-0.000040	1.82676
1	3	7	0.182440	0.182507	-0.000068	1.80333
1	1	10	0.187180	0.187207	-0.000027	1.78035
0	4	8	0.194730	0.194763	-0.000033	1.74549
1	3	8	0.200940	0.200956	-0.000016	1.71831
0	2	12	0.206070	0.206118	-0.000048	1.69679
0	4	9	0.215480	0.215671	-0.000191	1.65932
2	0	0	0.227800	0.227859	-0.000059	1.61383
0	2	13	0.236810	0.236865	-0.000055	1.58283
1	5	0	0.238190	0.238292	-0.000102	1.57824
0	0	14	0.241170	0.241060	0.000110	1.56846
1	3	10	0.245400	0.245232	0.000168	1.55488
2	0	4	0.247490	0.247537	-0.000047	1.54830
1	5	3	0.249320	0.249361	-0.000041	1.54261
2	2	0	0.256750	0.256871	-0.000121	1.52012
1	5	4	0.258010	0.257970	0.000039	1.51641
0	6	1	0.262380	0.262342	0.000038	1.50373
0	6	2	0.266010	0.266031	-0.000021	1.49343
2	2	3	0.268000	0.267940	0.000060	1.48788
1	5	5	0.268880	0.269040	-0.000160	1.48544
0	6	3	0.272210	0.272181	0.000029	1.47633
2	2	4	0.276550	0.276549	0.000001	1.46470
1	5	6	0.282540	0.282568	-0.000028	1.44909
2	2	5	0.287610	0.287618	-0.000008	1.43626
0	6	5	0.291850	0.291859	-0.000009	1.42579
0	4	12	0.293100	0.293155	-0.000055	1.42274

1	3	12	0.299370	0.299348	0.000022	1.40777
2	2	6	0.301370	0.301147	0.000223*	1.40309
0	6	6	0.305390	0.305388	0.000002	1.39382
0	2	15	0.305670	0.305739	-0.000069	1.39318
0	0	16	0.314790	0.314854	-0.000064	1.37285
2	2	7	0.317230	0.317136	0.000094	1.36756
0	4	13	0.323870	0.323902	-0.000032	1.35347
1	3	13	0.330200	0.330095	0.000105	1.34044
2	2	8	0.335610	0.335584	0.000026	1.32959
1	5	9	0.338090	0.337914	0.000176	1.32470
0	6	8	0.339690	0.339825	-0.000135	1.32158
1	1	15	0.340870	0.340945	-0.000075	1.31929
0	2	16	0.343830	0.343866	-0.000036	1.31360
2	4	2	0.348820	0.348828	-0.000008	1.30417
2	0	10	0.350900	0.350848	0.000052	1.30030
2	4	3	0.354900	0.354977	-0.000077	1.29295
0	4	14	0.357170	0.357109	0.000061	1.28883
1	5	10	0.361190	0.361282	-0.000092	1.28164
1	3	14	0.363350	0.363302	0.000048	1.27783
2	4	5	0.374790	0.374656	0.000134	1.25817
2	2	10	0.379880	0.379861	0.000019	1.24972
0	2	17	0.384490	0.384453	0.000037	1.24220
2	4	6	0.388010	0.388184	-0.000174	1.23655
0	4	15	0.392760	0.392776	-0.000016	1.22905
1	3	15	0.399110	0.398969	0.000141	1.21924
2	4	7	0.404250	0.404173	0.000077	1.21146
2	2	11	0.405660	0.405688	-0.000029	1.20935
1	7	0	0.412290	0.412367	-0.000077	1.19959
1	7	1	0.413510	0.413596	-0.000086	1.19782
1	7	2	0.417390	0.417286	0.000104	1.19224
2	4	8	0.422870	0.422622	0.000248*	1.18449
0	2	18	0.427380	0.427499	-0.000119	1.17822
1	7	4	0.432190	0.432045	0.000145	1.17165
2	2	12	0.434050	0.433976	0.000074	1.16914
1	3	16	0.437270	0.437096	0.000174	1.16482
1	5	13	0.446310	0.446145	0.000165	1.15296
1	7	6	0.456680	0.456643	0.000037	1.13980
1	1	18	0.462900	0.462704	0.000196	1.13212
2	2	13	0.464770	0.464724	0.000046	1.12984
0	8	2	0.469190	0.469118	0.000072	1.12450
1	7	7	0.472800	0.472632	0.000168	1.12020
0	8	3	0.475350	0.475268	0.000082	1.11719
0	8	4	0.483890	0.483877	0.000013	1.10729
1	7	8	0.491180	0.491080	0.000100	1.09904

NUMBER OF REFLECTIONS = 99

NUMBER OF REFLECTIONS USED = 97 FOR A GATE OF 0.00020

	PARAMETERS	STANDARD DEVIATIONS	LAST SHIFTS
A	= 3.227244	0.000169	-0.000000
B	= 9.044252	0.000316	-0.000000
C	= 21.963430	0.000887	0.000000

## REFINEMENT OF

ZR O2

MONOCLINIC

H	K	L	SINSQ(O)	SINSQ(C)	OBS-CALC	D ORS
---	---	---	----------	----------	----------	-------

WAVELENGTH = 1.54051

1	0	0	0.022933	0.022975	-0.000042	5.08630
0	1	1	0.043409	0.043396	0.000013	3.69694
1	1	0	0.044768	0.044838	-0.000070	3.64043
-1	1	1	0.059200	0.059232	-0.000032	3.16573
1	1	1	0.073439	0.073511	-0.000072	2.84231
0	0	2	0.086183	0.086132	0.000050	2.62376
0	2	0	0.087413	0.087453	-0.000040	2.60524
2	0	0	0.091834	0.091899	-0.000065	2.54175
-1	0	2	0.094738	0.094828	-0.000090	2.50249
0	2	1	0.109042	0.108986	0.000056	2.33259
2	1	0	0.113596	0.113763	-0.000166	2.28535
-1	1	2	0.116544	0.116691	-0.000147	2.25626
-2	1	1	0.120986	0.121017	-0.000030	2.21445
1	0	2	0.123316	0.123386	-0.000070	2.19343
-1	2	1	0.124756	0.124822	-0.000065	2.18074
1	1	2	0.145262	0.145250	0.000012	2.02096
-2	0	2	0.149377	0.149473	-0.000097	1.99294
-2	1	2	0.171589	0.171337	0.000252	1.85948
0	2	2	0.173617	0.173586	0.000032	1.84858
2	2	0	0.179328	0.179353	-0.000024	1.81891
-1	2	2	0.182307	0.182281	0.000026	1.80398
-2	2	1	0.186617	0.186606	0.000010	1.78303
2	0	2	0.206252	0.206590	-0.000338	1.69604
3	0	0	0.206656	0.206774	-0.000117	1.69438
2	2	1	0.215161	0.215165	-0.000004	1.66055
0	1	3	0.215777	0.215661	0.000115	1.65818
-1	1	3	0.217474	0.217217	0.000256	1.65170
1	3	0	0.219589	0.219745	-0.000156	1.64373
-3	1	1	0.228696	0.228751	-0.000055	1.61066
-1	3	1	0.234223	0.234138	0.000085	1.59155
-2	2	2	0.236923	0.236927	-0.000003	1.58245
1	3	1	0.248210	0.248417	-0.000207	1.54605
-3	0	2	0.250100	0.250068	0.000031	1.54020
1	1	3	0.260165	0.260055	0.000110	1.51012
-2	1	3	0.264832	0.264723	0.000109	1.49675
3	1	1	0.271633	0.271589	0.000045	1.47789
0	2	3	0.281290	0.281251	0.000039	1.45230
-1	2	3	0.282638	0.282807	-0.000169	1.44884
0	3	2	0.282919	0.282902	0.000017	1.44812
-1	2	3	0.282919	0.282807	0.000112	1.44812
2	3	0	0.288841	0.288669	0.000172	1.43319
-1	3	2	0.291674	0.291598	0.000076	1.42622
2	2	2	0.294116	0.294043	0.000073	1.42028
-2	3	1	0.296052	0.295923	0.000128	1.41563
1	3	2	0.320138	0.320156	-0.000018	1.36134
2	3	1	0.324628	0.324482	0.000146	1.35189
1	2	3	0.325387	0.325645	-0.000258	1.35031
3	2	1	0.337305	0.337179	0.000126	1.32624
-1	0	4	0.338839	0.338946	-0.000107	1.32324
-2	3	2	0.345945	0.346243	-0.000298	1.30958
0	4	0	0.349988	0.349813	0.000175	1.30199
-4	0	0	0.367598	0.367597	0.000001	1.27042
0	4	1	0.371458	0.371346	0.000112	1.26380
-4	1	1	0.382362	0.382435	-0.000074	1.24565
0	3	3	0.390400	0.390568	-0.000168	1.23276
-1	0	4	0.395961	0.396063	-0.000102	1.22408
-4	0	2	0.396695	0.396613	0.000082	1.22294
-2	1	4	0.401292	0.401175	0.000116	1.21592
3	3	0	0.403501	0.403543	-0.000042	1.21258
2	2	3	0.416064	0.415988	0.000076	1.19414
-3	2	3	0.424104	0.423768	0.000336	1.18276
-1	2	4	0.426087	0.426399	-0.000312	1.18001
0	2	4	0.432292	0.431983	0.000309	1.17151
1	3	3	0.435151	0.434961	0.000190	1.16765
-2	3	3	0.439320	0.439629	-0.000310	1.16210
3	3	1	0.446488	0.446495	-0.000008	1.15274
-2	4	1	0.448672	0.448966	-0.000294	1.14993
4	2	0	0.455233	0.455051	0.000182	1.14161
-3	0	4	0.465376	0.465628	-0.000252	1.12910
2	4	1	0.477676	0.477525	0.000151	1.11447
1	2	4	0.483458	0.483516	-0.000058	1.10778
3	1	3	0.486603	0.486691	-0.000089	1.10420
2	0	4	0.493777	0.493546	0.000231	1.09615
-4	1	3	0.497744	0.497583	0.000160	1.09177

NUMBER OF REFLECTIONS = 74

NUMBER OF REFLECTIONS USED = 74 FOR A GATE OF 0.00040

PARAMETERS	STANDARD DEVIATIONS	LAST SHIFTS
A = 5.148434	0.000410	0.000000
B = 5.209265	0.000413	0.000000
C = 5.317997	0.000381	-0.000000
BETA = 99.235773	0.006552	-0.000002

## REFINEMENT OF

BA CL<sub>2</sub>H<sub>2</sub> O MONOCLINIC

H	K	L	SINSQ(O)	SINSQ(C)	OBS-CALC	D OBS
WAVELENGTH = 1.54051						
0	1	1	0.016650	0.016654	-0.000004	5.96936
1	1	0	0.018040	0.018122	-0.000082	5.73478
0	2	0	0.019940	0.019944	-0.000004	5.45472
-1	0	1	0.024330	0.024328	0.000002	4.93814
1	0	1	0.025240	0.025280	-0.000040	4.84831
-1	1	1	0.029260	0.029314	-0.000054	4.50295
1	1	1	0.030250	0.030266	-0.000016	4.42866
0	2	1	0.031620	0.031612	0.000008	4.33165
-1	2	1	0.044180	0.044272	-0.000092	3.66456
1	2	1	0.045160	0.045224	-0.000064	3.62458
0	0	2	0.046650	0.046672	-0.000022	3.56623
0	1	2	0.051640	0.051658	-0.000018	3.38955
2	0	0	0.052470	0.052543	-0.000073	3.36263
0	3	1	0.056580	0.056542	0.000038	3.23820
2	1	0	0.057470	0.057529	-0.000059	3.21302
1	3	0	0.058030	0.058010	0.000020	3.19748
1	1	2	0.065720	0.065746	-0.000026	3.00459
-2	1	1	0.068190	0.068245	-0.000055	2.94967
-1	3	1	0.069160	0.069202	-0.000042	2.92892
2	1	1	0.070120	0.070149	-0.000029	2.90880
2	2	0	0.072490	0.072487	0.000003	2.86085
1	2	2	0.080650	0.080704	-0.000054	2.71227
-2	2	1	0.083220	0.083203	0.000017	2.67006
0	4	1	0.091430	0.091445	-0.000015	2.54736
1	4	0	0.092840	0.092913	-0.000073	2.52794
-2	0	2	0.097300	0.097311	-0.000011	2.46932
2	0	2	0.101070	0.101120	-0.000050	2.42283
-2	1	2	0.102240	0.102297	-0.000057	2.40893
-1	4	1	0.104060	0.104104	-0.000044	2.38777
2	1	2	0.106090	0.106106	-0.000016	2.36482
-2	3	1	0.108130	0.108133	-0.000003	2.34240
0	1	3	0.109960	0.109998	-0.000038	2.32283
-1	0	3	0.116640	0.116719	-0.000079	2.25533
1	0	3	0.119580	0.119576	0.000004	2.22744
2	2	2	0.120960	0.121064	-0.000104	2.21469
-1	1	3	0.121660	0.121706	-0.000046	2.20831
-3	0	1	0.128430	0.128462	-0.000032	2.14932
2	4	0	0.132250	0.132320	-0.000070	2.11805
3	1	1	0.136290	0.136304	-0.000014	2.08642
1	5	0	0.137750	0.137787	-0.000037	2.07534
-1	4	2	0.138610	0.138632	-0.000022	2.06889
1	2	3	0.139430	0.139520	-0.000090	2.06280
1	4	2	0.140550	0.140537	0.000013	2.05456
-2	3	2	0.142250	0.142185	0.000065	2.04225
2	4	1	0.144920	0.144940	-0.000020	2.02335
2	3	2	0.145890	0.145994	-0.000104	2.01661
-3	2	1	0.148410	0.148406	0.000004	1.99942
1	5	1	0.149920	0.149931	-0.000011	1.98932
3	3	0	0.163010	0.163096	-0.000086	1.90778
0	5	2	0.171340	0.171323	0.000017	1.86082
-3	3	1	0.173230	0.173336	-0.000106	1.85065
3	3	1	0.176260	0.176193	0.000067	1.83467
0	6	0	0.179600	0.179498	0.000102	1.81753
2	4	2	0.180800	0.180896	-0.000096	1.81149
0	0	4	0.186740	0.186688	0.000052	1.78244
-2	5	1	0.187810	0.187910	-0.000100	1.77736
2	5	1	0.189810	0.189815	-0.000005	1.76797
0	6	1	0.191280	0.191166	0.000114	1.76116
3	4	0	0.198100	0.197999	0.000101	1.73058
1	4	3	0.199440	0.199353	0.000087	1.72476
-1	1	4	0.202940	0.202905	0.000035	1.70982
-1	6	1	0.203900	0.203826	0.000074	1.70579
2	3	3	0.205310	0.205286	0.000024	1.69992
0	2	4	0.206620	0.206632	-0.000012	1.69453
-3	4	1	0.208080	0.208238	-0.000158	1.68857
3	3	2	0.212510	0.212625	-0.000115	1.67088
4	1	0	0.215110	0.215158	-0.000048	1.66075
-3	1	3	0.223840	0.223935	-0.000095	1.62804
2	5	2	0.225920	0.225771	0.000149	1.62053
0	5	3	0.229850	0.229663	0.000187	1.60662
0	3	4	0.231480	0.231563	-0.000083	1.60095
-2	4	3	0.234430	0.234475	-0.000045	1.59085

-2	0	4	0.235380	0.235422	-0.000042	1.58763
-1	6	2	0.238300	0.238353	-0.000053	1.57787
1	6	2	0.240210	0.240258	-0.000048	1.57159
-3	4	2	0.241820	0.241814	0.000006	1.56635
2	6	1	0.244600	0.244661	-0.000061	1.55742
3	2	3	0.247390	0.247463	-0.000073	1.54861
2	1	4	0.247980	0.248026	-0.000046	1.54677
-3	5	1	0.253120	0.253113	0.000007	1.53099
4	3	0	0.255180	0.255047	0.000133	1.52479
3	5	1	0.255840	0.255970	-0.000130	1.52283
1	7	0	0.257470	0.257452	0.000018	1.51800
-4	1	2	0.258020	0.258022	-0.000002	1.51638
4	0	2	0.260420	0.260653	-0.000233*	1.50938
-3	3	3	0.263820	0.263823	-0.000003	1.49962
0	4	4	0.266470	0.266465	0.000005	1.49214
-4	2	2	0.273050	0.272980	0.000070	1.47405
2	6	2	0.280650	0.280617	0.000032	1.45396
2	5	3	0.285080	0.285063	0.000017	1.44262
2	3	4	0.287850	0.287915	-0.000065	1.43566
4	4	0	0.289940	0.289949	-0.000009	1.43048
3	5	2	0.292550	0.292402	0.000148	1.42408
3	6	0	0.297780	0.297720	0.000060	1.41152
1	6	3	0.299090	0.299074	0.000016	1.40842
4	4	1	0.303380	0.303522	-0.000142	1.39843
1	7	2	0.305110	0.305077	0.000033	1.39446
-2	7	1	0.307580	0.307575	0.000005	1.38885
1	1	5	0.312310	0.312203	0.000107	1.37829
-2	4	4	0.315200	0.315199	0.000001	1.37196
1	5	4	0.326500	0.326380	0.000120	1.34801
0	8	1	0.330660	0.330775	-0.000115	1.33950
-5	0	1	0.337540	0.337682	-0.000142	1.32578
4	4	2	0.340490	0.340430	0.000060	1.32003
-3	6	2	0.341560	0.341535	0.000025	1.31796
-2	1	5	0.344460	0.344468	-0.000008	1.31240
3	6	2	0.347190	0.347249	-0.000059	1.30723
4	5	1	0.348430	0.348396	0.000034	1.30490
0	7	3	0.349320	0.349329	-0.000009	1.30324
3	5	3	0.352240	0.352170	0.000070	1.29782
-5	2	1	0.357610	0.357626	-0.000016	1.28804
3	7	0	0.362520	0.362539	-0.000019	1.27929
0	8	2	0.365760	0.365779	-0.000019	1.27361
2	2	5	0.368950	0.368949	0.000001	1.26809
0	4	5	0.371480	0.371477	0.000003	1.26377
-1	8	2	0.377880	0.377963	-0.000083	1.25302
1	8	2	0.379700	0.379867	-0.000167	1.25001
-2	3	5	0.384360	0.384357	0.000003	1.24241
-4	4	3	0.389220	0.389248	-0.000028	1.23463
3	4	4	0.390440	0.390400	0.000040	1.23270
-2	7	3	0.398920	0.399015	-0.000095	1.21953
-3	0	5	0.402950	0.402780	0.000170	1.21341
2	7	3	0.404670	0.404728	-0.000058	1.21083
4	1	4	0.409390	0.409465	-0.000075	1.20383
3	7	2	0.412020	0.412067	-0.000047	1.19998
-5	3	2	0.415220	0.415180	0.000040	1.19535
-5	4	1	0.417370	0.417459	-0.000089	1.19227
2	6	4	0.422360	0.422538	-0.000178	1.18520
0	1	6	0.424890	0.425034	-0.000144	1.18167
-5	1	3	0.431370	0.431251	0.000119	1.17276
-4	5	3	0.434090	0.434122	-0.000032	1.16908
3	2	5	0.437120	0.437008	0.000112	1.16502
4	6	2	0.440280	0.440151	0.000129	1.16083
-1	7	4	0.442260	0.442236	0.000024	1.15823
1	7	4	0.445800	0.446045	-0.000245*	1.15362
-4	7	1	0.464320	0.464252	0.000068	1.13038
-2	9	1	0.467310	0.467129	0.000181	1.12676
0	6	5	0.471360	0.471198	0.000162	1.12191
6	1	0	0.478030	0.477874	0.000156	1.11406
3	6	4	0.490190	0.490121	0.000069	1.10015
-5	5	2	0.494870	0.494956	-0.000087	1.09494
2	2	6	0.498180	0.498249	-0.000069	1.09129
4	6	3	0.500490	0.500396	0.000094	1.08877

NUMBER OF REFLECTIONS = 143

NUMBER OF REFLECTIONS USED = 141 FOR A GATE OF 0.00020

PARAMETERS	STANDARD DEVIATIONS	LAST SHIFTS
A = 6.721821	0.000209	-0.000000
B = 10.908276	0.000330	0.000000
C = 7.132084	0.000224	-0.000000
BETA = 91.101905	0.002833	-0.000019







LIST OF PUBLISHED AE-REPORTS

1-340 (See back cover earlier reports.)

341. Nonlinear dynamic model of power plants with single-phase coolant reactors. By H. Vollmer. 1968. 26 p. Sw. cr. 10:--.

342. Report on the personnel dosimetry at AB Atomenergi during 1967. By J. Carlsson and T. Wahlberg. 1968. 10 p. Sw. cr. 10:--.

343. Friction factors in rough rod bundles estimated from experiments in partially rough annuli - effects of dissimilarities in the shear stress and turbulence distributions. By B. Kjellström. 1968. 22 p. Sw. cr. 10:--.

344. A study of the resonance interaction effect between <sup>235</sup>U and <sup>239</sup>Pu in the lower energy region. By H. Häggblom. 1968. 48 p. Sw. cr. 10:--.

345. Application of the microwave discharge modification of the Wilzbach technique for the tritium labelling of some organics of biological interest. By T. Gosztonyi. 1968. 12 p. Sw. cr. 10:--.

346. A comparison between effective cross section calculations using the intermediate resonance approximation and more exact methods. By H. Häggblom. 1969. 64 p. Sw. cr. 10:--.

347. A parameter study of large fast reactor nuclear explosion accidents. By J. R. Wiesel. 1969. 34 p. Sw. cr. 10:--.

348. Computer program for inelastic neutron scattering by an anharmonic crystal. By L. Bohlin, I. Ebbsjö and T. Höjberg. 1969. 52 p. Sw. cr. 10:--.

349. On low energy levels in <sup>185</sup>W. By S. G. Malmkog, M. Höjberg and V. Berg. 1969. 18 p. Sw. cr. 10:--.

350. Formation of negative metal ions in a field-free plasma. By E. Larsson. 1969. 32 p. Sw. cr. 10:--.

351. A determination of the 2 200 m/s absorption cross section and resonance integral of arsenic by pile oscillator technique. By E. K. Sokolowski and R. Bladh. 1969. 14 p. Sw. cr. 10:--.

352. The decay of <sup>191</sup>Os. By S. G. Malmkog and A. Bäcklin. 1969. 24 p. Sw. cr. 10:--.

353. Diffusion from a ground level point source experiment with thermoluminescence dosimeters and Kr 85 as tracer substance. By Ch. Gyllander, S. Hollman and U. Widemo. 1969. 23 p. Sw. cr. 10:--.

354. Progress report, FFN, October 1, - September 30, 1968. By T. Wiedling. 1969. 35 p. Sw. cr. 10:--.

355. Thermodynamic analysis of a supercritical mercury power cycle. By A. S. Roberts, Jr. 1969. 25 p. Sw. cr. 10:--.

356. On the theory of compensation in lithium drifted semiconductor detectors. By A. Lauber. 1969. 45 p. Sw. cr. 10:--.

357. Half-life measurements of levels in <sup>210</sup>Pb. By M. Höjberg and S. G. Malmkog. 1969. 14 p. Sw. cr. 10:--.

358. A non-linear digital computer model requiring short computation time for studies concerning the hydrodynamics of the BWR. By F. Reisch and G. Vayssier. 1969. 38 p. Sw. cr. 10:--.

359. Vanadium beta emission detectors for reactor in-core neutron monitoring. By I. Ö. Andersson and B. Söderlund. 1969. 26 p. Sw. cr. 10:--.

360. Progress report 1968. Nuclear chemistry. 1969. 38 p. Sw. cr. 10:--.

361. A half-life measurement of the 343.4 keV level in <sup>175</sup>Lu. By M. Höjberg and S. G. Malmkog. 1969. 10 p. Sw. cr. 10:--.

362. The application of thermoluminescence dosimeters to studies of released activity distributions. By B.-I. Rudén. 1969. 36 p. Sw. cr. 10:--.

363. Transition rates in <sup>141</sup>Dy. By V. Berg and S. G. Malmkog. 1969. 32 p. Sw. cr. 10:--.

364. Control rod reactivity measurements in the Ågesta reactor with the pulsed neutron method. By K. Björens. 1969. 44 p. Sw. cr. 10:--.

365. On phonons in simple metals II. Calculated dispersion curves in aluminium. By R. Johnson and A. Westin. 1969. 124 p. Sw. cr. 10:--.

366. Neutron elastic scattering cross sections. Experimental data and optical model cross section calculations. A compilation of neutron data from the Studsvik neutron physics laboratory. By B. Holmqvist and T. Wiedling. 1969. 212 p. Sw. cr. 10:--.

367. Gamma radiation from fission fragments. Experimental apparatus - mass spectrum resolution. By J. Higbie. 1969. 50 p. Sw. cr. 10:--.

368. Scandinavian radiation chemistry meeting, Studsvik and Stockholm, September 17-19, 1969. By H. Christensen. 1969. 34 p. Sw. cr. 10:--.

369. Report on the personnel dosimetry at AB Atomenergi during 1968. By J. Carlsson and T. Wahlberg. 1969. 10 p. Sw. cr. 10:--.

370. Absolute transition rates in <sup>188</sup>Ir. By S. G. Malmkog and V. Berg. 1969. 16 p. Sw. cr. 10:--.

371. Transition probabilities in the 1/2+(631) Band in <sup>235</sup>U. By M. Höjberg and S. G. Malmkog. 1969. 18 p. Sw. cr. 10:--.

372. E2 and M1 transition probabilities in odd mass Hg nuclei. By V. Berg, A. Bäcklin, B. Fogelberg and S. G. Malmkog. 1969. 19 p. Sw. cr. 10:--.

373. An experimental study of the accuracy of compensation in lithium drifted germanium detectors. By A. Lauber and B. Malmsten. 1969. 25 p. Sw. cr. 10:--.

374. Gamma radiation from fission fragments. By J. Higbie. 1969. 22 p. Sw. cr. 10:--.

375. Fast neutron elastic and inelastic scattering of vanadium. By B. Holmqvist, S. G. Johansson, G. Lodin and T. Wiedling. 1969. 48 p. Sw. cr. 10:--.

376. Experimental and theoretical dynamic study of the Ågesta nuclear power station. By P. A. Bliselius, H. Vollmer and F. Akerhielm. 1969. 39 p. Sw. cr. 10:--.

377. Studies of Redox equilibria at elevated temperatures 1. The estimation of equilibrium constants and standard potentials for aqueous systems up to 374°C. By D. Lewis. 1969. 47 p. Sw. cr. 10:--.

378. The whole body monitor HUGO II at Studsvik. Design and operation. By L. Devell, I. Nilsson and L. Venner. 1970. 26 p. Sw. cr. 10:--.

279. ATOSPHERIC DIFFUSION. Investigations at Studsvik and Ågesta 1960-1963. By L.-E. Häggblom, Ch. Gyllander and U. Widemo. 1969. 91 p. Sw. cr. 10:--.

380. An expansion method to unfold proton recoil spectra. By J. Kockum. 1970. 20 p. Sw. cr. 10:--.

381. The 93.54 keV level <sup>90</sup>Sr, and evidence for 3-neutron states above N=50. By S. G. Malmkog and J. McDonald. 1970. 24 p. Sw. cr. 10:--.

382. The low energy level structure of <sup>231</sup>U. By S. G. Malmkog, V. Berg, A. Bäcklin and G. Hedlin. 1970. 24 p. Sw. cr. 10:--.

383. The drinking rate of fish in the Skagerack and the Baltic. By J. E. Larsson. 1970. 16 p. Sw. cr. 10:--.

384. Lattice dynamics of NaCl, KCl, RbCl and RbF. By G. Raunio and S. Rolandson. 1970. 26 p. Sw. cr. 10:--.

385. A neutron elastic scattering study of chromium, iron and nickel in the energy region 1.77 to 2.76 MeV. By B. Holmqvist, S. G. Johansson, G. Lodin, M. Salama and T. Wiedling. 1970. 26 p. Sw. cr. 10:--.

386. The decay of bound isobaric analogue states in <sup>28</sup>Si and <sup>28</sup>Si using (d, n<sub>γ</sub>) reactions. By L. Nilsson, A. Nilsson and I. Bergqvist. 1970. 34 p. Sw. cr. 10:--.

387. Transition probabilities in <sup>189</sup>Os. By S. G. Malmkog, V. Berg and A. Bäcklin. 1970. 40 p. Sw. cr. 10:--.

388. Cross sections for high-energy gamma transition from MeV neutron capture in <sup>208</sup>Pb. By I. Bergqvist, B. Lundberg and L. Nilsson. 1970. 16 p. Sw. cr. 10:--.

389. High-speed, automatic radiochemical separations for activation analysis in the biological and medical research laboratory. By K. Samsahl. 1970. 18 p. Sw. cr. 10:--.

390. Use of fission product Ru-106 gamma activity as a method for estimating the relative number of fission events in U-235 and Pu-239 in low-enriched fuel elements. By R. S. Forsyth and W. H. Blackadder. 1970. 26 p. Sw. cr. 10:--.

391. Half-life measurements in <sup>191</sup>I. By V. Berg and A. Höglund. 1970. 16 p. Sw. cr. 10:--.

392. Measurement of the neutron spectra in FRO cores 5, 9 and PuB-5 using resonance sandwich detectors. By T. L. Andersson and M. N. Qazi. 1970. 30 p. Sw. cr. 10:--.

393. A gamma scanner using a Ge(Li) semi-conductor detector with the possibility of operation in anti-coincidence mode. By R. S. Forsyth and W. H. Blackadder. 1970. 22 p. Sw. cr. 10:--.

394. A study of the 190 keV transition in <sup>141</sup>La. By B. Berg, A. Höglund and B. Fogelberg. 1970. 22 p. Sw. cr. 10:--.

395. Magnetoacoustic waves and instabilities in a Hall-effect-dominated plasma. By S. Palmgren. 1970. 20 p. Sw. cr. 10:--.

396. A new boron analysis method. By J. Weitman, N. Däverhög and S. Farvolden. 1970. 26 p. Sw. cr. 10:--.

397. Progress report 1969. Nuclear chemistry. 1970. 39 p. Sw. cr. 10:--.

398. Prompt gamma radiation from fragments in the thermal fission of <sup>235</sup>U. By H. Albinsson and L. Lindow. 1970. 48 p. Sw. cr. 10:--.

399. Analysis of pulsed source experiments performed in copper-reflected fast assemblies. By J. Kockum. 1970. 32 p. Sw. cr. 10:--.

400. Table of half-lives for excited nuclear levels. By S. G. Malmkog. 1970. 33 p. Sw. cr. 10:--.

401. Needle type solid state detectors for in vivo measurement of tracer activity. By A. Lauber, M. Wolgast. 1970. 43 p. Sw. cr. 10:--.

402. Application of pseudo-random signals to the Ågesta nuclear power station. By P.-A. Bliselius. 1970. 30 p. Sw. cr. 10:--.

403. Studies of redox equilibria at elevated temperatures 2. An automatic divided-function autoclave and cell with flowing liquid junction for electrochemical measurements on aqueous systems. By K. Johansson, D. Lewis and M. de Pourbaix. 1970. 38 p. Sw. cr. 10:--.

404. Reduction of noise in closed loop servo systems. By K. Nygaard. 1970. 23 p. Sw. cr. 10:--.

405. Spectral parameters in water-moderated lattices. A survey of experimental data with the aid of two-group formulae. By E. K. Sokolowski. 1970. 22 p. Sw. cr. 10:--.

406. The decay of optically thick helium plasmas, taking into account ionizing collisions between metastable atoms or molecules. By J. Stevefelt. 1970. 18 p. Sw. cr. 10:--.

407. Zooplankton from Lake Magelungen, Central Sweden 1960-63. By E. Almquist. 1970. 62 p. Sw. cr. 10:--.

408. A method for calculating the washout of elemental iodine by water sprays. By E. Bachofner and R. Hesböl. 1970. 24 p. Sw. cr. 10:--.

409. X-ray powder diffraction with Guinier-Hägg focusing cameras. By A. Brown. 1970. 102 p. Sw. cr. 10:--.

List of published AES-reports (In Swedish)

1. Analysis by means of gamma spectrometry. By D. Brune. 1961. 10 p. Sw. cr. 6:--.

2. Irradiation changes and neutron atmosphere in reactor pressure vessels - some points of view. By M. Grounes. 1962. 33 p. Sw. cr. 6:--.

3. Study of the elongation limit in mild steel. By G. Östberg and R. Attermo. 1963. 17 p. Sw. cr. 6:--.

4. Technical purchasing in the reactor field. By Erik Jonson. 1963. 64 p. Sw. cr. 8:--.

5. Ågesta nuclear power station. Summary of technical data, descriptions, etc. for the reactor. By B. Lilliehöök. 1964. 336 p. Sw. cr. 15:--.

6. Atom Day 1965. Summary of lectures and discussions. By S. Sandström. 1966. 321 p. Sw. cr. 15:--.

7. Building materials containing radium considered from the radiation protection point of view. By Stig O. W. Bergström and Tor Wahlberg. 1967. 26 p. Sw. cr. 10:--.

Additional copies available from the Library of AB Atomenergi, Fack, S-611 01 Nyköping 1, Sweden.